Permafrost and climate in Europe: Monitoring and modelling thermal, geomorphological and geotechnical responses — Source link ↗

Charles Harris, Lukas U. Arenson, Hanne H. Christiansen, Bernd Etzelmüller ...+18 more authors

Institutions: Cardiff University, University of Alberta, University Centre in Svalbard, University of Oslo ...+8 more institutions

Topics: Permafrost, Global warming, Ice wedge, Effects of global warming and Climate change

Related papers:

- Permafrost in steep bedrock slopes and its temperature-related destabilization following climate change

- Permafrost thaw and destabilization of Alpine rock walls in the hot summer of 2003

- Three-dimensional distribution and evolution of permafrost temperatures in idealized high-mountain topography

- Permafrost creep and rock glacier dynamics

- Permafrost distribution in the European Alps: calculation and evaluation of an index map and summary statistics

Share this paper: 📘 🐦 in ✉

View more about this paper here: https://typeset.io/papers/permafrost-and-climate-in-europe-monitoring-and-modelling-1ihtzbpajq

Year: 2009

Permafrost and climate in Europe: monitoring and modelling thermal, geomorphological and geotechnical responses

Harris, C ; Arenson, L U ; Christiansen, H H ; Etzelmüller, B ; Frauenfelder, Regula ; Gruber, Stephan ; Haeberli, Wilfried ; Hauck, C ; Hölzle, M ; Humlum, O ; Isaksen, K ; Kääb, Andreas ; Kern-Lütschg, Martina A ; Lehning, M ; Matsuoka, N ; Murton, J B ; Noetzli, Jeannette ; Phillips, M ; Ross, N ; Seppälä, M ; Springman, S M ; Vonder Mühll, D

Abstract: We present a review of the changing state of European permafrost within a spatial zone that includes the continuous high latitude arctic permafrost of Svalbard and the discontinuous high altitude mountain permafrost of Iceland, Fennoscandia and the Alps. The paper focuses on methodological developments and data collection over the last decade or so, including research associated with the continent-scale network of instrumented permafrost boreholes established between 1998 and 2001 under the European Union PACE project. Data indicate recent warming trends, with greatest warming at higher latitudes. Equally important are the impacts of shorter-term extreme climatic events, most immediately reflected in changes in active layer thickness. A large number of complex variables, including altitude, topography, insolation and snow distribution, determine permafrost temperatures. The development of regionally calibrated empiricalstatistical models, and physically based process-oriented models, is described, and it is shown that, though more complex and data dependent, process-oriented approaches are better suited to estimating transient effects of climate change in complex mountain topography. Mapping and characterisation of permafrost depth and distribution requires integrated multiple geophysical approaches and recent advances are discussed. We report on recent research into ground ice formation, including ice segregation within bedrock and vein ice formation within ice wedge systems. The potential impacts of climate change on rock weathering, permafrost creep, landslides, rock falls, debris flows and slow mass movements are also discussed. Recent engineering responses to the potentially damaging effects of climate warming are outlined, and risk assessment strategies to minimise geological hazards are described. We conclude that forecasting changes in hazard occurrence, magnitude and frequency is likely to depend on process-based modelling, demanding improved understanding of geomorphological process-response systems and their impacts on human activity.

Springman, S M; Vonder Mühll, D (2009). Permafrost and climate in Europe: monitoring and modelling thermal, geomorphological and geotechnical responses. Earth-Science Reviews, 92(3-4):117-171.
DOI: https://doi.org/10.1016/j.earscirev.2008.12.002

Permafrost and climate in Europe: Monitoring and modelling thermal, geomorphological and geotechnical responses

Charles Harris [a,*], Lukas U. Arenson [b], Hanne H. Christiansen [c], Bernd Etzelmüller [d], Regula Frauenfelder [d], Stephan Gruber [e], Wilfried Haeberli [e], Christian Hauck [f], Martin Hölzle [e], Ole Humlum [d], Ketil Isaksen [g], Andreas Kääb [d], Martina A. Kern-Lütschg [a], Michael Lehning [h], Norikazu Matsuoka [i], Julian B. Murton [j], Jeanette Nötzli [e], Marcia Phillips [h], Neil Ross [k], Matti Seppälä [l], Sarah M. Springman [m], Daniel Vonder Mühll [n]

[a] School of Earth and Ocean Sciences, Cardiff University, CF10 3YE, UK
[b] Department of Civil and Environmental Engineering, University of Alberta, Edmonton, Alberta, Canada T6G 2W2
[c] Department of Geology, The University Centre in Svalbard, 9171 Longyearbyen, Norway
[d] Department of Geosciences, University of Oslo, Blindern, NO-0316 Oslo, Norway
[e] Department of Geography, University of Zurich, CH-8057 Zurich, Switzerland
[f] Institute for Meteorology and Climate Reasearch, Karlsruhe Institute of Technology, 76131 Karlsruhe, Germany
[g] The Norwegian Meteorological Institute, Blindern, 0313 Oslo, Norway
[h] WSL,Swiss Federal Institute for Snow and Avalanche Research, SLF Davos, CH-7260 Davos Dorf, Switzerland
[i] Graduate School of Life and Environmental Sciences, University of Tsukuba, Ibaraki 305-8572, Japan
[j] Department of Geography, University of Sussex, Brighton, BN1 9SJ, UK
[k] School of Geosciences, University of Edinburgh, West Mains Road, Edinburgh EH9 3JW, UK
[l] Department of Geography, University of Helsinki, Helsinki, FIN-00014, Finland
[m] Geotechnical Institute, ETH Zurich, CH-8093 Zürich, Switzerland
[n] The Swiss Initiative in Systems Biology, ETH-Zürich, CH-8092 Zürich, Switzerland

ARTICLE INFO

ABSTRACT

We present a review of the changing state of European permafrost within a spatial zone that includes the continuous high latitude arctic permafrost of Svalbard and the discontinuous high altitude mountain permafrost of Iceland, Fennoscandia and the Alps. The paper focuses on methodological developments and data collection over the last decade or so, including research associated with the continent-scale network of instrumented permafrost boreholes established between 1998 and 2001 under the European Union PACE project. Data indicate recent warming trends, with greatest warming at higher latitudes. Equally important are the impacts of shorter-term extreme climatic events, most immediately reflected in changes in active layer thickness. A large number of complex variables, including altitude, topography, insolation and snow distribution, determine permafrost temperatures. The development of regionally calibrated empirical-statistical models, and physically based process-oriented models, is described, and it is shown that, though more complex and data dependent, process-oriented approaches are better suited to estimating transient effects of climate change in complex mountain topography. Mapping and characterisation of permafrost depth and distribution requires integrated multiple geophysical approaches and recent advances are discussed. We report on recent research into ground ice formation, including ice segregation within bedrock and vein ice formation within ice wedge systems. The potential impacts of climate change on rock weathering, permafrost creep, landslides, rock falls, debris flows and slow mass movements are also discussed. Recent engineering responses to the potentially damaging effects of climate warming are outlined, and risk assessment strategies to minimise geological hazards are described. We conclude that forecasting changes in hazard occurrence, magnitude and frequency is likely to depend on process-based modelling, demanding improved understanding of geomorphological process-response systems and their impacts on human activity.

© 2008 Published by Elsevier B.V.

* Corresponding author. School of Earth and Ocean Sciences, Cardiff University, Main Building, Park Place, Cardiff CF10 3YE, UK. Tel.: +44 2920 874336; fax: +44 2920 874326.
E-mail address: harrisc@cardiff.ac.uk (C. Harris).

Contents

1. Introduction

Permafrost (perennially frozen ground) forms a major element of the global cryosphere and since it is thermally defined as ground that remains below 0 °C for at least two years (Permafrost Subcommittee NRC Canada, 1988), is particularly sensitive to climate change (Haeberli and Hohmann, 2008). The relationship between mean ground temperatures and mean air temperatures reflects complex interaction between a range of variables including aspect, surface cover, soil moisture status and winter snow depth (Burn, 2007). As a result, mean annual ground surface temperatures may vary by many degrees within a given region. In addition, the higher thermal conductivity of the frozen active layer in winter than the thawed active layer in summer results in mean annual temperature at the permafrost table somewhat lower than mean annual ground surface temperature (the difference is known as the "thermal offset"). This thermal offset is strongly influenced by moisture status. Thus ground temperatures may be spatially variable, and permafrost is frequently discontinuous in the sub arctic and in mid-latitude high mountains.

In this paper we review the current status of European permafrost, its response to past, present and likely future climate change, the likely impact this will have on periglacial landforms and processes, and potential consequences regarding hazard and risk to human infrastructure. A major stimulus for this research was the international project "Permafrost and Climate in Europe" (PACE) that commenced in 1997 (see Harris et al., 2001a), funded by the European Union, and subsequently the PACE21 programme (2003–2006) sponsored by the European Science Foundation. The present paper includes reference to earlier research and to parallel studies, but its focus is on the progress made in this last decade of European research. A number of national and international programmes continue to develop permafrost research in Europe and elsewhere; many under the auspices of the International Polar Year (see Brown et al., 2008; Romanovsk et al., 2008).

The geographical area considered here is the European sector, defined approximately by lines of longitude 30°E to 25°W, including Svalbard, Iceland, Fennoscandia and the Alps, but excluding Greenland and Russia (Fig. 1). In this zone, permafrost occurs largely in mountainous regions, in bedrock, superficial sediments, and sometimes in association with glaciers. The major regional contrast is between the Arctic Archipelago of Svalbard, and the lower latitude higher altitude mountains of Scandinavia and the Alps. In Svalbard, permafrost is continuous outside the glacier covered areas, and glaciers are polythermal, with permafrost extending beneath their margins. Interaction between glacier and permafrost therefore leads to distinctive depositional processes and landform assemblages (see Etzelmüller and Hagen, 2005). In lower latitude mountains, permafrost is discontinuous or sporadic (Brown et al., 1997) (Fig. 1), and glaciers are generally warm-based, though at higher elevations permafrost may well extend to cold-based glacier margins (Haeberli, 2005; Kneisel, 2003). In the high mountains, permafrost is strongly influenced by altitude and aspect (e.g. Hoelzle et al., 2001; Etzelmüller et al., 2001a), and recent progress in mapping and modelling permafrost distribution is discussed. In many cases, ground tempera-

tures are only a few degrees below zero, so that European mountain permafrost is highly sensitive to projected climate changes in the 21st century. Literature on the distribution and character of discontinuous and sporadic permafrost in European mountains was reviewed by King and Åkerman (1993), who included reference to permafrost occurrences in the Pyrenees, Carpathians and parts of European Russia, areas that are not dicussed in the present paper.

A major goal of the PACE Project was to establish a continental scale north-south transect of permafrost monitoring stations, and this was achieved through drilling six deep (>100 m) boreholes in frozen bedrock (Fig. 1) over the period 1998 to 2001. Data from a borehole drilled through ice-rich frozen debris in 1987 at Murtèl–Corvatsch, Switzerland, have also been included, and are discussed in this paper. The PACE borehole network provides a regional framework for long-term European permafrost monitoring within the context of the worldwide monitoring network of WMO, ICSU and other international organisations (Global Terrestrial Network on Permafrost, GTN-P, contributing to GCOS/GTOS, see for instance, Cihlar et al., 1997, Harris et al., 2001a). This network corresponds to Tier 1 (Large Transect) in the global hierarchical observing strategy (GHOST) of GTN-P (Harris and Haeberli, 2003), and is the basis for the present discussion on the current thermal status of European permafrost. Details of each borehole are given in Table 1. Further European networks of shallow boreholes are currently being established in order that local variability in permafrost thermal regime and detailed changes in permafrost distribution may be established (see for instance, Vonder Mühll et al., 2007, 2008).

The sensitivity of permafrost terrain to global warming has recently been emphasised (e.g. Nelson et al., 2001, 2002; Jorgenson et al., 2006) but attention has mainly been paid to arctic regions. The present thermal status of European permafrost reflects not only the prevailing environmental conditions, but also past climate cycles, since the response to perturbations in the upper boundary (ground surface) thermal condition are often of longer duration than that of the forcing climate signals. In the longer term, permafrost has evolved under the major climatic cycles of the Pleistocene. However the focus here is on responses to 20th and early 21st Century climate change, for which more recent and less extreme Holocene climate fluctuations provide the main context, and these are therefore briefly reviewed before we discuss the current and potential future status of European permafrost.

2. Holocene climate and permafrost evolution

2.1. Context

In the Northern Hemisphere, summer insolation peaked at 10–9 ka BP, when the last remnants of the large ice sheets retreated rapidly. Incoming solar radiation was approximately 40 W/m^2 higher than now (Berger and Loutre 1991). Since then the Northern Hemisphere summers have seen gradually decreasing incoming solar radiation. This has been important, especially for high latitudes during summer when daylight persists for 24 h (Bradley 1990). The late Holocene was punctuated by a number of 400–800 yr periods with either relatively warm or cold climate, such as the Medieval Warm Period (MWP; c. AD
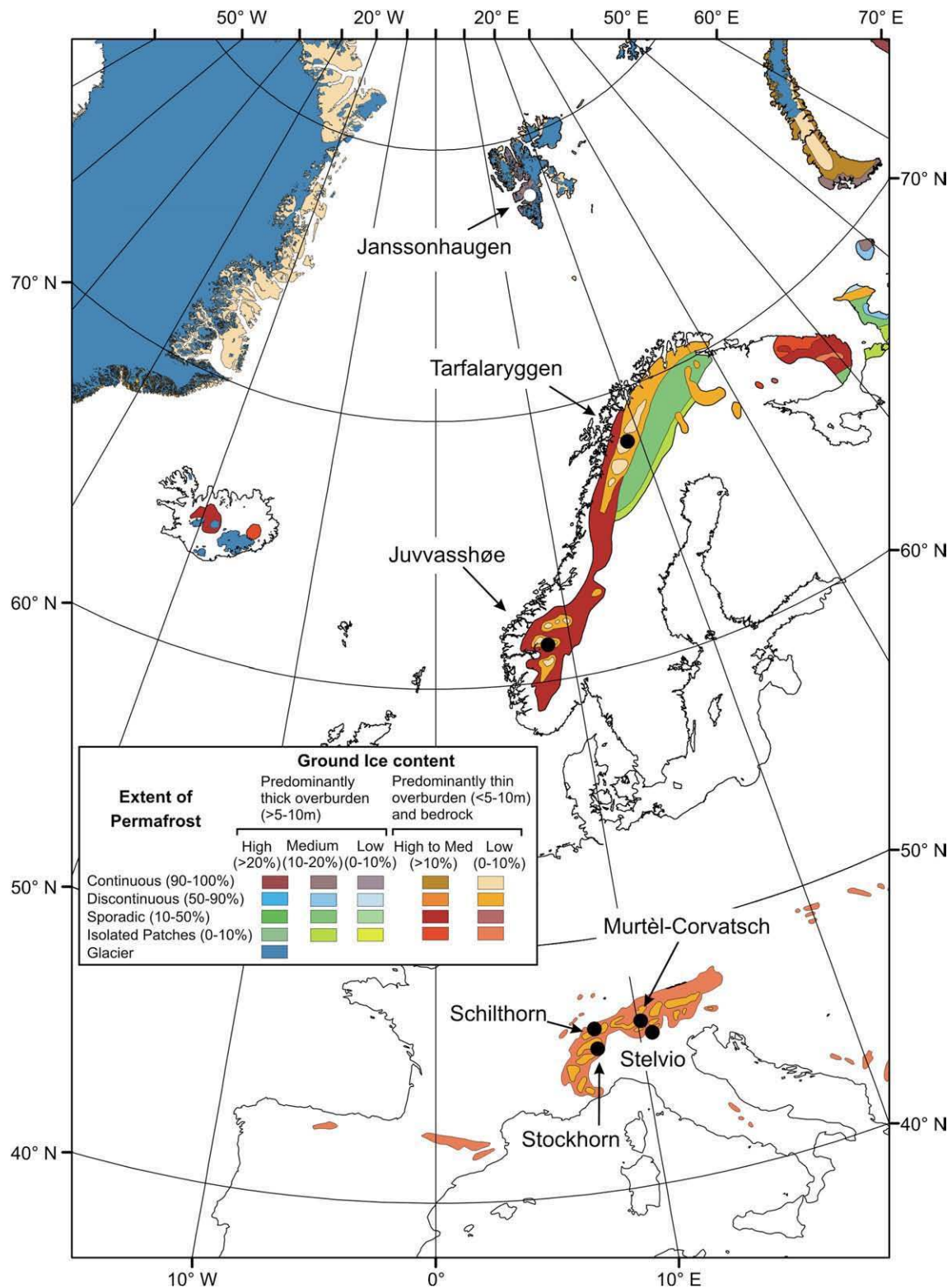
Fig. 1. Distribution of permafrost in the European sector according to the IPA Circum-Polar Map of Permafrost (Brown et al., 1997). The location of PACE boreholes is shown.

800–1200) or the Little Ice Age (LIA; c. AD 1300–1900). This overall Holocene climatic development is reflected in many regions of Europe, but to varying degrees.

A number of attempts have been made to develop dynamic regional and global time series temperature reconstructions for the last 1000 years (Mann et al., 1999; Shaopeng et al., 2000; Briffa et al., 2001; Moberg et al., 2005). With few exceptions, these are based on annually resolved proxies, particularly tree-rings, effectively limiting such studies to the last millennia when annual archives are widely available (Bradley, 1999). Observational evidence and numerical models suggest that climatic variability in large parts of Europe is closely linked to changes in the North Atlantic atmospheric and thermohaline circulation (for a recent overview, see Meincke 2002). The intensity of North Atlantic oceanic circulation governs energy

Table 1
Details of the PACE permafrost monitoring network

PACE boreholes and test sites		Janssonhaugen	Tarfalaryggen	Juvvashøe	Schilthorn	Stelvio Pass	Murtèl-Corvatsch	Stockhorn Plateau
		Svalbard Norway	Lapland Sweden	Jotunheimen Norway	Berner Oberland, Switzerland	Lombardia, Italy	Oberengadin Switzerland	Wallis Switzerland
Site description	Latitude	78°10′45″ N	67°55′ N	61°40′32″ N	46°33′34″ N	46°30′59″ N	46°26′ N	45°59′17″ N
	Longitude	16°28′15″ E	18°38′ E	08°22′04″ E	07°50′10″ E	10°28′35″ E	09°49′30″ E	07°40′31″ E
	Elevation a.s.l.	275 m	1540 m	1894 m	2909 m	3000 m	2670 m	3410 m
	Topography	Hill	Ridge	Plateau	Slope	Summit,	Rock glacier	Plateau on crest
	MAAT	−8 °C (estimated)	−6 °C (Estimated)	−4.5 °C (Estimated)	−4.3 °C	−3.7 °C (Sep 98–Sep 99)	−3 °C	−5.5 °C (Estimated)
1st borehole	Drilling date	April 1998	March 2000	April 1999	August 2000	1998	May/June 1987	July 2000
	Depth	102 m	100 m	129 m	101 m	100.3 m	62 m	100.7 m
	Chain length	(Vertical) 100 m	(Vertical) 100 m	(Vertical) 100+129 m	(Vertical) 100 m	(Vertical) 100	(Vertical) 58 m	(Vertical) 100 m
	Thermistor depths	PACE standard	PACE standard	PACE standard	PACE standard	24 (0.02–100 m)	52 (0.6–58 m)	PACE standard
2nd borehole	Drilling date	May 1998	March 2000	August 1999	October 1998			August .2000
	Depth	15 m	15 m	20 m	14 m			31 m
	Chain length	(Vertical)	(Vertical)	(Vertical)	(Vertical)			(Vertical)
	Thermistor	15 m	15 m	15 m	13.7 m			17 m
	Depths	PACE Standard	PACE Standard	PACE Standard	PACE Standard			PACE Standard

transfer to the atmosphere and regulates regional atmospheric pressure differences over Europe on timescales ranging from millennial to interannual (Hurrell 1995; Rodwell et al., 1999).

Climatic evolution is conveniently summarised by geographical subdivision into Arctic and Sub Arctic Maritime Europe, Northern Europe, and Central Europe, the latter two being roughly divided by the 55°N parallel. All dates quoted below are calibrated ages (calendar years).

2.2. The Western Arctic and Sub Arctic Maritime Zone: Iceland

In Iceland the early Holocene was characterized by progressive warming, rapidly retreating glaciers and development of a vegetation cover (e.g., Hallsdóttir, 1995; Ingólfsson et al., 1997). The Icelandic Holocene temperature maximum occurred between 8 and 4 ka BP, with summer temperatures 2–3 °C higher than present (Fig. 2) and extensive birch woodlands covering most of the lowlands (Einarsson, 1975; Hallsdóttir, 1995). The onset of colder and wetter climate began around 5 ka BP, and was marked by lowering of the mountain tree line and birch woods being replaced by heath and peatlands. By 4 ka BP

glaciers were expanding, but did not reach their Holocene maximum until the LIA in the later part of the 19th century (Gudmundsson, 1997). Given the high geothermal gradients that prevail in Iceland, much pre-existing permafrost probably disappeared rapidly during the mid Holocene climatic optimum, so that most of the present day Icelandic permafrost and associated landforms (palsas, rock glaciers and ice-cored moraines) were probably initiated during the onset of the late Holocene cooling c. 5 ka BP (Wangensteen et al., 2006), culminating in the Little Ice Age (Hamilton and Whalley, 1995).

2.3. The Eastern Arctic and Sub Arctic Maritime Zone: Svalbard

Sediment cores from the Nordic Seas near Svalbard indicate the first half of the Holocene to have been the warmest period during the last 13.4 ka (Koç et al., 1993) and in the Barents Sea, south of Svalbard, $\delta^{18}O$ data show early Holocene warming culminating between 9 and 6.5 ka BP (e.g., Ivanova et al., 2002). MAAT was 3–5 °C higher than today until c. 5 ka BP (e.g., Birks, 1991; Hjort, 1997; Salvigsen, 2002) (Fig. 2). Glacier margins on Svalbard and Franz Josef Land lay within the present ice limits until the Late Holocene, with high summer
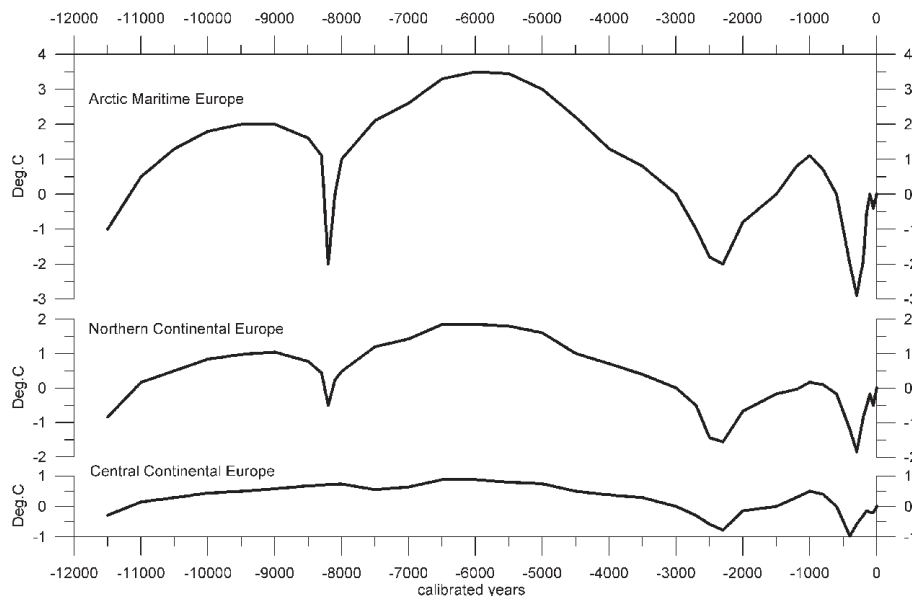

Fig. 2. Estimated Holocene air temperature changes in Arctic Maritime Europe, Northern Continental Europe and Central Continental Europe. Temperature units (vertical axes) approximate degrees Celsius, time axis in calibrated years. Modern temperature (late 20th century) is baseline for temperatures shown.

temperatures dominating glacier budgets (Svendsen and Mangerud 1997; Lubinski et al., 1999). After 5–4 ka BP the surface waters along western Svalbard cooled and air temperatures fell as the influence of Atlantic Water decreased (e.g. Koç and Jansen, 1994). Glacier expansion began in western Svalbard around 5–4 ka BP (Svendsen and Magerud, 1997), glaciers reaching a maximum around 2.3 ka BP and their Holocene maximum during the Little Ice Age (Furrer, 1994; Humlum et al., 2005). The long composite meteorological record from Svalbard indicates that MAAT during periods of the Little Ice Age was 4–6 °C below late 20th century values (Fig. 2).

Permafrost in many coastal locations probably disappeared in the early Holocene warm period, and was discontinuous to altitudes of 300–400 m, (Humlum et al., 2003; Humlum, 2005). In the main trunk valleys, permafrost was presumably eliminated by warm-based Weichselian glaciers (Humlum et al., 2003). Permafrost development was apparently controlled by Holocene cooling after around 3 ka BP (e.g. Büdel, 1977; Svensson, 1971; Jeppesen, 2001). Below the early Holocene marine limit (c.70–80 m asl.), permafrost evolution has been partly controlled by emergence totalling 15–30 m in eastern Svalbard and 5–10 m in western and central areas since 5 ka BP (Forman et al., 2004).

2.4. Northern Continental Europe

Holocene temperature variations in Northern Europe were apparently greatest in the NE and decreased towards the SW. Early Holocene summer temperatures were similar to today in Northern Scandinavia (e.g., Seppä and Birks, 2001) and Western Norway, (e.g., Karlén, 1998; Lauritzen and Lundberg, 1999) and the tree-line appears to have been close to its present position (e.g., Dahl and Nesje, 1996). Warming by 9.5–9 ka BP led to migration of pine forests and reduction in glaciers (Hyvärinen 1975; Karlén, 1988; Eronen and Zetterberg, 1996; Barnekow and Sandgren, 2001; Seierstad et al., 2002) and between 8 and 5.8 ka BP, MAAT rose to 2.5 °C, some 3 °C higher than today (e.g. Kultti et al., 2006), and glaciers in southern Norway virtually disappeared (Nesje and Kvamme, 1991; Nesje et al., 2000). Cooling, glacier expansion and tree line retreat followed (e.g., Korhola et al., 2002; Nesje et al., 2001; Matthews et al., 2005), with the periods 4.35–3.35 ka BP and post 1.35 ka BP having the severest winters during the entire Holocene (Blikra and Selvik, 1998).

During the succeeding Medieval Warm Period between AD 980 and 1250, winter air temperatures in Finland were up to 2 °C warmer than today (Tiljander et al., 2003) (see Fig. 2) although July temperatures were only marginally warmer (Seppä and Birks, 2002). Subsequent cooling in the Little Ice Age of the 18th–19th centuries saw glaciers in Norway reach their greatest Neoglacial extent (Nesje, 1992), with summer temperatures 0.5 to 1.6 °C lower than the reference period 1949–1963 (Matthews, 1976).

The mid-Holocene altitudinal limit for permafrost in Northern Europe probably lay around 150–300 m higher than today though local changes in snow cover duration and timing may have reduced or enhanced this altitudinal difference. The period from 5 ka BP to the Little Ice Age was characterised by lowering of permafrost altitudinal limits, though during the Medieval Warm Period the trend would have been reversed. Thermal inertia arising from latent heat effects would have limited complete permafrost degradation to marginal zones of ice-poor bedrock, and it is likely that present day permafrost distribution is currently adjusting to the warmer 20th century climate but still largely reflects that of the Little Ice Age (Juliussen and Humlum, 2008).

2.5. Central Europe

Generally, climate reconstructions from Central Europe do not show the large and coherent Holocene warming and cooling trends that characterise Northern Europe. On the basis of plant macrofossil and pollen evidence, Haas et al. (1998) suggest summer temperatures 0.7–0.9 °C above present values in the early Holocene. Following this period, temperature fluctuations within 1.0 °C of modern values have been reported (e.g. Haas et al., 1998; Davis et al., 2003) and alpine glaciers have responded periodically to such fluctuations (Hormes et al., 2001). The mid-Holocene thermal maximum at around 6 ka BP was more clearly defined in the west than in the east (Davis et al., 2003), and saw tree lines at their maximum altitudes (Haas et al., 1998; Wick and Tinner, 1997) though in NW Italy, the timberline was 100–200 m higher than today (Burga, 1991), corresponding to summer temperatures 1.5–3.0 °C above present day. Following the Holocene thermal maximum, summer temperatures declined in the west, although winter temperatures continued to increase (Davis et al., 2003). Alpine timberlines retreated (Tinner et al., 1996), and after 4.5 ka BP, bog surfaces were wetter (Barber et al., 1994).

The Medieval Warm Period, between AD 800 and 1100, led to glacier retreat in Switzerland (Holzhauser et al., 2005) and was followed by transition to the Little Ice Age. MAAT fell by about 1.5 °C (Filippi et al., 1999) culminating around AD 1850–1860 when Alpine glaciers reached their late Holocene maximum. Fluctuation in the permafrost altitudinal limits in Central Europe were probably less marked than in Northern Europe and would have been strongly modulated by variations in snow depth and duration. Permafrost advance during cooling would probably have been more rapid than permafrost retreat during warming, due to the thermal inertia associated with latent heat. In the highest Alpine peaks, that penetrated the Weichselian glaciers as nunataqs, permafrost may have survived from the last glaciation.

2.6. European climate during the 20th century

It is generally agreed that European climate during the 20th century has been characterised by warming. Slonosky et al. (2000, 2001) investigated the variability of the surface atmospheric circulation over Europe from 1774 to 1995 and found that records suggest episodes of more intense meridional circulation from 1822 to 1870, and stronger zonal westerlies from 1947 to 1995. The zonal flow appears to have been considerably more variable with more extreme values in the late 18th and early 19th centuries than in the 20th century. Luterbacher et al. (2004) investigated European seasonal and annual temperature variability, trends, and extremes since 1500, using multiproxy reconstructions of monthly and seasonal surface temperature fields. They found that the late 20th- and early 21st-century European climate is likely to be warmer than that of any time during the past 500 years. In central and western Europe from 1901 to 1999, the dominant trend has been for increasing winter precipitation intensity and frequency of moderately extreme events (Moberg and Jones, 2005). The length of dry spells in summer generally increased during the 20th century. Both the warm and cold tails of the temperature distribution in winter rose over the entire 20th century but notably low values in the cold tail for daily maximum temperatures (Tmax) and daily minimum temperatures (Tmin) occurred in the early 1940s.

To provide a geographical overview of 20th century temperature changes within Europe, monthly meteorological data from 318

Fig. 3. Mean Annual Air Temperatures observed at selected meteorological stations in Europe, near PACE boreholes. Heavy lines show the 11 years unweighted running average. (a) Svalbard, (b) Abisko, Sweden, (c) Dombås and Fokstugu, Norway and (d) Saentis, Switzerland. Note that in (c) a constant of 1.3 °C has been added to the Fokstugu data (stippled), in order to simulate modern continuation of the old Dombås data series. Data sources: the Norwegian Meteorological Institute, the Abisko Research Station, and NASA Goddard Institute (GISS).
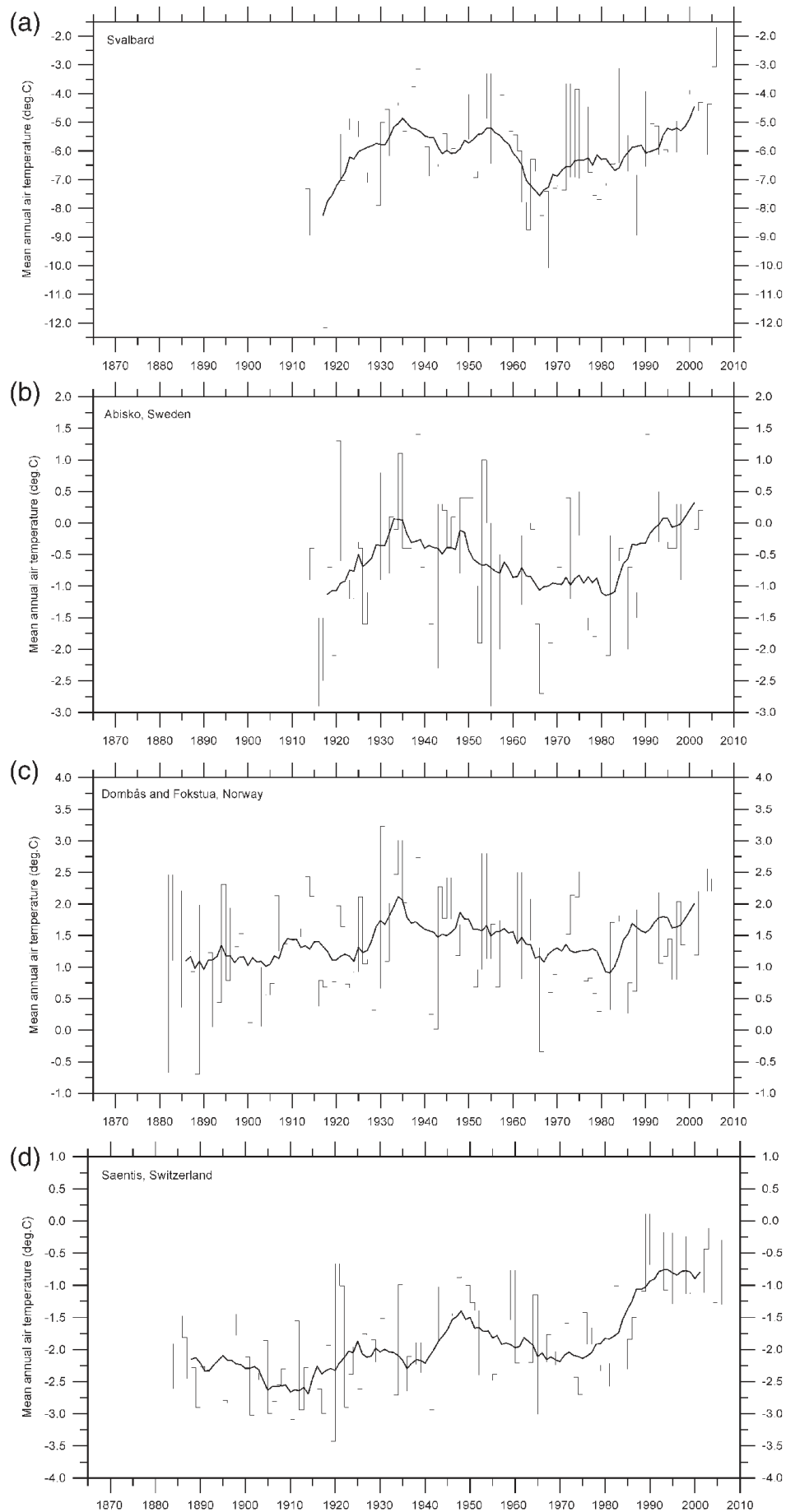
meteorological stations have been analysed. Data are largely derived from a database at the NASA Goddard Institute (GISS). All data have been homogenized, i.e. corrected for environmental change in the surroundings of the measuring instrument, and for errors arising at the point of measurement (known equipment or procedural faults, change of measuring site, change of surroundings, change of averaging method, etc.), before inclusion in the GISS database. However, some unknown inhomogeneities may still remain in the data set for some stations. A few series with missing data were encountered. In such cases, missing data were generated by comparison with the two nearest meteorological stations having continuous data for the months in question. Meteorological observations from 1880 to December 2005 have been used in the analysis.

Interannual temperature variations are known to be substantial, especially at high latitudes during winter. Both the global and the European mean annual air temperatures are characterised by 2–5 year oscillations which most likely are associated with oceanographic and volcanic effects. To reduce the influence of such short-term variations, the spatial pattern of change of 11 years unweighted running means was analysed, highlighting variability over longer time periods. Fig. 3 shows the mean annual air temperature (MAAT) record from selected meteorological stations. Several, but not all, display rising temperatures during the first 30–40 years of the 20th century, and then falling temperatures until 1970–1975, when a renewed temperature increase occurred. Thus, the climatic development within Europe during the observational period has not been uniform and in general, temperature variations (interannual, decadal or multi-decadal) tend to increase with latitude.

Selected time windows, centred on start and end year of the period considered, have been analysed to explore the spatial variability of climate trends. The calculated changes were spatially interpolated across the entire European continent between 32°N and 72°N (for mapping reasons Svalbard was omitted), using a standard kriging algorithm. This interpolation procedure is widely considered one of the more flexible interpolation methods, producing a smooth map with few "bulls' eyes". The method is suitable for gridding almost any type of data set, especially those with a heterogeneous point distribution, such as the present meteorological data set (Polyak, 1996). The results of the spatial surface temperature analyses are shown in Fig. 4.

Between 1900 and 1940, MAAT increased in western and northern Europe (including Iceland), while most of the remaining part of Europe experienced only small changes. Due to their geographical locations, most of the PACE borehole sites experienced increasing air temperatures during this period, especially the two northernmost boreholes (Svalbard and Sweden). The period from 1940 to 1975 was one of widespread cooling in the Arctic, affecting Iceland and Svalbard (Fig. 4), but in continental Europe cooling was confined to the northern and western regions. At the same time, regions in Eastern Europe experienced slight warming and Central and Southern Europe experienced relatively minor changes.

Most of the PACE borehole sites in this period experienced relatively small changes in MAAT, again with the exception of the boreholes in Sweden and Svalbard (Figs. 3 and 4). Widespread climate warming has been recorded in Europe in the period 1975 to 2000. On an annual basis, this has been most pronounced in SW Europe and in central Scandinavia (Fig. 4). Seasonally, however, there are large regional deviations from these overall annual trends. Winters (Fig. 4, lower right panel, DJF) have been characterised by rising temperatures in western and northern Europe, especially within a region stretching from central Scandinavia to southern Russia. Spring (Fig. 4, lower right

panel, MAM) has been characterised by increasing temperatures over most of Europe, but most pronounced in the central and southwestern regions. Summers (Fig. 4, lower right panel, JJA) have warmed everywhere, but especially in southern Europe, and autumn temperatures (Fig. 4, lower right panel, SON) have been characterised by spatial variability.

All PACE borehole sites have been exposed to atmospheric warming in all seasons since 1975. The warming has been especially pronounced during the autumn and winter for the northernmost boreholes. For boreholes in central Europe the warming has been greatest during spring and summer. The response of near-surface permafrost temperatures to changes in air temperature are very strongly modulated by snow thickness and duration, and since the seasonal trends identified above also correspond to changes in snow regime, any attempt to model impacts of climate change on permafrost temperatures cannot be based simply on mean annual air temperatures and precipitation, but must also consider seasonal changes, with particular emphasis on snow cover thickness and duration.

## 3. Monitoring permafrost temperatures and active layer thickness

3.1. Geothermal conditions in mountain permafrost

The geothermal regime of mountain permafrost is strongly influenced by the nature of the ground surface (especially the temporal and spatial variability of snow cover, together with local topography), the nature of the substrate (spatial and depth variation in lithology and ice content) and the regional geothermal heat flux (see for instance Harris et al., 2003a,b). At lower elevations, local hydrology might also be significant. Time scales of climatically-forced cycles of ground surface temperature range from daily, through seasonal, annual, decadal, century to millennial, with corresponding differences in magnitude. Thus, geothermal profiles are generally in a transient state, continually adjusting to changes in the upper boundary temperature that propagate downwards into the ground (e.g. Beltrami and Harris, 2001).

Ground temperature data from permafrost boreholes are particularly well suited to the detection of changes in the surface boundary condition that can be interpreted as climate signals (e.g. Lachenbruch and Marshall, 1986), mainly because heat advection by ground water or air circulation is often negligible. The geothermal profile is, therefore, primarily a function of heat conduction, depending on heat flux from the Earth's interior and heat flux arising from the energy exchanges that occur at the ground surface. Downward propagation of temperature changes at the permafrost table may take considerable time, and is accompanied by progressive attenuation. The annual thermal cycle generally penetrates to a depth of 15–20 m, but larger perturbations in surface temperature of longer periodicity may penetrate much deeper and take much longer to do so. Thus, changes in the subsurface thermal gradient provide a record of the recent ground surface temperatures.

Geothermal time series obtained from monitoring of permafrost represent a systematic running mean that filters the higher frequency signal at the ground surface and preserves only the low frequency, long-term signals (cf. Lachenbruch and Marshall, 1986). Thus, records of ground temperatures below the depth of zero annual amplitude may provide direct evidence of thermal trends at the permafrost table during recent decades (e.g., Osterkamp and Romanovsky, 1999; Osterkamp, 2008; Cermak et al., 2000; Romanovsky and Osterkamp, 1995).

Fig. 4. Spatial distribution of changes in surface mean annual air temperature 1900–1940, 1040–1975 and 1975–2000, based on 11-year unweighted running temperature means, comparing unweighted averages for the periods 1895–1905, 1935–1945, 1970–1980 and 1995–2005. Temperature interval 0.2 °C. Lower right panel shows seasonal changes for the period 1975–2000. DJF = December, January, February, MAM = March, April, May, JJA = June, July, August, SON = September, October, November. Data sources the Norwegian Meteorological Institute, the Abisko Research Station, and NASA Goddard Institute (GISS).
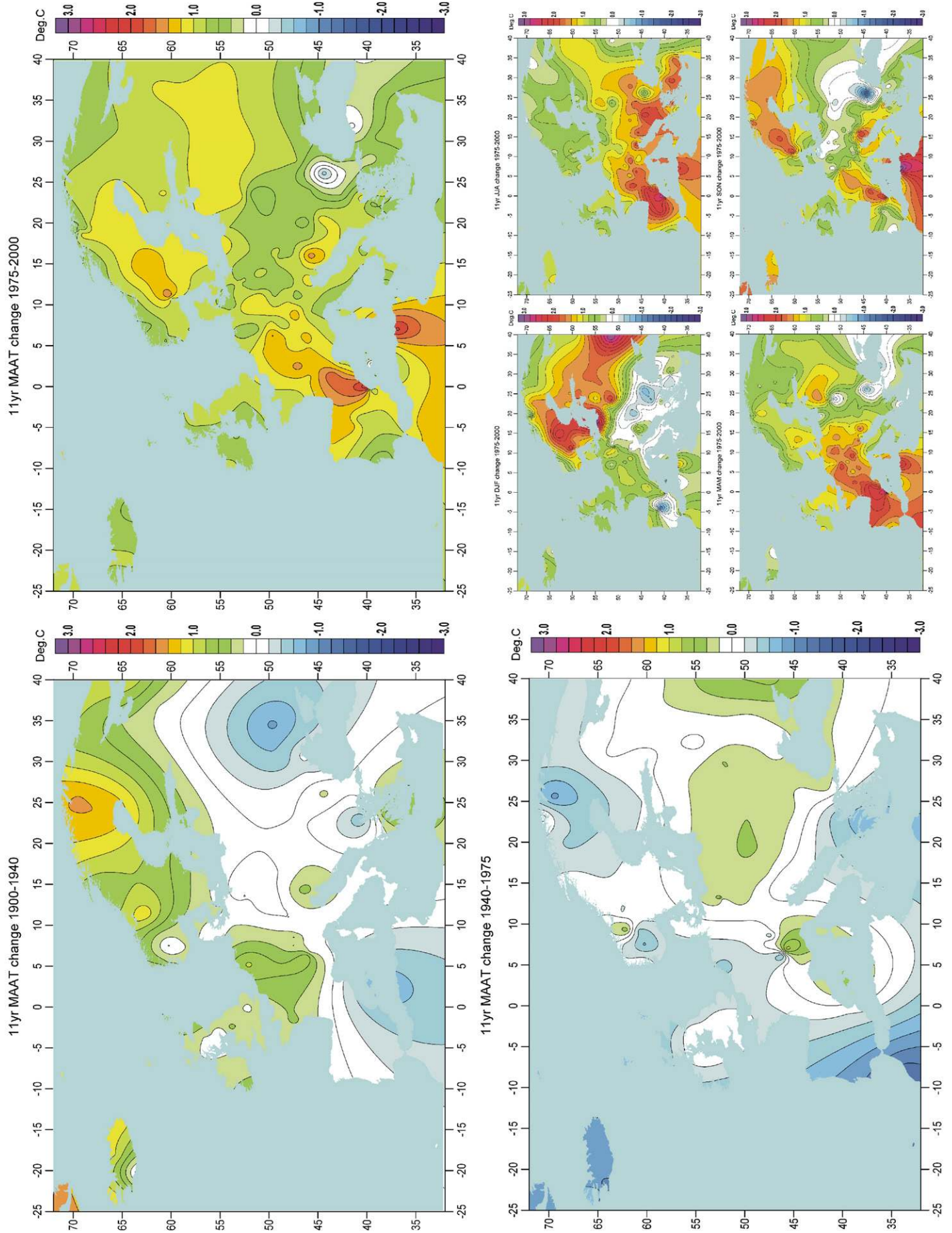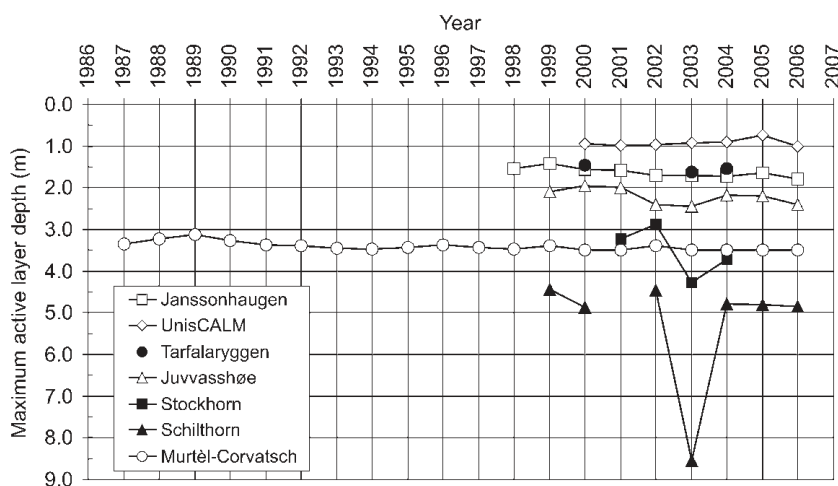
Fig. 5. Maximum annual active layer depth. The thickness of the active layer during each thaw season is estimated using an exponential best-fit between all thermistors in the boreholes. Daily temperature records are used. At Janssonhaugen and Juvvasshøe, data series were obtained from nearby 15–20 m deep control boreholes (Isaksen et al., 2001 see Table 1).

In the Arctic, the mean annual ground temperature and the thermal response of the surface to the passage of the seasons can vary significantly as one passes from, for instance, dry to wet habitats, gravel beaches, ponds, lakes and rivers (Gold and Lachenbruch, 1973). In addition, variable snow cover, especially in early winter, exerts an important influence on ground temperatures, causing strong lateral variations (e.g., Goodrich, 1982; Vonder Mühll et al., 1998; Zhang, 2005). In mountain permafrost, the problem of 3-dimensonality of the thermal field is complicated further by the often complex surface geometry and by strong spatial heterogeneity of the surface conditions and temperatures (Gruber et al., 2004c). Circulation of water and air within coarse blocks in typical steep slopes may result in highly variable and sometimes extreme thermal offsets (e.g., Hoelzle et al., 2001). Thus, permafrost ground temperatures may integrate effects of several processes involved in the heat transfer regime of the air-ground boundary. This integration modulates the thermal signal conducted downwards into the permafrost below. Therefore, interpretation of measured temperature profiles should be undertaken carefully, with particular attention being paid to the strong 3-dimensional effects of rugged alpine topography (Kohl, 1999; Gruber et al., 2004c) (see Section 7).

3.2. The European mountain permafrost borehole network

Currently seven boreholes form the core network of the PACE permafrost monitoring network (Fig. 1, Table 1) (Harris et al., 2003a,b). In the Alps, bedrock boreholes have been drilled and instrumented at Schilthorn (Vonder Mühll et al., 2000; Harris et al., 2001a, 2003a,b; Harris and Isaksen, 2008) and Stockhorn (Gruber et al., 2004c) in Switzerland and at the Stelvio Pass in Italy (Guglielmin et al., 2001). At Schilthorn an additional oblique 100 m borehole was drilled to study the influence of topography on the thermal regime (Vonder Mühll et al., 2004). In Scandinavia and Svalbard, boreholes have been installed at Juvvasshøe, Jotunheimen (Norway), Tarfalaryggen (Sweden) and Janssonhaugen (Svalbard) (Sollid et al., 2000; Isaksen et al., 2001). The boreholes extend to a depth of 100 m or more.

Borehole casing, sensors and data logging equipment were assembled according to guidelines provided by the PACE project in order to standardise procedures and ensure comparability between sites (Harris et al., 2001a). This also ensured reliability and serviceability. Periodic recalibration of the installed thermistors is possible and the holes remain accessible for other probes in future. Borehole temperatures were measured with negative temperature coefficient (NTC) thermistors, namely Yellow Spring Instruments YSI 44006

with a resistance of about 2.95×10^4 Ω at 0 °C, with a temperature coefficient of about 5% per °C. The absolute accuracy is estimated at ±0.05 °C and the relative accuracy at ±0.02 °C. Depths of thermistors followed the general instructions for the PACE boreholes and levels were: 0.2 m, 0.4 m, 0.8 m, 1.2 m, 1.6 m, 2.0 m, 2.5 m, 3.0 m, 5.0 m, 7.0 m, 9.0 m, 10.0 m, 13.0, 15.0 m, 20.0 m, 25.0 m, 30.0 m and 10 m spacing to 80.0 m, and then denser again to 100.0 m. The measurement interval of the thermistors in the upper 15 m of the control borehole is every 6 h. Temperatures of the thermistors below 5 m in the main boreholes are taken once every 24 h. For more details on borehole instrumentation, see Isaksen et al. (2001). In addition, time series data from the Murtèl–Corvatsch borehole (Switzerland), drilled in 1987 to a depth of 58 m in creeping frozen ice-rich rock debris are available (Vonder Mühll and Haeberli, 1990; Hoelzle et al., 2002).

3.3. Active layer thickness

Summer surface temperatures at the Scandinavian and Svalbard borehole sites are significantly lower at than those in the Alps, so that active layers are shallower in the former than in the latter (Harris et al., 2003a,b). Fig. 5 shows the maximum annual active layer depth at each PACE borehole, together with data from the UNISCALM site in Adventdalen, Svalbard where the substrate is frozen silt (this forms part of the Circumpolar Active Layer Monitoring (CALM) network of the GTN-P, (Christiansen and Humlum, 2008)). The UNISCALM site is less than 15 km from Janssonhaugen. Maximum and minimum active layer thickness recorded in each time series is given in Table 2. The Alpine boreholes, plus the Scandinavian sites at Juvvasshøe and Tarfalaryggen showed maximum active layer depths in 2003, while in Svalbard maximum summer thaw penetration occurred in 2006.

Table 2

Maximum and minimum active layer depths recorded at European PACE boreholes

| Site	Minimum thickness (m)	Year with minimum thickness	Maximum thickness (m)	Year with maximum thickness
Janssonhaugen, Svalbard	1.42	1999	1.80	2006
UNISCALM, Svalbard	0.75	2005	1.00	2006
Tarfalaryggen, Sweden	1.45	2000	1.63	2003
Juvvasshøe, Norway	1.95	2000	2.45	2003
Schilthorn, Switzerland	4.43	1999	8.55	2003
Stockhorn, Switzerland	2.88	2002	4.27	2003
Murtèl–Corvatsch, Switzerland	3.12	1999	3.5	2003, 2004, 2005
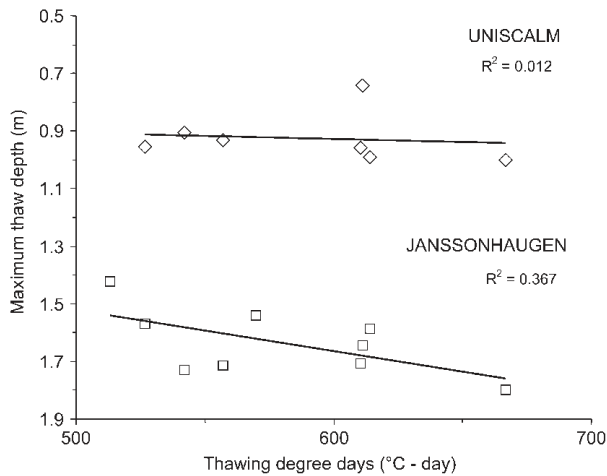
Fig. 6. Relationship between cumulative above zero degree days and active layer thickness, Janssonhaugen and the Longyearbyen CALM site, Svalbard.

On Svalbard, the mean air temperature in December–May 2005–2006 was as high as −4.8 °C, which is 8.2 °C above the 1961–1990 average. This is 2.8 °C higher than the previous record from 1954, amounting to an offset of 3.7 standard deviations from the mean (Isaksen et al., 2007a). In southern Norway, the summers of 2002 and 2003 were among the warmest recorded, and in the Alps, summer 2003 saw sustained record temperatures, in Switzerland approximately 3 °C higher than the 1961–1990 average for the three month period June, July and August (Schär et al., 2004). Active layer responses depended largely on the composition and ice content of the ground, with higher ice contents limiting thaw penetration because of greater latent heat demand (see Murtèl–Corvatsch (Switzerland) in Table 2).

On Janssonhaugen, where permafrost comprises ice-poor bedrock, the extreme 2005–2006 winter temperature, coupled with summer 2006 air temperatures ~2 °C above the 1961–1990 normal, resulted in the earliest commencement of thawing during spring 2006 in the 8-year borehole record, and in late summer 2006 the active layer thickness exceeded previous years by 0.18 m (Isaksen et al., 2007b). At Juvvasshøe, southern Norway, again in ice-poor bedrock, active layer depths were 20% greater in the 2003, 2004 and 2006 summers than in previous years. Snow cover at Janssonhaugen and Juvvasshøe is usually thin or absent, surfaces are normally dry and water content in the ground is low, so that active layer thickness is well correlated with local summer air temperatures on an inter-annual basis.

At the UNISCALM site, where winter snow thickness is generally less than 0.3–0.4 m and ground cooling in winter is sufficient to promote thermal contraction cracking, the average active layer depth was 0.93 m over the period 2000–2006, with a minimum of 0.74 m recorded in 2005 and a maximum of 1.0 m in 2006. Thus, the 2006 active layer thickness was 0.07 m greater than average, though only slightly greater than that recorded in 2001. It is possible that ice contents increase in the permafrost immediately below the active layer at this site, reducing thaw penetration during extreme years. The active layer, however, is less ice-rich, as evidenced by the 2006 thaw depth exceeding that in 2005 by as much as 0.26 m (Christiansen and Humlum, 2008).

In the Alpine boreholes, the response to the extreme summer of 2003 varied considerably. At Murtèl-Corvatsch in the Swiss Alps, active-layer thickness ranged between 3.1 and 3.5 m within the 19-year observation period, with a trend towards increasing depths (Fig. 5). In the ice-rich frozen debris at Murtèl–Corvatsch, the large latent heat requirement restricted active layer thickening in 2003, though the active-layer was deeper than had previously been recorded (Fig. 5). In the two Swiss bedrock boreholes, Stockhorn and Schilthorn, minimum recorded active layer thickness over the past 5–6 years was just less than 3 m at Stockhorn and just less than

4.5 m at Schilthorn. The depth of thaw penetration in the extreme summer of 2003 at Schilthorn was around twice the average of the previous years, and at Stockhorn it increased by around 30%, indicating strong heat conduction coupled with possible convective heat transfer by water (e.g. Gruber et al., 2004b).

Plotting maximum active layer depths against the summer accumulated above zero degree days for Janssonhaugen with a frozen bedrock substrate and the UNISCALM site, with a frozen silt substrate, demonstrates that active layer thawing is largely driven by summer air temperatures (Fig. 6). Scatter within the plots results from several factors, including the degree of cooling in the previous winter and the duration of spring snow cover, while differences in the coefficients largely reflect contrasting active layer and permafrost ice contents (and hence latent heat) between sites. The presence of an ice-rich "transient layer" in the transition zone between the active layer and the permafrost in non-bedrock locations such as Adventdalen acts as a thermal buffer, slowing active layer thickening during warmer than average summers (Shur et al., 2005).

3.4. Permafrost temperature profiles

The greater altitudinal range and steeper topographic gradients in the Alps leads to considerably greater ground temperature variability among the Swiss boreholes than among those in Scandinavia (Harris et al., 2003a,b, Harris and Isaksen, 2008). In Svalbard, in the continuous permafrost zone, spatial variation is considerably less than in the Alps. Fig. 7 shows updated ground temperature profiles from all the sites, recorded in April 2005. Seasonal temperature variations influence the upper 15–20 m and data from this zone are less useful in analysing interannual to decadal variations in ground temperatures than the thermal gradients recorded at greater depths.

The smooth profile at Janssonhaugen on Svalbard suggests little geothermal disturbance by non-climate sources (cf. Isaksen et al., 2000b). Here the temperature gradient at 25 m is 0.010 °C m^{-1} and this increases to 0.037–0.038 °C m^{-1} at 95 m. At Tarfalaryggen and Juvvasshøe the thermal gradients in the upper 40–50 m of bedrock are negative (temperatures increasing with depth), the temperature gradient changing from −0.015 °C m^{-1} at 25 m to 0.010–0.011 °C m^{-1} at 95 m in the Tarfalaryggen borehole and −0.011 °C m^{-1} at 25 m to 0.010–0.011 °C m^{-1} at 126.5 m in Juvvasshøe. Large-scale topographic influence may partly explain the low geothermal gradients at Tarfalaryggen and Juvvasshøe since adjacent valleys extend ~400
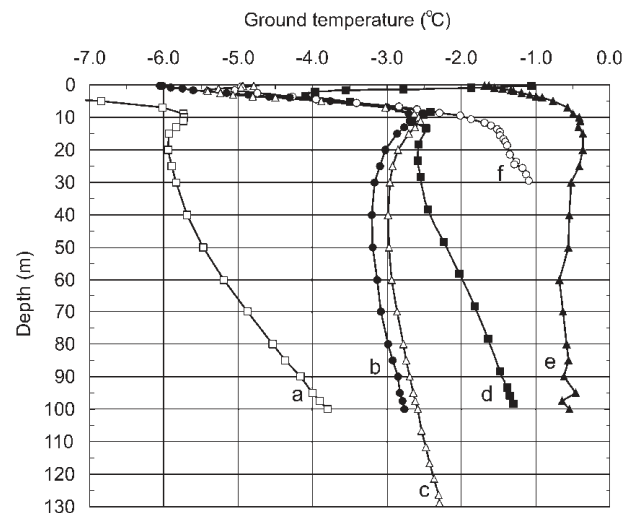

Fig. 7. Ground temperature profiles in permafrost at (a) Janssonhaugen, (b) Tarfalaryggen, (c) Juvvasshøe, (d) Stockhorn, (e) Schilthorn and (f) Murtèl-Corvatsch. Data recorded 22nd April 2005 (temperature profile at Juvvasshøe below 100 m depth recorded manually 1st October 2000). The upper 15–20 m of the boreholes are influenced by the annual temperature fluctuations.

and ~1100 m respectively below the ground surface altitudes of the two boreholes. To obtain undisturbed vertical heat flow values, the boreholes should probably be at least 5 to 10 times deeper (Isaksen et al., 2007a).

In the Alps, the temperature profiles are highly disturbed by topography (Gruber et al., 2004c). The position of the Stockhorn borehole on the Stockhorn plateau has a major influence on its temperatures and temperature gradients at depth. This effect was demonstrated by Gruber et al. (2004c) in a simple model experiment showing the coexistence of both positive (temperature increasing with depth) and negative near-surface geothermal gradients in adjacent vertical profiles, even under steady state conditions. At Schilthorn, permafrost temperatures are close to 0 °C. Analyses of data series indicate that the permafrost temperature is influenced by latent heat effects and convective heat transfer by water. In combination with topographical effects this makes the interpretation of transient signals contained in the temperature profile on Schilthorn an extremely complex problem (Gruber et al., 2004c).

The three boreholes in Svalbard and Scandinavia are located on plateaux or ridges with minor topographic relief within a radius of 100–200 m, smooth ground surfaces, and uniform snow conditions. This ensures little disturbance from small-scale 3-dimensional thermal effects in the upper parts of the boreholes (Isaksen et al., 2007a), as opposed to possible effects of the larger scale relief at greater depths. All three boreholes show a significant warm-side deviation in their thermal profiles to 70 m depth (Fig. 7), that is most likely associated with surface warming during the last few decades, with the greatest change occurring in the northernmost borehole in Svalbard (cf. Harris et al., 2003b; Isaksen et al., 2001). Upward extrapolation to the surface of the temperature gradient between 30–20 m depths indicates surface temperature changes with a magnitude of ~1.4 °C, ~1.1 °C and ~1.0 °C for Janssonhaugen, Tarfalaryggen and Juvvasshøe respectively (Isaksen et al., 2007a). There is no evidence that the observed anomalies in the upper part of the thermal profiles reflect factors other than past changes in ground surface temperatures. In addition, the similarity of the two thermal profiles from Tarfalaryggen and Juvvasshøe suggest a general common effect, that is, a warming of the upper permafrost surface.

3.5. Recent trends in permafrost temperatures

On Murtèl–Corvatsch, temperatures have been measured since 1987 in the 58 m deep borehole. Between 1987 and 1994, the uppermost 25 m warmed rapidly (Vonder Mühll and Haeberli, 1990; Vonder Mühll et al., 1998). At 11.6 m below the surface, the temperature rose by approximately 1.0 °C during this period (Fig. 8). Mean annual surface temperature is estimated to have increased from −3.3 °C (1988) to −2.3 °C (1994), and probably exceeded previous maximum temperatures during the 20th century (Hoelzle et al., 2002). During the following two years (1994–1996), winter snowfall was low, resulting in intense cooling of the ground and permafrost temperatures returning to values similar to those in 1987 (Fig. 8). Since 1996, interannual variations in permafrost temperatures have increased slightly. In 2000/2001 snow came very early and in some places reached maximum values in early winter. During winter 2001/2002 a new period of intense cooling occurred due to exceptionally late snow fall. Since 2002 temperatures have been rising. Overall, permafrost warming during the 18 years of observations at Murtèl–Corvatsch was about 0.5 °C at 11.6 m (Fig. 8) and 0.3 °C at 21.6 m (Fig. 9). At 21.6 m the temperature in 2005 was −1.3 °C, the highest since readings began. Winter snow thickness, coupled with its date of arrival and disappearance, clearly plays a critical role in interannual ground temperature fluctuations.

On Stockhorn and Schilthorn, the episode of intensive cooling found in the Murtèl–Corvatsch series during winter 2001/2002 is also clearly visible at 13.3 m and 13.0 m depth respectively (Fig. 8), but data
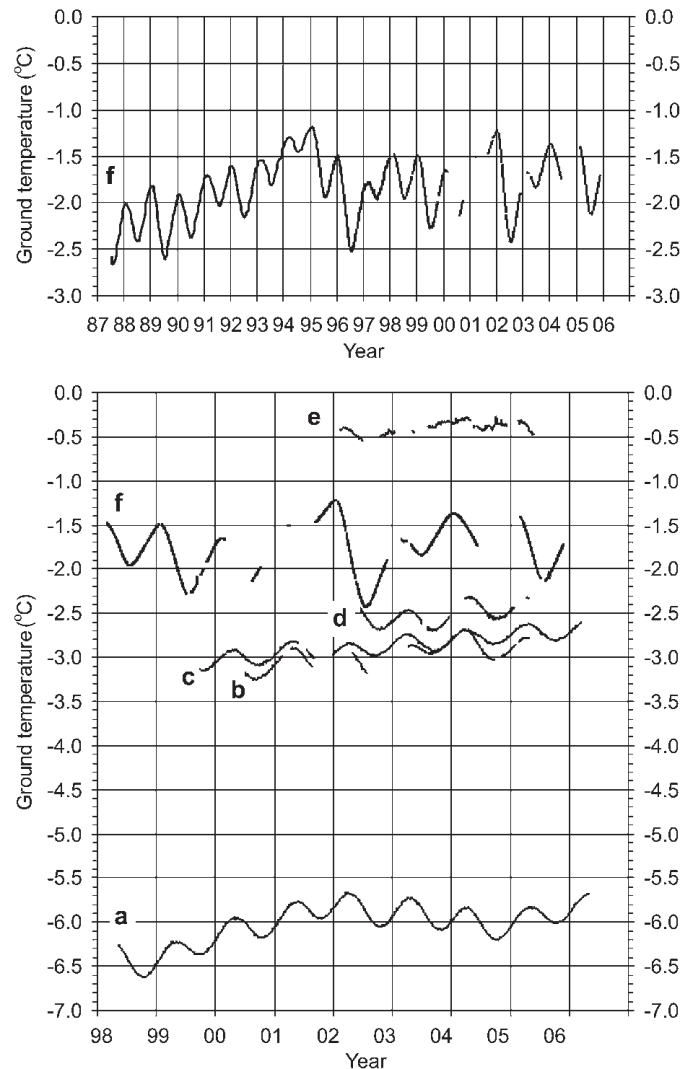

Fig. 8. Observed ground temperatures at the depth where seasonal fluctuations are less than, 0.5 °C. (a) Janssonhaugen (13.0 m), (b) Tarfalaryggen (13.0 m), (c) Juvvasshøe (13.0 m), (d) Stockhorn (13.3 m), (e) Schilthorn (13.0 m) and (f) Murtèl–Corvatsch (11.6 m). At Schilthorn data were smoothed and filtered due to some errors in the data logger and periods of refreezing of meltwater in the bedrock.

series are too short to draw conclusions on longer term temperature changes. It is concluded that interpretation of ground temperature series from the Alps must take account of the complex relationship between the ground surface and atmospheric temperatures, particularly the strong modulating affect of snow conditions (see below; Harris et al., 2003a,b). The significance of the interaction between snow cover and ground surface/subsurface characteristics in influencing ground surface temperature offsets from air temperature has been emphasised by Hoelzle and Gruber (2008) using data from the Murtèl–Corvatsch and Schilthorn borehole sites. At the Nordic sites of Janssonhaugen, Tarfalaryggen and Juvvasshøe, wind action maintains relatively snow-free conditions in winter, and the relationship between air-, ground surface- and ground temperatures is much stronger, resulting in a climate signal that penetrates the permafrost with no large perturbations caused by changing near-surface and surface conditions (Isaksen et al., 2007b).

Continuous ground temperature monitoring just below the depth of zero annual amplitude over periods from five to seven years on Janssonhaugen, Tarfalaryggen and Juvvasshøe show that the ground temperature has increased by 0.36 °C, 0.27 °C and 0.24 °C respectively at 20 m depth (Fig. 9). Observed warming is statistically significant to
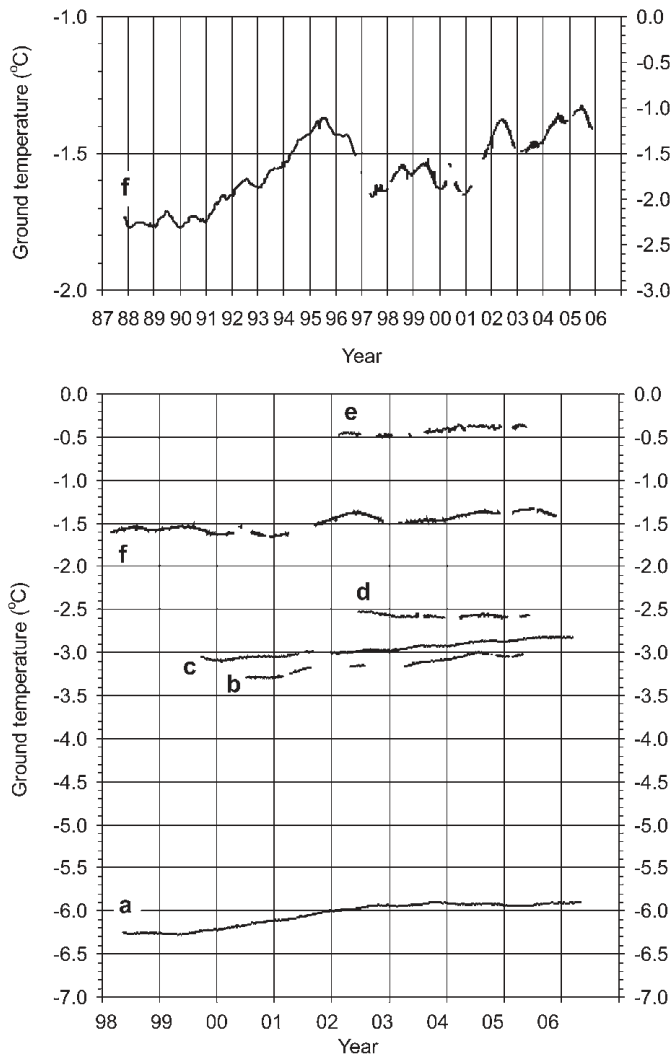
Fig. 9. Observed ground temperatures at the depth where annual amplitude is less than 0.1 °C, that is just below the approximate depth of zero annual amplitude. (a) Janssonhaugen (20.0 m), (b) Tarfalaryggen (20.0 m), (c) Juvvasshøe (20.0 m), (d) Stockhorn (23.3 m), (e) Schilthorn (20.0 m) and (f) Murtèl–Corvatsch (21.6 m). At Schilthorn data were smoothed and filtered due to some errors in data logger and periods of refreezing of meltwater in the bedrock.

If the thermal responses observed within the PACE mountain borehole network are indicative of longer term trends, major changes in permafrost distribution may be anticipated through the 21st Century. It is also clear that on a seasonal time scale, extreme summer temperatures may lead to large increases in bedrock active layer depths, and are likely to increase the scale and frequency of mountain slope instability (see Section 8.2). The PACE boreholes provide a regional framework for monitoring European mountain permafrost geothermal responses to climate change, and additional networks of shallow (up to 20 m) boreholes in both the Alps and the Nordic countries (e.g. Vonder Mühll et al., 2004; Sollid et al., 2003; Ødegård et al., 2008) provide more detailed information on local variability.

Of particular importance in this respect are three permafrost monitoring boreholes installed in central and northeastern Iceland in 2004 (Farbrot et al., 2007; Etzelmüller et al., 2007, 2008), at altitudes of between 890–930 m a.s.l. (Fig. 11). All are shallow (12–22 m deep), and penetrate thin sediment into basaltic bedrock. Observed permafrost temperatures below the depth of seasonal temperature fluctuation were between −1 °C and 0 °C, and at the Snæfell and Gagnheiði boreholes, permafrost thickness was estimated to be 30–35 m, with active layers around 2 m and 4 m respectively. At Hágöngur, permafrost was thin, temperatures were close to zero and the active layer was around 6 m deep. Meteorological data indicate that mean annual ground surface temperatures for the past few years in Iceland have been 0.5–1 °C higher than those for the 1961–90 period (Etzelmüller et al., 2007). At the Gagnheiði and Snæfell boreholes, temperature profiles show warm-side deviation from steady state, suggesting recent rises in the upper boundary temperature (Fabrot et al., 2007).

One-dimensional thermal modelling suggests that increases in mean daily surface air temperatures of (a) 0.01 °C a^{-1} and (b) 0.03 °C a^{-1} would cause permafrost to disappear in 160 and 100 years respectively at Snæfell, and 125 and 75 years respectively at Gagnheiði (Farbrot et al., 2007; Etzelmüller et al., 2008). Higher ice contents explain the slower response at Snæfell than at Gagnheiði. The influence of snow cover on the ground thermal regime at these sites was quantified by Etzelmüller et al. (2008), by damping the winter air temperatures by a nival factor

60 m depth at all three Nordic sites (Isaksen et al., 2007a). This strongly supports previous interpretation by Isaksen et al. (2001) and Harris et al. (2003b) that most of the anomalies observed in the geothermal profiles (cf. Fig. 7) are associated with surface warming.

In all boreholes the temperature signal below a depth of 20 m is free of any response to annual or shorter-term temperature variations. At these depths, any recorded systematic temperature time variations must correspond to a longer period of several years and it is possible to calculate the actual rate of temperature change as a function of depth (Fig. 10). Below 50–60 m depth, longer time-series than those currently available are required to identify thermal trends. Calculated warming rates over the past several decades based on the recorded temperature trends at a depth of between 40 and 50 m correspond with present decadal warming rates at the permafrost table, in the order of 0.04–0.07 °C yr^{-1}, the highest rates being on Janssonhaugen and Tarfalaryggen (Isaksen et al., 2007a). Higher rates of permafrost warming are reported in northern Alaska, rates tending to increase with increasing latitude (Osterkamp, 2008) while observed permafrost warming rates over the past 30 years in Siberia are somewhat lower (Romanovsky et al. 2008).

Fig. 10. Observed present-day temperature change as a function of depth below the depth of annual amplitude. Time series generally start one year or more after establishment of the boreholes to minimise influence from borehole drilling. In addition, analyses of the data series are based on whole years (3–7 years) to reduce any systematic errors in the dataloggers and measurements. Data periods are at Janssonhaugen 26.04.1999–25.04.2006, Tarfalaryggen 20.04.2001–19.04.2005, Juvvasshøe 26.02.2000–25.02.2006, Stockhorn 15.06.2002–31.05.2005 and Schilthorn 20.05.2002–19.05.2005.
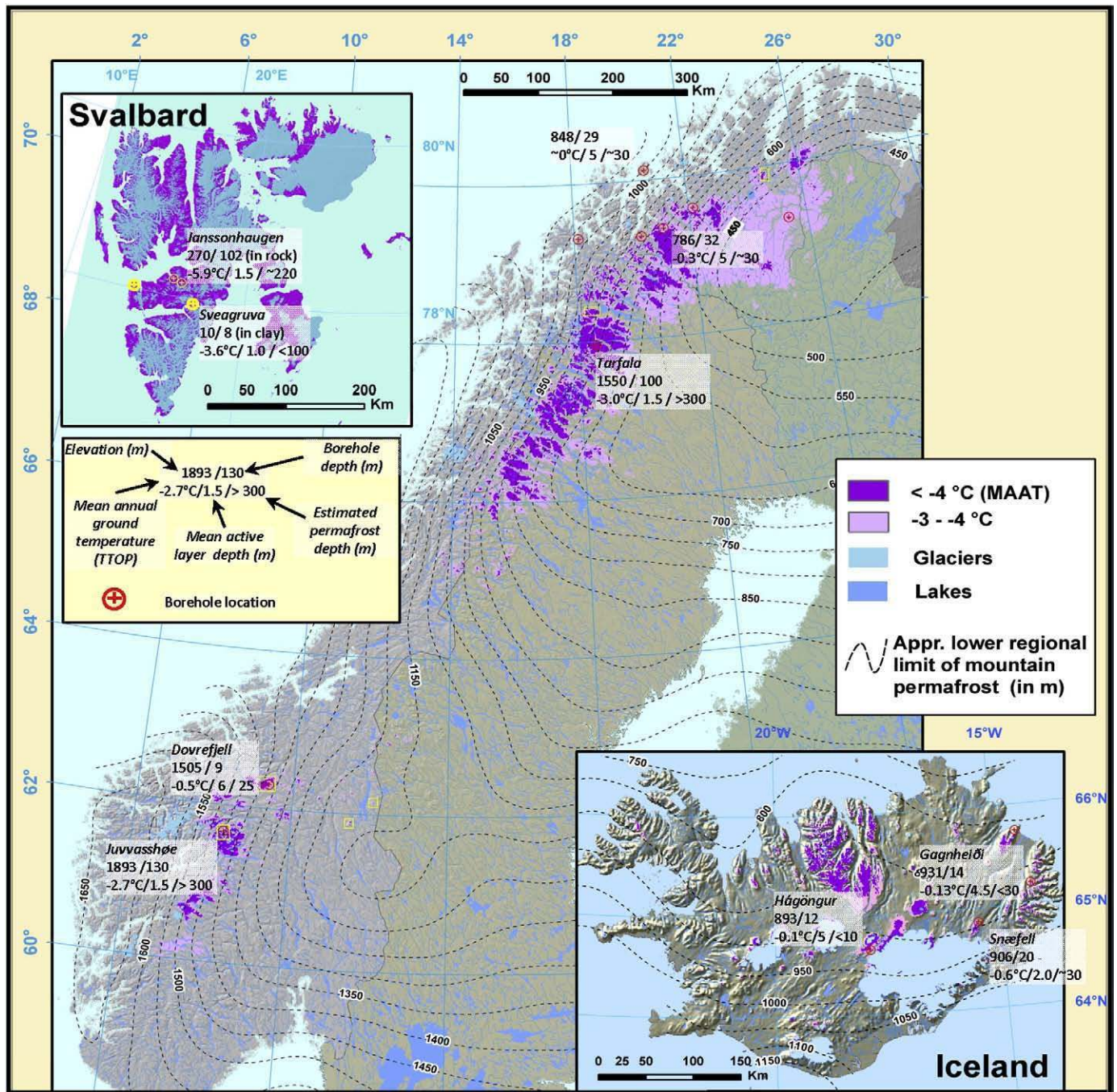
Fig. 11. Permafrost map of the Nordic countries. The approach selected here is based on a relation between gridded air temperature data and permafrost existence not considering snow and topographic heterogeneity. The dashed contour lines indicate the regional lower limit of discontinuous mountain permafrost. Existing shallow boreholes in Scandinavia are shown, including key thermal parameters and average active layer thickness. On most sites, several boreholes are drilled in different topographic positions and with varying depths. The map is compiled at the University of Oslo (UiO), Norway, based on data provided by UiO, met.no, UNIS and NGU.

(between 0 and 1), following equilibrium modelling approaches (see Riseborough et al., 2008). The study indicated critical snow cover thresholds, where permafrost is stable, aggrading or degrading for different snow cover scenarios. Modelled temperature evolution since 1955 suggested that the present-day permafrost thicknesses reflect cooling in the late 1960s/early 1970s. This rapid permafrost thermal response is in part a reflection of the shallowness of the permafrost layer, but also the influence of high geothermal heat fluxes that at Snæfell are around 150 mW m^2, approximately five times the values at the Scandinavian PACE borehole sites (cf. Isaksen et al., 2001).

4. Modelling mountain permafrost thermal condition and spatial distribution

4.1. Modelling approaches

Unlike the other cryospheric phenomena such as glaciers or sea ice, permafrost is a largely invisible phenomenon. Therefore, modelling based on thorough process understanding is the best method for estimating permafrost spatial distribution patterns in the past, present and future. In recent years, several attempts have been made to

develop and improve spatial modelling of mountain permafrost distribution (Etzelmüller et al., 2001a; Hoelzle et al., 2005). Appropriate models are useful to a wide range of permafrost-related environmental issues, including the evaluation of climate-change scenarios, large- and local-scale mapping, surface process studies, and environmental concerns such as natural hazards and ground engineering.

Modelling capability for mountain areas has progressively improved over the past decade, not least as a result of the EU-funded PACE-project (Harris et al 2001a, Riseborough et al., 2008). The selection of a particular methodology often depends on the objectives, the scale and the application for which the models are developed. On a more local-scale, process-oriented numerical approaches and sensitivity studies with respect to process interactions and feedbacks within the mountain permafrost system have received more attention, focusing on the interface between atmosphere and ground surface as well as within the uppermost layers of the ground. On a larger regional scale, empirical–statistical models have been developed and applied. For mountain areas in Europe in general, the preferred modelling methodology is now changing from more stochastic and empirical to more numerical approaches.

In this section, we review the currently available typology of models at various levels of sophistication and spatio-temporal scales, and we present new data and results relating to permafrost modelling in mountainous regions.

4.2. Spatial and temporal scales of permafrost distribution modelling

A simplified conceptual distinction between the influence of 'Climate', 'Topography' and 'Ground Condition' can be made on the basis of scale (Gruber, 2005). Latitude plus large-scale atmospheric/ oceanic circulation patterns mainly determines weather and climate patterns on a global and continental scale. At a regional to local scale (areas covering several square kilometres) topography strongly overprints weather and climate. Terrain geometry controls air temperature by elevation, orographic precipitation, and solar radiation via the insolation angle and shading. Locally, surface and subsurface properties further influence the translation of the "climatic" signal into ground temperatures. Factors such as snow cover, air or water movement and ground surface characteristics influence different (often non-conductive) thermal processes that have an important overall influence on the total energy and mass exchange of the system. Thus, many process models are applicable only at regional to local scales in which complex models are able to simulate transient 3D-temperature fields with some restrictions (see below). A major problem exists in bridging continental and local scales, and this is particularly important for the application of climate scenarios when the outputs from Regional Climate Models (RCMs) have to be downscaled to meet the needs of local scale permafrost models.

The coarse resolution of certain models is in most cases appropriate for overview maps and long-term predictive models. However, many applied and scientific applications are concerned with the identification of more local distribution patterns of forms, processes and potential slope instability (Harris et al., 2001a), demanding refined models with higher resolutions. Such models need an increasing number of input parameters and better calibration but are essential for a better process understanding and for transient extrapolations into the future within complex three-dimensional mountain topography.

As permafrost is a thermal system with slow response to climate forcing, the present state of permafrost is in part a function of former climatic conditions and present day climate changes will in turn affect the future thermal state of permafrost. The response time of permafrost depends mainly on the thermal conductivity, the ice content and the thickness of the frozen ground. Empirical models neglect important feedback mechanisms such as atmosphere/snow/permafrost-interactions and do not take into consideration transient conditions at depth. Even in relatively warm and thin discontinuous mountain permafrost, propagation of a warming trend through the entire permafrost thickness is typically measured in decades to centuries. PACE-borehole thermal data support the contention that alpine permafrost thickness and its distribution in marginal areas most probably still reflect maximum Holocene cooling during the Little Ice Age that culminated in the 19th century (see Section 2).

4.3. Recent developments

Today, mountain permafrost distribution models combine stochastic with deterministic elements and include two main types; regionally calibrated empirical-statistical models, and more physically based numerical models (Etzelmüller et al., 2001a,b, Hoelzle et al., 2001, Riseborough et al., 2008). Several model approaches calculate the main energy exchange processes in one dimension (Goodrich, 1978; Stähli et al., 1996; Zhang et al., 2001; Riseborough, 2002; Gruber et al., 2004b; Farbrot et al., 2007; Etzelmüller et al., 2008). More recently, attempts have been made to apply equlibrium models such as the TTOP-approach (Riseburough, 2002) in European mountain environments (Juliussen and Humlum, 2007; Etzelmüller et al., 2008). Both transient and the equilibrium approaches have been applied, though only at specific locations; spatial modelling remains a future task.

Empirical-statistical distributed permafrost models directly relate documented permafrost occurrences to topoclimatic factors (altitude, slope and aspect, mean air temperature, solar radiation), that can easily be measured or computed (Jorgenson and Kreig, 1988; Hoelzle and Haeberli, 1995; Hoelzle, 1996; Imhof, 1996; King and Kalisch, 1998; Li et al., 1998; Etzelmüller et al., 2001b; Kneisel et al., 2000a; Gruber and Hoelzle, 2001; Lugon and Delaloye, 2001; Tanarro et al., 2001; Duchesne et al., 2003; Mustafa et al., 2003; Wright et al., 2003; Heggem et al., 2005; Nyenhuis et al., 2005). In some studies this model type is also used for paleo-reconstructions and simulating future scenarios (Frauenfelder and Kääb, 2000; Lambiel and Reynard, 2001; Frauenfelder et al., 2001; Janke, 2005). In these models, the energy and mass exchange processes at the surface and within the active layer are not treated explicitly. Therefore, these models can be seen as a grey box with topoclimatic factors being selected according to their relative influence in the total energy balance exchange. This simplification results in advantages and disadvantages: empirical–statistical permafrost distribution models are easily applied, need only limited input parameters and are quite reliable if well calibrated locally or regionally. They are, however, yes/no-functions about the presence or absence of permafrost, primarily applicable to certain areas. They assume steady-state conditions and neglect the influence of the complex heat fluxes within the three dimensional topography. Extrapolations in time and space may lead to uncertain or even misleading results.

Process-oriented models focus on more detailed understanding of the energy fluxes between the atmosphere and the permafrost (Romanovsky et al., 1997; Wegmann et al., 1998; Kukkonen and Safanda, 2001; Marchenko, 2001; Riseborough, 2002; Stocker-Mittaz et al., 2002; Isaksen et al., 2003; Kasymskaya et al., 2003; Oelke and Zhang, 2003; Gruber et al., 2004b; Ling and Zhang, 2004). They explicitly parameterise solar radiation, turbulent heat fluxes, surface albedo, heat conduction, etc., are often complex and need a correspondingly large amount of precisely measured or computed data. Such approaches allow for spatio-temporal extrapolation and are especially well suited for sensitivity studies with respect to interactions and feedbacks involved with climate-change scenarios (Salzmann et al., 2007a,b). They enable surface temperatures to be computed and, hence, thermal conditions at depth and transient effects in complex topography to be estimated (Noetzli et al., 2007).

However, the proper investigation of uncertainties is an important element of the application of this type of model.

4.4. Regional-scale modelling

Regional-scale modelling operates on a ground resolution of 100 m or more, depending on the heterogeneity and size of the area modelled. Such regional models aim to give a first indication of permafrost distribution, with limited accuracy demands, identifying the areas of permafrost abundance. A simple climate-permafrost model based on the relationahip between gridded Mean Annual Air Temperature (1961–90, MAAT) values (Tveito et al., 2001) to permafrost existence has been used to generate a permafrost map of the Nordic countries (Fig. 11). However, the approach does not consider snow conditions and topographic heterogeneity. A MAAT map was generated by reducing air temperatures at official climate stations to sea level, interpolating between the stations, and subsequently estimating the air temperatures for real elevations using a constant lapse rate. For studies in southern Norway it has been shown that an annual air temperature of −3 to −4 °C is a good estimate for the regional limit of the lower mountain permafrost boundary (e.g. King, 1986; Ødegård et al., 1996; Etzelmüller et al., 2003). For Iceland, a value of −3 °C was derived, based on ground surface temperature (GST) measurements in different sites in northern and eastern Iceland (Etzelmüller et al., 2007). This approach is justified by the fact that most areas of permafrost in the Nordic countries have more gentle topography than the Alps (Etzelmüller et al., 2003), where large topographic effects strongly influence permafrost distribution.

Predicted permafrost distribution was compared with observations in different regions, including southern Norway (Heggem et al., 2005; Isaksen et al., 2002), northern Norway (Farbrot et al., 2008; Isaksen et al., 2008) and Iceland (Etzelmüller et al., 2007; Farbrot et al., 2007). All validation indicated that the general permafrost pattern is well reproduced and shows a decrease in the lower permafrost limit from west to east in Scandinavia though local variations are not represented. In Iceland, the predicted southwards increase in altitude of the permafrost limit is due to more maritime and snow-rich conditions in Southeastern Iceland. In Scandinavia, mountain permafrost distribution clearly exceeds the glacier coverage, while in Iceland it seems to be in the same order of magnitude.

A regional map of potential permafrost distribution at a scale of 1:50,000 for the Swiss Alps has recently been published by the Swiss Federal Office for the Environment (Map realization: Geotest, GEO7, Academia Engiadina). The map is based on two different approaches. The empirical model uses as input the digital elevation model of the Federal Office of Topography (DHM25, swisstopo). The potential permafrost calculation distinguishes three different high alpine ground surface characteristics with a) coarse debris, b) bedrock and c) glaciers and water (see Fig. 12). For the calculation, a permafrost index was generated based on the topographic parameters. For all calculations of permafrost distribution in non-bedrock and non-glaciated areas, the well-known 'rules of thumb' developed by (Haeberli, 1975) and implemented in a GIS by (Keller, 1992) were used. For bedrock, an index was developed, based on energy balance models and on field validations (Gruber et al., 2003a,b, 2004b). For glaciers and water surfaces no calculations were performed. This index approach to estimate permafrost distribution is only very approximate, and the resulting map contains considerable uncertainties relating to the influence of topography on a variety of heat transfer mechanisms.

4.5. Local-scale modelling

During the PACE project, a distributed energy balance model was developed with the aim of investigating and simulating the interactions between the ground, the snow cover and the atmosphere (Mittaz et al., 2002; Stocker-Mittaz et al.; 2002; Gruber, 2005). Progress has been made in modelling the major energy fluxes, but there remain many challanges. Firstly, the model is still not able to produce a sufficiently accurate estimation of snow cover and secondly, the coupling between atmosphere and ground where ground cover comprises coarse debris (non-conductive heat transfer) is not satisfactorily included. Therefore, as a first approach, more simple systems have been selected for detailed process modelling to avoid complex
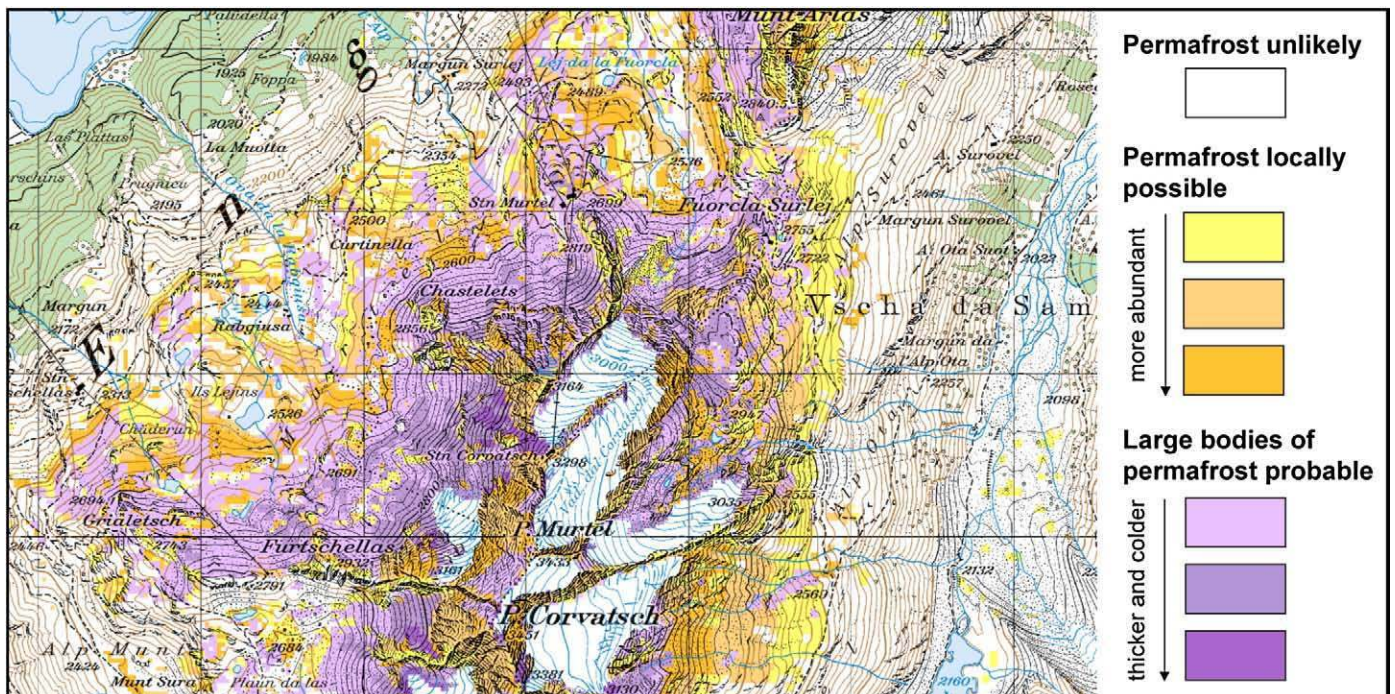

Fig. 12. Potential permafrost distribution as shown by the new Swiss Permafrost Map 1:50,000 (subsection of map sheet "Julierpass") published by the Swiss Federal Office for the Environment (FOEN) and realized by Geotest, GEO7 and Academia Engiadina.

interactions with snow cover or complex materials such as coarse debris. Steep alpine rock walls represent such a system and allow more straightforward modelling with better estimation of uncertainties. The model was validated by several rock temperature loggers placed in steep rock walls at different altitudes with different aspects (Gruber et al., 2003a,b, 2004a,b).

In many areas with limited coverage of meteorological stations, statistical–empirical modelling is still in use. Most common is the bottom temperature of snow (BTS) method (Haeberli, 1973), where field data are related to topo-climatic factors, establishing a statistical relationship between BTS temperatures and these factors (Hoelzle & Haeberli 1995; Hoelzle 1996). Recently, more sophisticated statistical methods such as logistic regression have been utilised, simulating permafrost probability in a region (Brenning et al., 2005; Lewkowicz and Ednie, 2004; Heggem et al., 2005; Lewkowicz and Bonnaventure, 2008). The most important topo-climatic factors are the altitude and potential incoming radiation, while the potential topographic wetness in a region also seems to play a significant role (Heggem et al., 2005). These models do not explain the heat transfer processes, but result in an easily obtainable map of permafrost occurrence and distribution in a region, and thus have an applied value.

Multi-criteria approaches within a GIS framework have been applied to generate maps of "permafrost favourability" in regions where meteorological data is restricted. Here, scores are derived for single factors (elevation, topographic wetness, potential solar radiation, vegetation) based on simple logistic regression or basic process understanding, and the sum of the derived probabilities is used as a measure of permafrost favourability in a given location within the framework of a multi criteria analysis (Etzelmüller et al., 2006; Fig. 13). The index maps are in this case the map layers representing the spatially distributed attributes that are found to contribute to the favourability (f) of permafrost existence, ranging between 0 and 1. The f-values obtained were statistically related both to measured ground surface temperatures and ground resistivities obtained by DC electrical resistivity. The approach is well suited for both local and regional surveys of permafrost distribution, but less applicable for studies of the impact of climate change.

In general, DEM-derived topographic parameters coupled with satellite-image derived information offers the potential for more accurate permafrost distribution modelling in remote areas (e.g. Etzelmüller et al., 2001a,b). For instance, Heggem et al. (2006) estimated the spatial distribution of annual Ground Surface Temperature (GST) based on measured GST in different landscape categories defined by a classification of topographic parameters (elevation, potential solar radiation, wetness index) and satellite-image derived factors (forest and grass cover). A sine-function was adapted to the
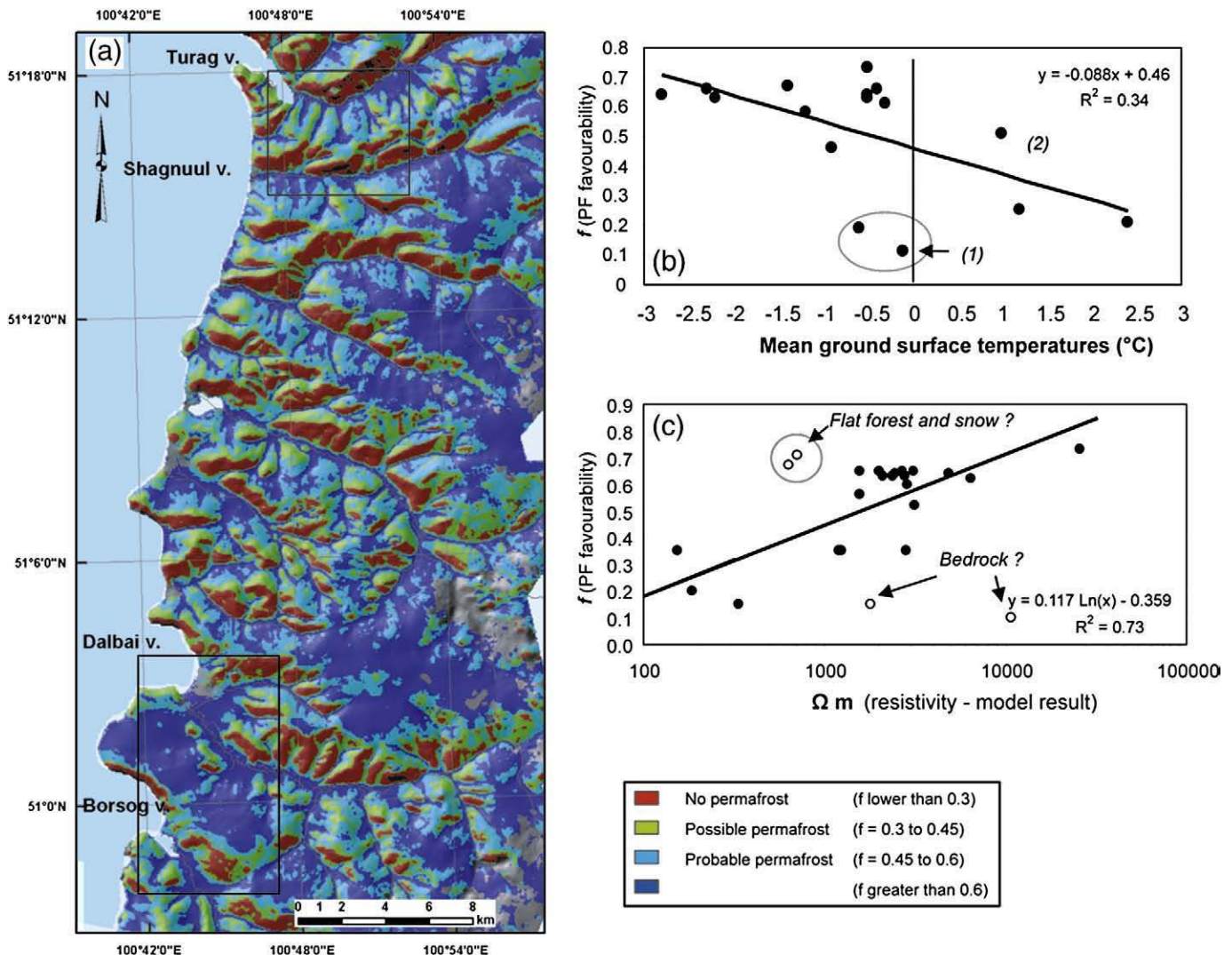

Fig. 13. Permafrost favourability mapping based on multi-criteria approaches within a GIS framework. (a) Permafrost favourability map (reproduced after Etzelmüller et al., 2006). (b) Plot of ground surface temperature against permafrost favourability. (c) Plot of modelled resistivity at 8 m depth vs. permafrost favourability. The regression equation was developed without including the marked outliers (from Etzelmüller et al., 2006).
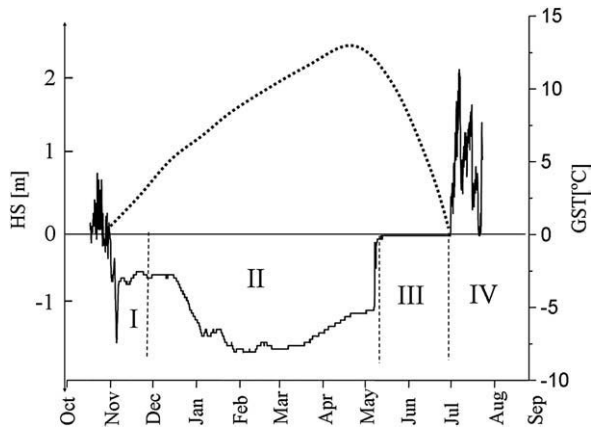
Fig. 14. The interaction between seasonal snow cover (i.e. snow depth (HS), dotted line) and ground surface temperature (GST, solid line) can be divided into four stages reflecting different thermal effect of the snow cover: I) the ground cooling non-insulating early snow cover, II) the ground warming, insulating snow cover in winter III) the snow-melt season in spring and IV) the snow-free stage in summer.

measured GST curves, parameterised with the temperature amplitude and mean annual temperature. This allowed the simulation of the GST field for changing temperature or snow cover (amplitude).

4.6. The significance of snow

The importance of snow cover arises largely from its low thermal conductivity (depending on density and microstructure (Fierz and Lehning, 2001; Luetschg and Haeberli, 2005)), its high surface albedo, and the energy sink provided by latent heat demand during snowmelt (Mellor, 1977; Sturm et al., 1997; Zhang, 2005). Ground under a snow depth greater than 60–80 cm can be regarded as effectively thermally insulated from the atmosphere (Keller and Gubler, 1993; Hanson and Hoelzle, 2004). Typically, the role of snow cover changes through the year over four distinct time periods (Fig. 14) and the timing and duration of these periods can have a considerable influence on mean annual ground temperatures (Goodrich, 1982; Harris and Corte, 1992; Keller, 1994; Seppälä, 1994; Luetschg et al., 2004). In autumn and early winter, an absence of snow or the presence of a thin cover, allows conduction of heat from the ground surface, and if thin snow is present, additional ground cooling arises from the high albedo of the snow surface. Increasing snow thickness then effectively insulates the ground surface from air temperature variation. During the spring thaw, melt-water percolation results in constant ground surface temperatures close to zero, this period lasting up to one or two weeks in the Arctic and Sub-Arctic (Zhang, 2005), but up to several months at the foot of steep avalanche slopes in mountain areas (e.g. Luetschg, 2005). Finally, during the summer snow-free season, ground surface temperatures reflect daily air temperature and radiation fluctuations.

Modelling approaches show differences in emphasis between arctic permafrost regions and mid-latitude mountains. In the Arctic, 1-D modelling generally includes complex hydrothermal processes associated with the freezing and thawing of a fine-grained and water rich active layer, but the thermal effect of seasonal snow cover is often simplified (e.g. Goodrich, 1982). Zhang and Stamnes (1998) and Zhang et al. (2001) using a one-dimensional heat flux model concluded that in high latitude permafrost, ground temperatures are most strongly affected by air temperatures, though soil moisture and the onset date of snow cover and the snow thickness were also shown to be critical for the persistence of marginal permafrost.

Corresponding modelling of mid-latitude mountain permafrost places greater emphasis on the complexities of seasonal snow cover, but generally treats the substrate as a less humid, coarse-grained non-frost susceptible soil in which conductive heat fluxes dominate. An

example is a three-year simulation of the ground temperature evolution of a 16 m thick dry, coarse blocky ground layer (Luetschg, 2005). Simulations utilised the SNOWPACK model (Lehning et al., 1999; Bartelt and Lehning, 2002), which allows significant temporal changes in snow properties to be included, and was extended to incorporate underlying soil layers (Luetschg et al., 2003). The snow and soil are simulated respectively as three-component (air, water and ice) and four-component (air, water, ice and soil grains) materials (Fierz and Lehning, 2001; Lehning et al., 2002a,b). Mass and energy transport and phase change processes are treated in the same way in the snow and soil layers. For gravitational water transport, a bucket water transport algorithm is applied that for some soil layers is a crude approximation (Lehning et al., 2002a). The four stages in the role of snow cover with respect to ground thermal conditions outlined earlier are clearly indicated (Fig. 15). More recently, the model has been developed into a distributed model system to simulate Alpine surface processes in general, including snow redistribution by wind, terrain influences on the surface energy balance, snow-soil-vegetation interactions and runoff (Lehning et al., 2006, 2008).

4.7. Validation

Validation of permafrost modelling against measured data must be an integral part of the model development process. As permafrost is thermally defined, the most secure validation data are derived from boreholes instrumented to measure ground temperatures. The PACE borehole network provided initial European data sets, but since then numerous additional borehole networks have been established. Measurements of the bottom temperature of the winter snow cover (BTS) combined with selected ground temperature loggers, are suitable for validation purposes for broader areas, e.g. for validation of regional empirical or energy balance models. Geophysical methods, such as DC resistivity tomography and seismic soundings are especially useful for detection of ice rich permafrost grounds in a local scale (see Section 6). Geoelectrical soundings have proved to be very useful, clearly mapping the transition zones between permafrost and no permafrost, allowing relationships to altitudinal or surface cover effects to be established (Hauck et al., 2004; Isaksen et al., 2002, Etzelmüller et al., 2006). On specific sites, where meteorological stations are available, other important variables, such as measured air
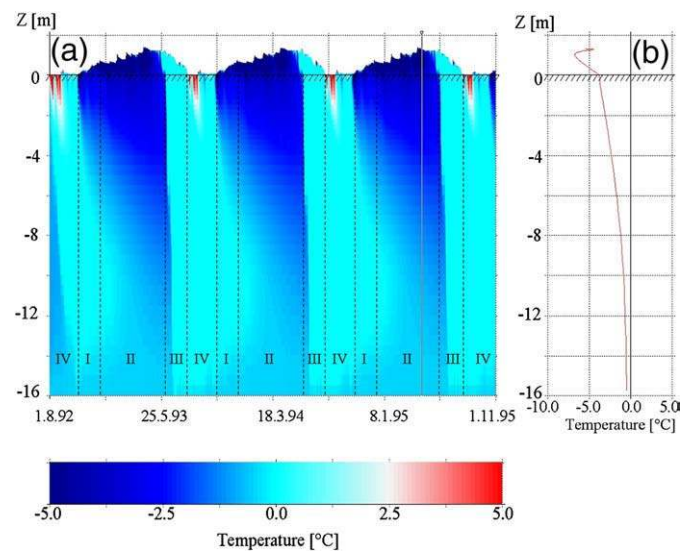

Fig. 15. (a) SNOWPACK three-year simulation run of the ground temperature evolution with time and depth for a 16 m thick dry, coarse blocky soil, including the influence of the seasonal snow cover. (b) Winter temperature profile through the soil and snow layers.
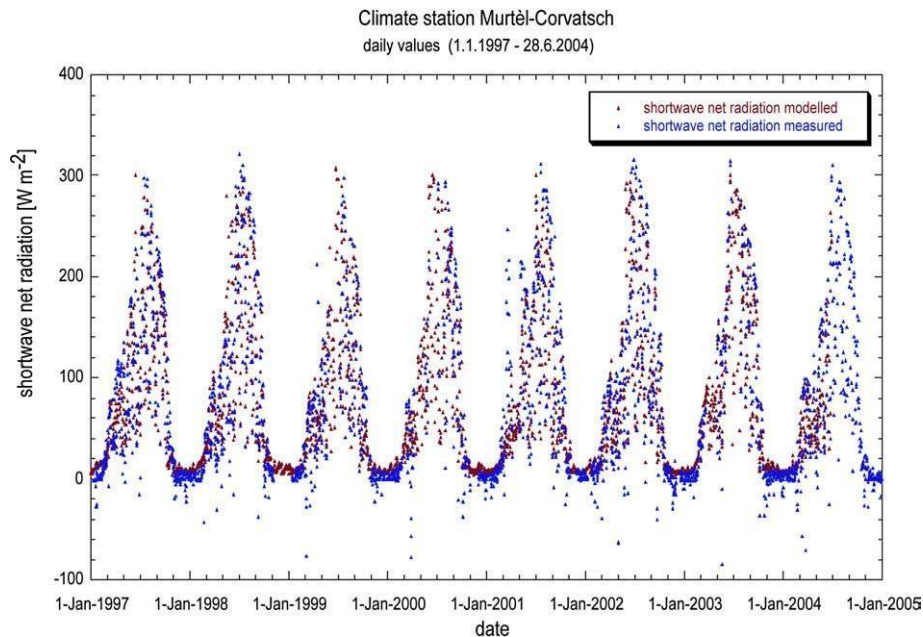
Fig. 16. Modelled and measured Shortwave net radiation in Wm^{-2} at the climate station Corvatsch–Murtèl, Upper Engadin, Switzerland.

or ground temperatures, thickness of snow cover, or radiation can be used as validation for the modelled variables (e.g. Fig. 16), especially when applying physical models.

4.8. Perspectives on mountain permafrost modelling

The main challenges for the development of more sophisticated and reliable permafrost distribution models can be summarised as follows. Firstly, there remains a need for field measurement and numerical modelling of processes within the main types of ground material such as bedrock, fine-grained debris and coarse, ice-rich debris. Several factors strongly influence the ground thermal regime in these materials and many of these are still poorly understood. Of particular importance is the influence of snow cover, and the need to model the spatial variability of snow thickness and duration. In addition, more accurate modelling of the role of ice within bedrock and fine and coarse debris, heat transfer by percolating water, and the effects of general local inhomogeneities is required. Secondly, validation of models should include the application of modern measurement technology using appropriate sensors. This requires collaborative research between a numbers of specialists. Thirdly, improved evaluation of uncertainties and uncertainty propagation within measurements and models is required. Fourthly, scaling issues between different models and between models and validation data need to be addressed, and finally, the modelling sequence Global Circulation Models–Regional Circulation Models–Energy Balance Models–Heat Transfer Models within three-dimensional topography should be further improved. The focus should be modelling transient effects, which requires coupling of time-dependent surface and subsurface ground thermal conditions. This is a prerequisite for realistic modelling of impacts of potential future climate-change scenarios in relation to possible permafrost degradation or aggradation.

5. Geophysical characterisation of frozen ground

One of the main problems in assessing future permafrost response to climate change is a lack of 3-dimensional information relating to subsurface composition, ice content and structure. Since a number of geophysical properties alter significantly when phase change of water occurs, surface based geophysical methods represent a cost-effective approach to permafrost mapping and characterisation, and when

repeated through time, monitoring of changing ground conditions. Measurements are largely non-invasive, making geophysical methods very suitable for monitoring purposes. An earlier review of geophysical and geomorphological methods of detecting and mapping mountain permafrost is provided by King et al. (1992). Scott et al. (1990) have discussed geophysical investigations in arctic regions and Vonder Mühll et al. (2001) and Hauck and Vonder Mühll (2003a) described mountain permafrost applications. Recent overviews of geophysical methods for the application in periglacial environments are provided in Hauck and Kneisel (2008) and Kneisel et al. (2008).

5.1. Geophysical properties

In permafrost studies, key properties of interest are temperature and ice content. Without a borehole, these properties cannot be observed directly, and borehole data may not be representative of a larger area of complex terrain. The detection and characterisation of permafrost from the surface depends on those characteristics that differentiate it from surrounding non-cryotic (temperature above zero) ground. These are mainly related to differences in physical properties of earth materials containing either frozen or unfrozen water. The degree of variation depends on water/ice content, pore size, pore water chemistry, ground temperature and pressure on the material (Scott et al., 1990). Three commonly used geophysical parameters for differentiating between frozen and unfrozen material are:

(a) electrical resistivity, which in moist porous rocks and soils increases markedly at the freezing point, and in fine-grained soils continues to increase exponentially until most of the pore water is frozen (e.g. King et al., 1988; McGinnis et al., 1973; Daniels et al., 1976; Pearson et al., 1983; Hauck, 2002);

(b) dielectric permittivity, which governs the propagation speed of georadar waves, also changes significantly between frozen and unfrozen material, with the and dielectric constant having values of 3–4 for ice, around 6 for frozen sediment, around 25 for unfrozen sediment and 80 for fresh water (Moorman et al., 2003); and

(c) seismic compressional- and shear-wave velocities that increase sharply on freezing in most moist porous materials, the increase being more pronounced as porosity increases (McGinnis et al., 1973).

The presence of saline pore waters leads to freezing point depression, and significantly affects all three of the above geophysical properties (Pandit and King, 1978). Geoelectrical approaches are sensitive even to small changes in unfrozen water at sub-zero temperatures, but seismic energy is transmitted primarily through the solid matrix, so once the pore volume is largely ice filled, further changes in unfrozen water content produce only negligible changes in velocity (Pearson et al., 1983). In permafrost terrain, the effects of topography, high electrical contact resistance and scattering of georadar by boulders may also cause difficulties. The use of capacitive-coupled resistivity systems (Timofeev et al., 1994; Hauck and Kneisel, 2006; de Pascale et al., 2008) or electromagnetic induction methods (e.g. Harada et al., 2000; Hauck et al., 2001; Bucki et al., 2004, Yoshikawa et al., 2006) have proved effective in overcoming problems of high contact resistance.

5.2. Resistivity surveys

Most geophysical case studies of mountain permafrost reported in the literature have involved applications of sounding methods that provide 1-D distributions of physical properties as functions of depth and/or lateral mapping methods that supply information on the horizontal variations of physical properties over a narrow depth range (e.g. Ikeda, 2006). Only recently have applications of 2-D imaging (tomographic inversion) techniques to mountain permafrost been published. These imaging techniques provide more reliable and more complete information than the sounding and lateral mapping methods by generating a 2-D ground model.

Electrical Resistivity Tomography (ERT) has been successfully applied to map and characterise different permafrost structures in mountain terrain (e.g. Kneisel et al., 2000b; Ishikawa et al., 2001; Vonder Mühll et al., 2001; Hauck and Vonder Mühll, 2003b; Marescot et al., 2003; Kneisel, 2004; Heggem et al., 2005; Krautblatter and Hauck 2007). In winter, however, it may be impossible to use ERT surveys as a dry snow cover acts as an electrical insulator. To overcome this problem, de Pascale et al. (2008) used a capacitative-coupled ERT system, the so-called OhmMapper instrument, that allows standard ERT measurements without the need for galvanic contact. For monitoring purposes, measurements are repeated at certain time intervals using a permanently installed electrode array. The fixed-
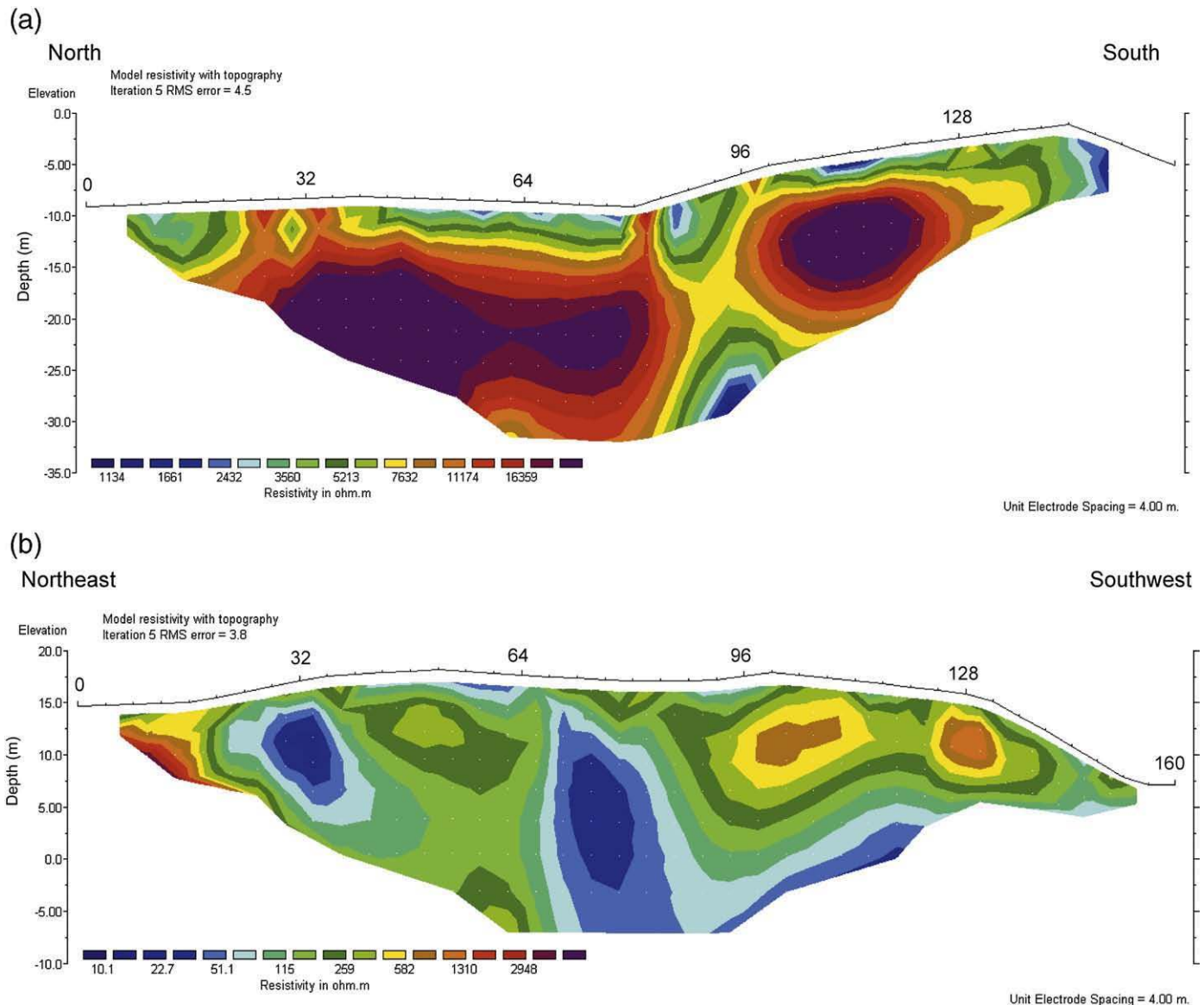

Fig. 17. Electrical resistivity tomograms through contrasting pingo types in Svalbard. (a) Innerhytte pingo, Adventdalen, above the marine limit. (b) Longyear pingo, Adventdalen, below the marine limit.

electrode array effectively filters resistivity variations due to variable electrode contacts or geological background variations, as mainly temporal resistivity changes are determined (Hauck, 2002; Hilbich et al., 2008a).

An example of the application of ERT surveys to investigate the nature and distribution of ground ice is provided by a recent study of the internal structure of open system pingos in Svalbard by Ross et al. (2007). At Innerhytte Pingo, located above the marine limit in Adventdalen, electrical resistivity tomography surveys identified a 3–4 m thick layer of relatively low to intermediate resistivity (1500–

6000 Ω m), and a zone of high resistivity (6000–30,000 Ω m) that extends to depths in excess of 20–25 m below the ground (Fig. 17a) and likely corresponds to a complex core of injection ice. These data are in accordance with resistivity values of pingo ice in Alaska (4500–18,000 Ω m) (Yoshikawa et al., 2006). In contrast, exceptionally low resistivity values (predominantly 10–400 Ω m, but up to 4000 Ω m) characterise the internal structure of Longyear Pingo (Fig. 17b), a younger and smaller open system pingo located below the marine limit in Adventdalen. This suggests that its core is dominated by segregation ice within a fine matrix of saline marine sediments.
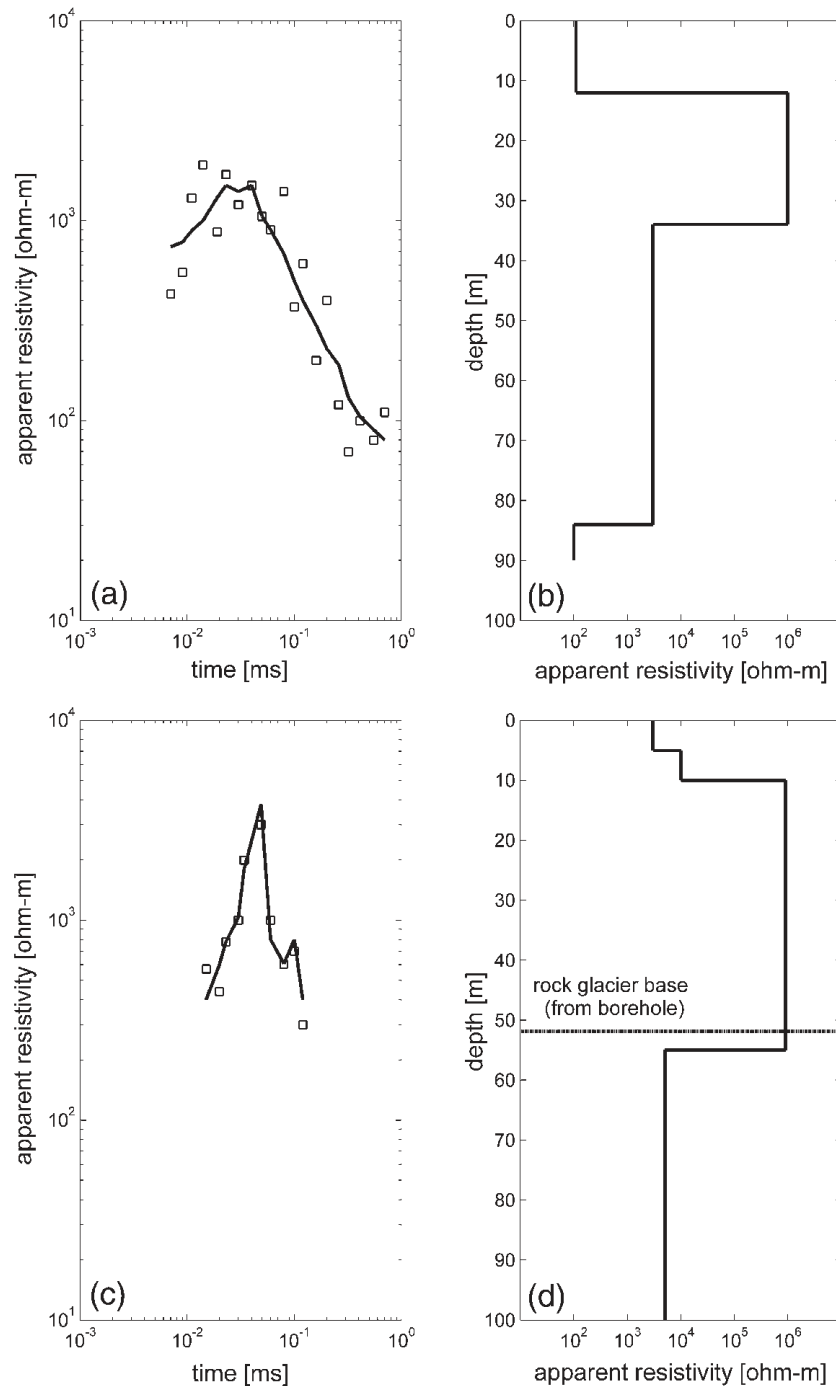

Fig. 18. Offset transient electromagnetic sounding data. (a) Measured (square symbols) and modelled (solid line) apparent resistivity values Muragl Rock Glacier, Swiss Alps. (b) Derived resistivity model, Muragl Rock Glacier, Swiss Alps. (c) Measured (square symbols) and modelled (solid line) apparent resistivity values Murtèl Rock Glacier, Swiss Alps. (d) Derived resistivity model, Murtè/Rock Glacier, Swiss Alps. Depth of rock glacier base is marked by the horizontal line. In both field sites the high-resistive zones correspond to massive ground ice in the rock glacier core.

5.3. Electromagnetic induction mapping

Electromagnetic (EM) induction techniques measure the electrical conductivity (1/resistivity). A wire loop carrying an electrical current produces a primary magnetic dipole field, and this dipole field is varied either by using an alternating current operating in the frequency-domain (FEM method) or by terminating it (transient methods operating in the time-domain (TEM)). This time-varying magnetic field induces very small eddy currents in the Earth. The eddy currents generate a secondary magnetic field, that may be sensed by a receiver loop at the surface. The more conductive the subsurface, the larger are the eddy currents and the larger is the measured secondary field, which in turn allows the ground conductivity to be determined by a simple proportional relation (McNeill, 1980). In the case of FEM, further data processing is required, and the lateral variability of the bulk conductivity of the uppermost subsurface layer is determined, but with no or limited depth information (e.g. Hauck et al., 2001; Cannone et al., 2003). However, EM induction sounding allows the determination of vertical conductivity variations, and commonly utilises transient electromagnetic systems (TEM), measuring the induced secondary magnetic field in the transmitter-off periods, when the primary magnetic is terminated. The response of the subsurface in terms of the decaying amplitude of the secondary magnetic field is measured as a function of time and therefore of depth.

To illustrate the effectiveness of this approach, results of a recent assessment of permafrost status in the rock glaciers Muragl and Murtèl, Swiss Alps (Musil et al., 2002; Maurer and Hauck, 2007) are presented in Fig. 18. Voltages measured during offset TEM sounding were transformed into apparent resistivities (Fig. 18a and c) and finally inverted to yield a specific resistivity model with depth (Fig. 18b and d). The results indicate an approximately 10 m thick unfrozen surface layer ($\rho < 1$ KΩm), which is slightly overestimated by the TEM, and a 20 m (Muragl) and 40 m (Murtèl) thick frozen layer ($\rho > 500$ KΩm) above the assumed bedrock layer ($\rho < 10$ KΩm), which is in good agreement with complementary geophysical and borehole data (Maurer and Hauck, 2007).

5.4. Ground Penetrating Radar (GPR)

Ground Penetrating Radar (GPR) has been successfully used to study permafrost distribution and structure in the Arctic and Antarctica for many years (e.g. Arcone et al., 1998a,b; Moorman et al., 2003; Munroe et al., 2007; Dallimore and Davis, 1987). Attenuation is highest (and therefore penetration lowest) in low-resistive earth materials (usually having a high liquid water content, particularly where pore water is saline) and in fine-grained sediments (even when frozen), where penetration depths can be less than 1 m. GPR is therefore best suited to investigating the unfrozen active layer in summer, and ice-rich permafrost. GPR surveys in mountain permafrost can be more difficult due to the low signal-to-noise ratio that arises from complex reflections within blocky layers, and can mask the true layer horizons. For high-resolution investigations, antennae with dominant frequencies between 20 and 100 MHz have proved to be suitable (Lehmann and Green, 2000; Isaksen et al., 2000a; Berthling et al., 2000) and adequate coupling of the antennae to the ground is extremely important. Data processing can include amplitude scaling to enhance later arriving events, and frequency filtering in the time and space domains to remove system noise and improve the coherency of reflected signals (Gross et al., 2003). If reliable velocity information is available, migration may be used to convert the processed time sections to equivalent depth sections. To account for the effects of strong topographic relief, special purpose topographic migration algorithms may be applied (Lehmann and Green, 2000).

In an arctic setting, GPR survey has recently been applied to investigate the internal structure of the open system pingo known as Riverbed pingo, located above the marine limit in Adventdalen (Ross et al., 2005, 2007). Reflections 0–7.5 m below the ground surface dipping sub-parallel to the surface (Fig. 19) were interpreted on the basis of geological evidence (Yoshikawa, 1993) as interbedded units of ground-ice and frozen partially disaggregated shale bedrock. The lack of basal reflections and poor signal penetration suggest attenuation of
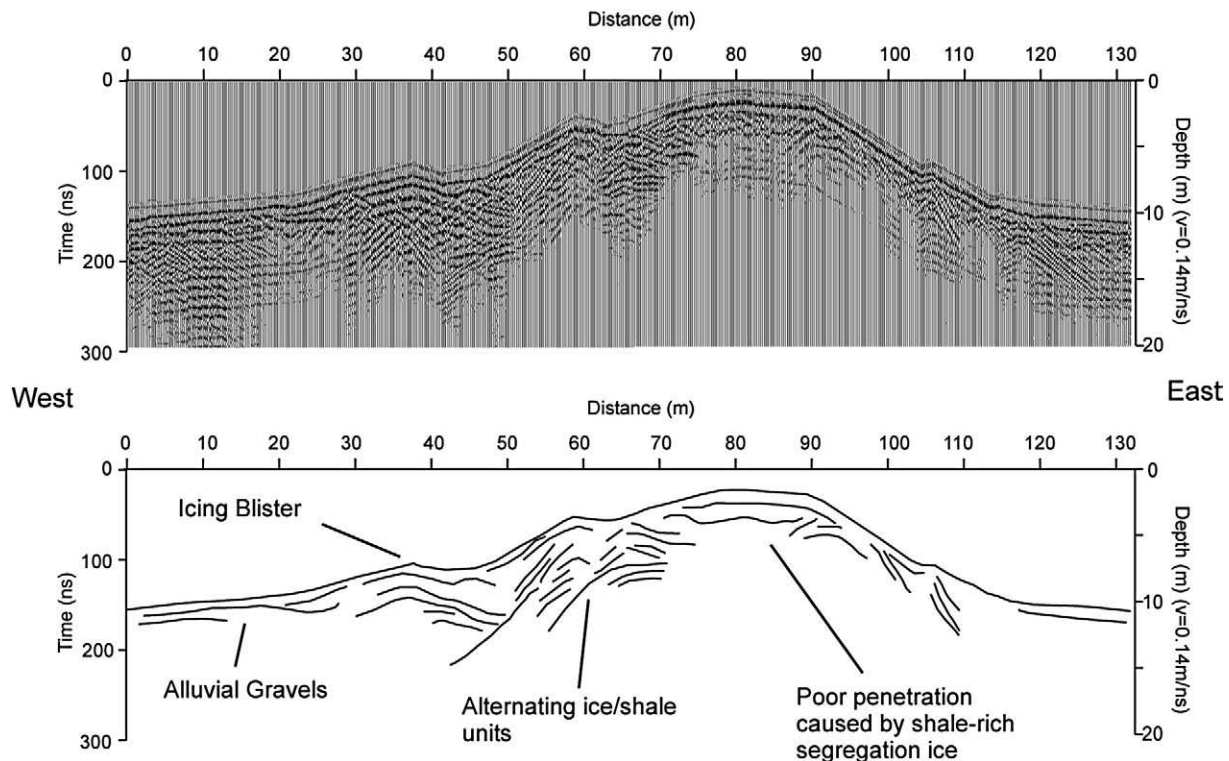

Fig. 19. Ground penetrating radar profile (100 Mhz), Riverbed pingo, Adventdalen, Svalbard.
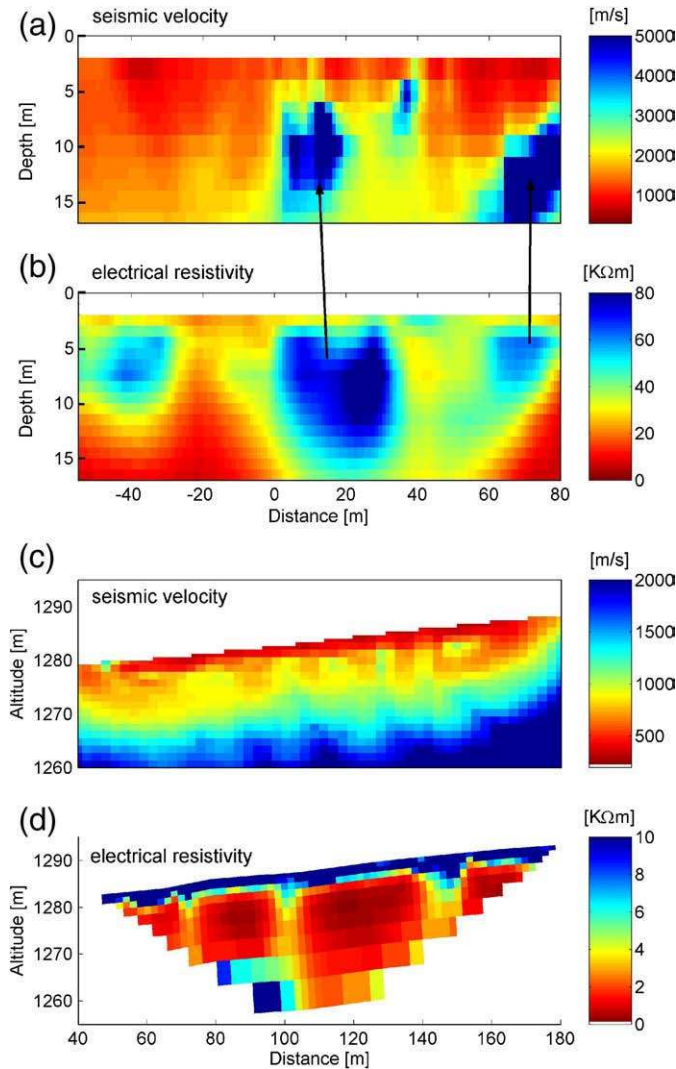
Fig. 20. Refraction seismic and DC resistivity inversion results for two field sites. (a) refraction seismics Val Bever, Switzerland. (b) DC resistivity Val Bever. (c) refraction seismics Juvvasshoe, Norway. (d) DC resistivity Juvvasshoe. The high-velocity anomalies (2500–4500 m/s, marked with the solid lines) in (a) indicate buried ice occurrences and the very low velocities (<500 m/s) in the uppermost 1–2 m in (c) indicate the presence of air-filled cavities (taken from Hauck and Vonder Mühll, 2003b).

the EM signal by the bedrock, and possibly a pingo core rich in segregation ice rather than massive intrusive ice.

5.5. Refraction seismic techniques

Refraction seismics has a long tradition in permafrost studies (e.g. Timur, 1968; Zimmerman and King, 1986; King et al., 1988; Ikeda, 2006). The P-wave velocity distribution can be used as a complementary indicator to resistivity for the presence of frozen material. The method is especially useful for differentiatiation between the presence of subsurface ice and air, and to determine the top of the permafrost layer, as the contrast for the P-wave velocity between the unfrozen top layer (= active layer, 400–1500 m/s) and the permafrost body (2000–4000 m/s) is usually large. For most permafrost applications using a sledgehammer as seismic source, depth penetration is slightly smaller than the corresponding penetration depth of resistivity surveys with similar horizontal survey lengths. Interpretation techniques are often based on layered models, but this may be of limited use for very heterogeneous ground conditions in mountainous environments. As with the ERT technique, tomographic inversion

schemes can be used for more reliable 2D interpretation (Musil et al., 2002; Hauck et al., 2004; Maurer and Hauck, 2007).

5.6. Crosshole methods

Conceptually, most geophysical techniques can also be applied by placing the sources in one borehole and receivers in another. Crosshole tomography provides detailed 2D information in the plane containing the two boreholes. The multiple illumination of subsurface targets provided by crosshole geometries results in more reliable and higher resolution than can be provided by most surface-based techniques. Ideally, the borehole separation should be about half the borehole depth. To date, crosshole methods have been used only where very detailed subsurface information is needed and boreholes are already present (e.g. Delisle et al., 2003; Musil et al., 2006) and since measurements are confined to the plane between the two boreholes, they are best combined with additional surface-based geophysical measurements (Maurer and Hauck, 2007).

5.7. Combined geophysical measurements

Since the environmental effects of permfrost degradation in a future changing climate depend largely on ground ice content, the similarity in resistivity between ice, air and certain rock types may present a problem in the interpretion of resistivity data. In such cases,
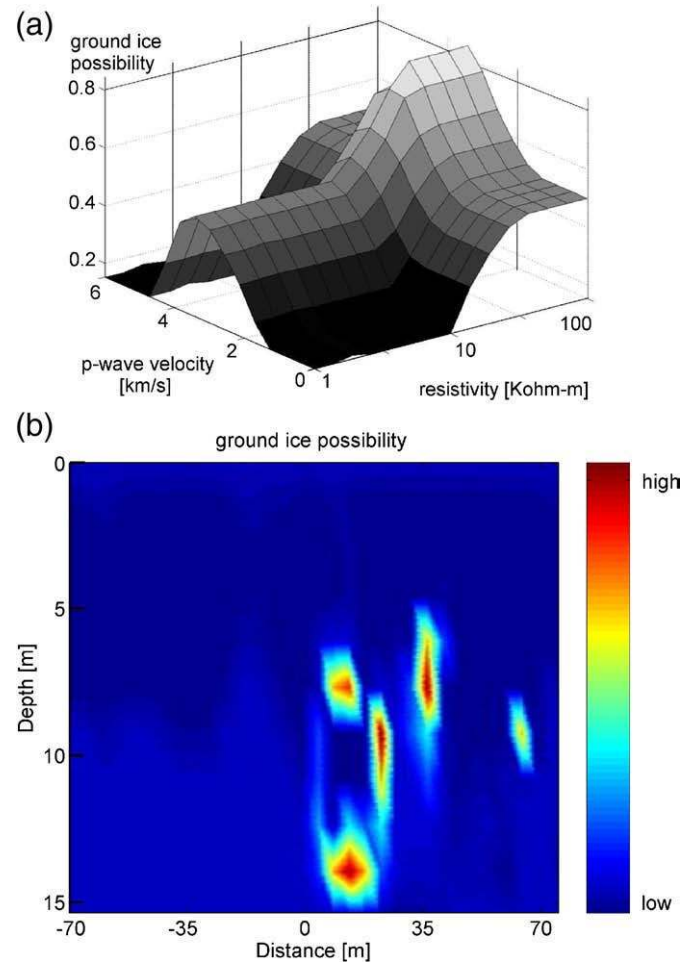

Fig. 21. (a) Decision surface for the fuzzy inference system for ground ice detection. Each value of seismic velocity (in km/s) and electrical resistivity (in Kohm-m)) is associated with a degree of possibility for ground ice (z-axis). (b) Degree of possibility for ground ice for an example from Val Bever, Switzerland (based on data in Fig. 20 (a) and (b)).

it is necessary to use more than one geophysical method to improve interpretation in terms of permafrost delineation, ice content or stratigraphy. Complementary methods include (a) refraction seismics and ERT (Fig. 20), since the former differentiates between ice and water and the latter between ice and air, and (b) ERT and GPR, since ERT identifies the presence or absence of ice, whilst structural information is provided by GPR (e.g. Hauck and Vonder Mühll, 2003b; Farbrot et al., 2005; Otto and Sass, 2006). Other combinations, such as ERT, FEM and seismics (Hauck et al., 2004), TEM, seismics and GPR (Bucki et al., 2004), ERT, seismics, GPR and TEM (Maurer and Hauck, 2007) or even ERT, GPR, seismics and three different EM methods (Yoshikawa et al., 2006) may also been applied.

Newer approaches combine information from several geophysical data sets in a quantitative way. Hauck and Wagner (2003) used a fuzzy-logic approach to delineate those regions where the occurrence of ground ice was most likely. The input data were derived from ERT and refraction seismic surveys, the output indicated the "degree of ice content" (but not the ice content itself), that is the possibility of ground-ice occurrence. The fuzzy inference system used is based on nine rules, all linking low, medium and high resistivity and velocity values to a corresponding output (low, medium and high ice content). A practical view of the rule system is shown as a decision surface showing the likelihood of ground ice at Val Bever in Switzerland (Fig. 21a), where each pair of velocity (Fig. 20a) and resistivity (Fig. 20b) data points is associated with a possibility of ground-ice occurrence (Fig. 21b).

Another possibility is the so-called 4-phase model (Hauck et al., 2005, 2008), which is based on two well-known geophysical mixing rules for electrical resistivity (Archie, 1942) and seismic P-wave velocity (Timur, 1968). Due to the presence of four phases within the frozen material (rock/soil matrix, unfrozen water, ice and air), the respective volumetric fractions of the phases in the subsurface cannot be quantified by using one method alone. Using the above mixing

rules and a combination of electric and seismic data sets, the respective volumetric fractions of each phase (e.g. the ice content) can be approximated.

5.8. Monitoring permafrost change

In principle, all the above methods can be used to monitor changes by repeated measurements using the same survey geometry. ERT is possibly the most effective for monitoring ice content, and GPR for active layer thickness. A fixed 30 electrode array along a 58 m survey line was permanently installed at Schilthorn in September 1999 (Hauck, 2002). Resistivity surveys were made by connecting a standard 4-channel resistivity meter to a manual switchbox for each of the selected electrode configurations. Since September 1999 monitoring has included daily, seasonal and annual time scale studies (Hauck, 2002; Schudel, 2003; Völksch, 2004; Scherler, 2006, Hilbich et al., 2008a; Noetzli et al., 2008) confirming the effectiveness of the approach. Fig. 22 shows an example from 1999–2004, where the annual variation of the resistivity in the uppermost 10 m was determined. Instead of analysing the resulting resistivity tomograms in terms of absolute values, the resistivity change based on the first September measurement in 1999 are shown. Whereas the annual resistivity changes at greater depths were in the order of 10% until 2002, the anomalously warm summer of 2003 in the Alps caused a resistivity decrease of more than 30%, indicating substantial melting of permafrost. This coincides with a deepening of the active layer from 5 m to 9 m, as measured in a nearby borehole (Hilbich et al., 2008a).

Monitoring programmes at permafrost sites considered particularly sensitive to warming, such as potential debris flow source areas with high ground ice contents, or sites with structures sensitive to ground settlement, may in future incorporate such geophysical monitoring, coupled with ground temperature measurements, as an effective method of obtaining early indications of changes in ice
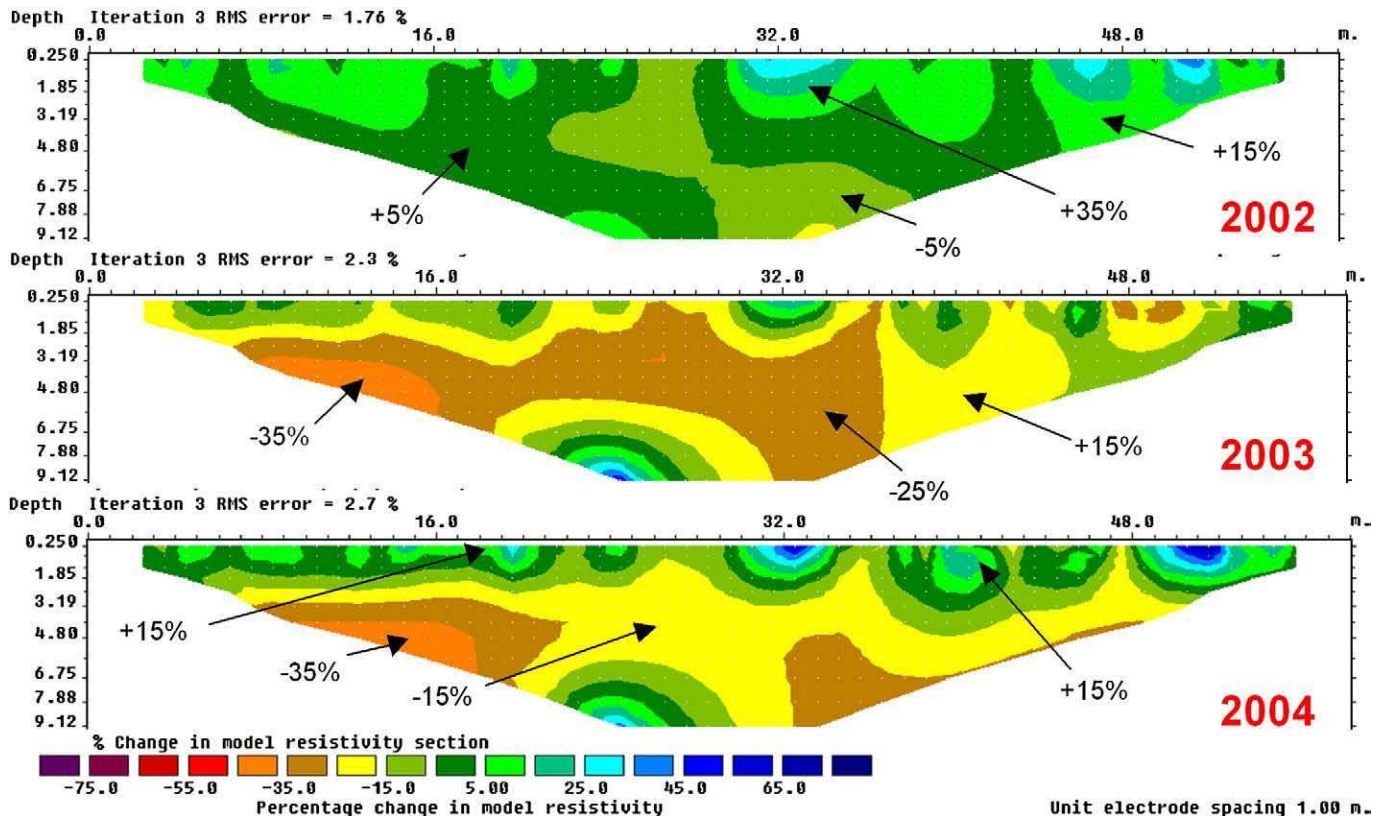

Fig. 22. Relative change in resistivity calculated for 3 ERT profiles in time-lapse mode for the years 2002–2004, each related to the baseline year 1999. Orange colours indicate regions with decreased resistivities due to thaw processes.

content or active-layer thickness. As a first step, long-term geophysical monitoring has now been included in the Swiss PERMOS network including the three PACE monitoring sites Murtél, Stockhorn and Schilthorn (Hilbich et al., 2008b; Noetzli et al., 2008).

6. Rock weathering

Climate-related changes in permafrost geothermal regime may lead to changes in the nature, intensity and the frequency of occurrence of many geomorphic processes. Changes in process intensity and type are associated with thawing (and sometimes simply warming) of permafrost and may lead to significant landscape response. Frequently such processes depend fundamentally on the nature and volume of ice formed during ground freezing and lost during ground thawing. Bedrock weathering in permafrost regions includes a number of physical and chemical processes, their nature and intensity varying both spatially and temporally according to environmental and geological conditions. Rock freezing and thawing may occur over a range of time scales, in the longer term as permafrost aggrades and degrades in response to climate change, seasonally as active layers

thaw and refreeze and seasonal frost penetrates then thaws, or over diurnal or shorter time scales, when frost is likely to penetrate into the near surface only (Fig. 23).

The change in phase of water from liquid to solid and vice versa within bedrock plays a critical role in reducing rock strength and eventually breaking the rock down (e.g. Rapp, 1960; Sass, 2005a; Stoffel et al., 2005). The 9% volumetric expansion accompanying phase change has traditionally been considered the main causal mechanism of frost weathering, though recently the role of ice segregation within certain bedrock lithologies has been recognised as potentially of greater significance. The main difference between the two is that the former arises from *in situ* freezing of water, while the latter involves water migration within freezing or frozen ground. Volumetric expansion occurs at the freezing point of the water ooccupying pores or cracks and requires a high saturation level (>90%) of the rock. In contrast, ice segregation can occur in unsaturated rocks. The presence of capillary and adsorbed water with a freezing point below 0 °C allows unfrozen pore water to migrate through partially frozen rock to supply progressive growth of ice lenses. The resulting rock fracture can occur at temperatures considerably below 0 °C (e.g. Walder and
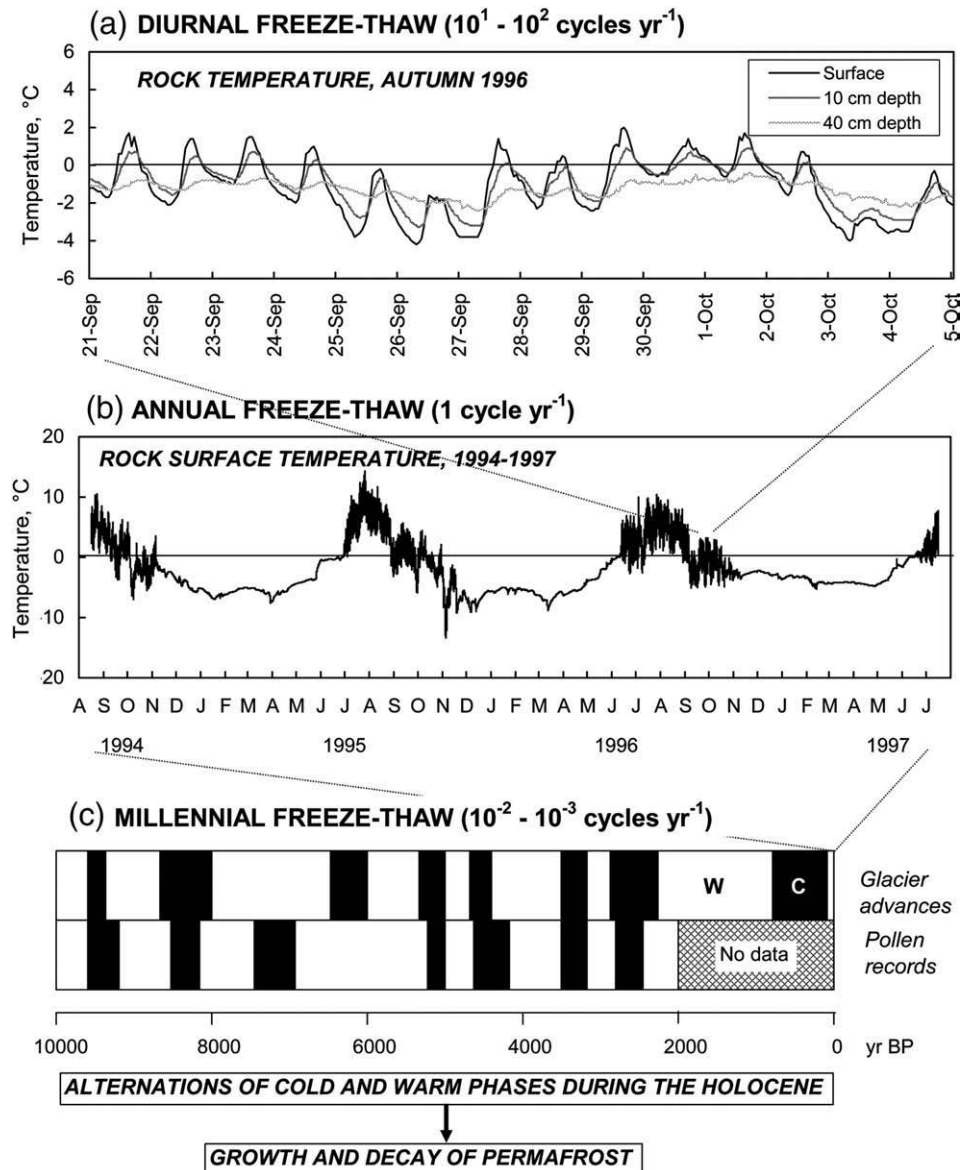

Fig. 23. Diurnal, annual and millennial freeze-thaw cycles in the Alps. A and B are based on data from Murtèl-Corvatsch Southern Swiss Alps. C is compiled and simplified from Gamper (1993) and Burga (1993).
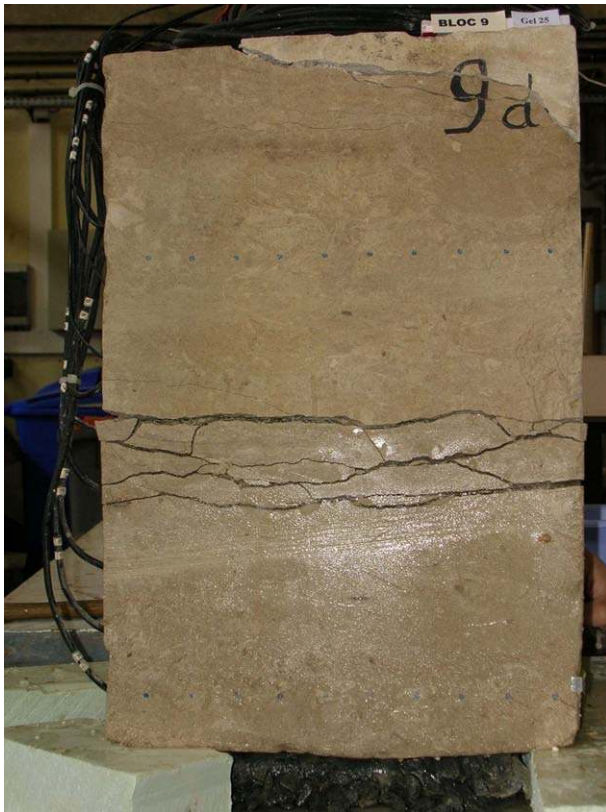
Fig. 24. Fractures formed by ice segregation in near-surface permafrost and the base of the active layer in moist chalk. The fractures are filled with segregated ice. The block of chalk is 450 mm high and 300 mm wide, and at the start of the experiment was unweathered and lacked visible fractures. The upper half of the block was subjected to 24 cycles of active-layer freezing and thawing, while the lower half remained as permafrost. The mean active-layer depth was 240 mm (SD±36 mm).

Hallet, 1985; Akagawa and Fukuda, 1991; Hallet et al., 1991; Murton et al., 2001), depending partly on the pore structure (e.g. Matsuoka, 2001a). Recent summaries of weathering processes, rates and products in cold regions are given by Hall et al. (2002), Murton et al. (2006) and Matsuoka and Murton (2008).

6.1. Ice segregation in frozen bedrock: laboratory and field evidence

In frost-susceptible soils, migration of water downwards from the active layer to the underlying permafrost leads to ice segregation and formation of an ice-rich zone, directly beneath the active layer, that thaws only during infrequent extreme summer events (Cheng, 1983; Schur, 1988; Shur et al., 2005). Field observations of fine-grained porous bedrock in the Arctic reveal a similar layer of ice-rich, fractured rock within the upper few metres of permafrost. Büdel (1982) observed an ice-rich layer, which he termed the "ice rind", within a variety of sedimentary rocks (e.g. Triassic marly limestones, shales and arkoses) in the continuous permafrost zone of southwest Barents Island, Svalbard. Büdel attributed the ice rind to thermal contraction cracking and infilling of fractures with hoar frost. Subsequent Canadian observations from Melville Island (French et al., 1986), Ellesmere Island (Hodgson et al., 1991) and the Western Arctic Coast (Mackay, 1999) indicate a similar layer in the upper layer of permafrost within Mesozoic sedimentary rocks. In these cases, the ice was interpreted as segregated ice.

It has been unclear until recently if ice can fracture intact bedrock subject to natural freezing regimes, or whether it simply enlarges existing fractures or does both. This question is important, because if ice segregation in bedrock permafrost is widespread, then there may be considerable potential for significantly increased rock slope

instability associated with rising ground temperatures and thickening active layers in a period of climate warming. Laboratory modelling has now begun to elucidate the process of ice segregation in bedrock.

If freezing processes in porous rock are fundamentally the same as those in frost-susceptible soils (Walder and Hallet, 1986), then ice lenses will concentrate in wet rock just beneath the top of the permafrost and in the base of the active layer, leading to pervasive fracturing at these depths. To test this hypothesis, an experimental methodology was developed and systematic experiments were carried out to simulate a bedrock active layer above permafrost that in winter freezes from the ground surface downwards and from the permafrost table upwards (Murton et al., 2000, 2001, 2006). The experiments clearly demonstrated that ice segregation fractures the upper layer of permafrost and the base of the active layer in moist chalk (a porous limestone). At the beginning of the experiments the chalk was unweathered and lacked visible fractures. But after repeated cycles of active-layer freezing and thawing, fractures filled with segregated ice had formed in the uppermost permafrost and in the lower part of the active layer.

Fig. 24 shows an example of an experimental block 450 mm high in which net heave of the rock surface was almost 13 mm over the course of 24 seasonal cycles. The dominant fractures are more or less horizontal, which is expected because the isotherms were parallel to the permafrost table. The permafrost table determines the depth of ice segregation. Heave data indicate that ice segregation and fracture occur not only during upward freezing (early winter) of the active layer but also during the late stages of thaw cycles (late summer) as water migrates down below the base of the active layer and into the underlying permafrost) (Fig. 25), as occurs in summer in Arctic permafrost soils (Mackay, 1983). In summary, the experiments showed that moist, porous rock behaves remarkably like moist, frost-susceptible soil, with both substrates experiencing ice enrichment and fracture/fissuring of near-surface permafrost. It appears that significant concentrations of segregated ice are most likely in the transition zone between the active layer and the permafrost, as a result of downward migration of water in summer and upward advance of freezing at the beginning of the winter (Murton et al., 2001, 2006; Sass, 2005b).

Laboratory modelling discussed above indicates clearly that given adequate water supply, ice segregation produces a zone of ice-bonded fractured bedrock immediately below the permafrost table. In general,
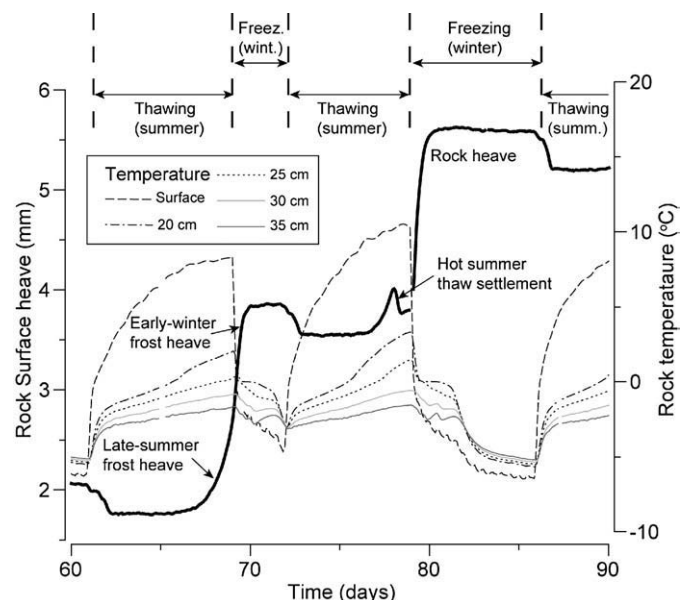

Fig. 25. Temperatures and frost heave during laboratory simulation of three annual cycles of active layer freezing and thawing in chalk bedrock.
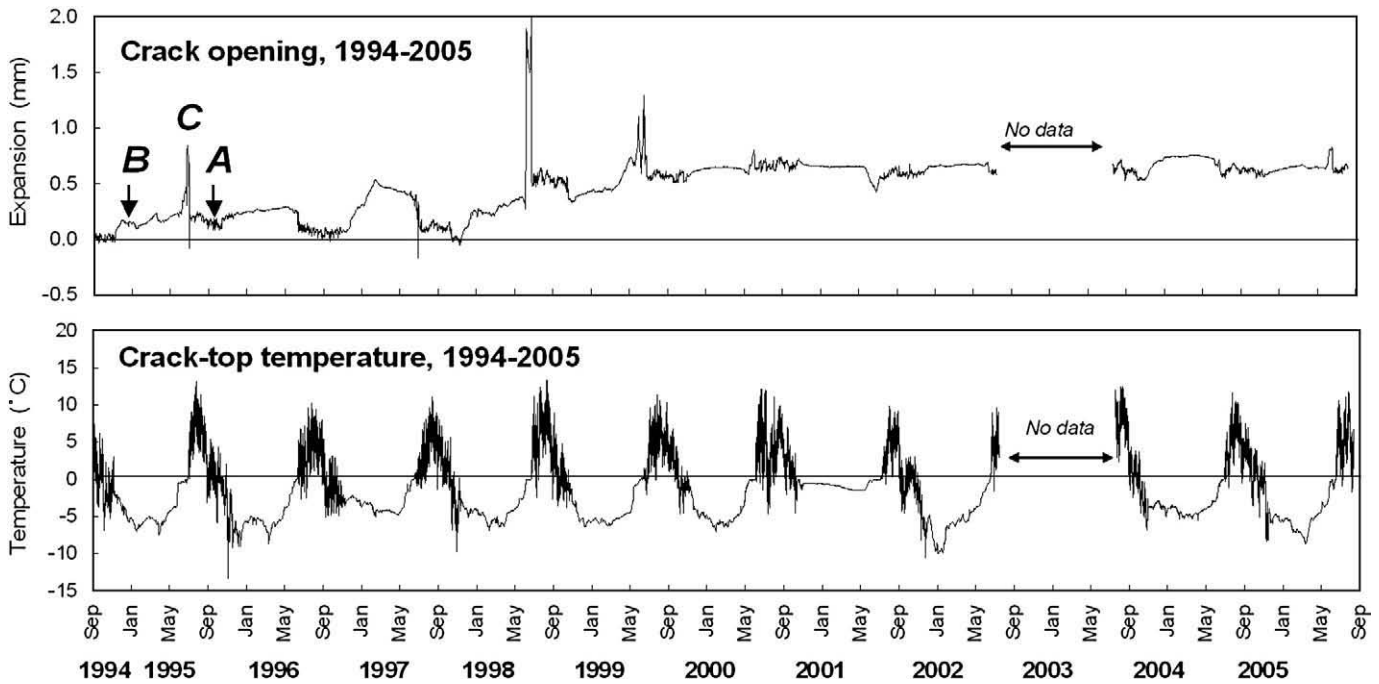
Fig. 26. Monitoring frost wedging at MW site (Murtèl–Corvatsch). Three types of movements (Types A–C) are identified. Note significant permanent opening from 1997 to 1999.

the importance of ice segregation relative to in-situ volume expansion increases with decreasing thermal gradients and increasing duration of freezing (Powers and Helmuth, 1953; Walder and Hallet, 1985). Rempel and co-workers (2004) suggest that the maximum possible disjointing pressure is governed by the temperature depression below the bulk-melting point, even in the absence of large temperature gradients, and therefore slow ice segregation in bedrock may be possible at greater depths where the frozen permeability of rock limits the actual amount of heave produced. Thus, over long timescales, ice segregation may be highly significant in frozen steep bedrock slopes where the presence of ice-rich fractured bedrock may be critically important in releasing rock falls and rock slides during climate-induced warming and permafrost degradation (see Section 7 of this paper).

6.2. Temporal scales of frost weathering

A high frequency of frost cycles is likely to be most effective within the outermost decimetre of bedrock, leading to the spalling off of relatively small (up to pebble size) rock fragments (Matsuoka, 1994) though lack of moisture may considerably reduce the number of effective freeze-thaw cycles (e.g. Prick, 2003). Seasonal freezing progresses much more slowly – over a period of a few months – but penetrates deeper into the bedrock. The annual freezing and thawing depth varies with the surface freezing or thawing index, thermal conductivity and moisture content of the rock, but may reach several metres (Matsuoka, 1994; Wegmann and Gudmundsson, 1999; Gruber et al., 2004a).

The roles of diurnal and annual freeze-thaw cycles in rock weathering have recently been evaluated through long-term field measurements of near-surface rock temperatures and rock joint widening at rockwalls near the altitudinal boundary between the permafrost zone and seasonal frost zone in the Engadine, Swiss Alps (Matsuoka et al., 1997, 1998, 2003; Matsuoka, 2008). Here three types of rock joint widening were distinguished (Fig. 26): repetitive and frequent opening and closing of the order of 10^{-2} mm during diurnal freeze-thaw cycles in autumn and in early summer (type A); widening of 0.1–0.5 mm that accompanied seasonal freezing in early winter (type B); and finally, widening (often exceeding 0.5 mm) at the onset of seasonal thawing, probably resulting from refreezing of snow melt

entering the rock joint at a subfreezing temperature (type C). At Murtèl–Corvatsch, these events resulted in permanent widening of the joint at a rate of 0.06 mm a^{-1} over 11 years (1994–2005), with most change associated with significant type C events.

The rate of surficial rock weathering resulting from diurnal freezing and thawing may be significantly affected by climate changes through an increase or decrease in cycle frequency, or through modification of ground surface insulation arising from changes in vegetation or snow-cover. An increase in mean annual air temperature is also likely to deepen the active layer by thawing of the uppermost part of the permafrost, and hence increase the potential thickness of rock fall material.

7. Rockfalls and rockslides

7.1. Field monitoring of annual debris production from rock walls

In the Swiss Alps, production of pebble-sized (and smaller) rock debris has been observed annually by collecting recently fallen rock
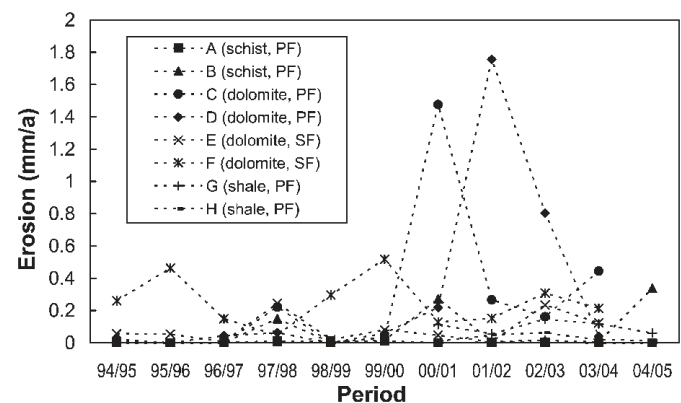

Fig. 27. Inter-annual variations in the annual rockwall retreat computed from the volume of rock debris released from painted quadrangles. PF: Bedrock underlain by permafrost. SF: Bedrock subjected to seasonal frost.

fragments released from painted quadrangles 50 cm × 50 cm wide at sites in the Engadine, (Matsuoka et al., 2003; Matsuoka, 2008). For each quadrangle, the total volume of fragments was converted to the annual rockwall erosion. The observed rockwall erosion rates were about 0.1 mm a^{-1} on average, although this was increased by sporadic occurrences of extreme rates (1.5–1.8 mm a^{-1}) (Fig. 27). The interannual variability of the debris production rate is likely to depend mainly on the freeze-thaw cycle frequency, snow-cover and moisture availability (Sass, 2005a,b).

Average rockwall retreat rates calculated on the basis of these measurements were much lower than the long-term rates estimated from the volume and age of talus rock glaciers in the Alps (e.g. 1–2 mm a^{-1}: Haeberli et al., 2001). This indicates that falls of pebble-sized and smaller rock fragments only account for up to 10% of the long-term rockwall retreat. In other words, seasonal or episodic larger scale boulder falls govern the long-term evolution of these alpine rockwalls. One such boulder fall, equivalent to about 100 m^3 in total volume (or around 2.5 mm of rockwall retreat), was recorded at Murtèl–Corvatsch in mid June 1997 (Matsuoka, 2008). Rockfalls comprising large boulders tend to occur in summer in response to progressive seasonal thaw penetration and/or refreezing of meltwater (e.g. Rapp, 1960; Matsuoka and Sakai, 1999; Stoffel et al., 2005). An increase in scale and frequency of such rockfall events would, therefore, contribute to a significant increase in the overall rate of rockwall retreat (see below).

7.2. The role of permafrost in the initiation of rockfall events

Atmospheric and ground temperatures are strongly coupled on steep mountain bedrock slopes due to the absence of an insulating interface of snow, vegetation and soil material. Climatically-driven permafrost degradation can lead to increased instability leading to a serious increase in hazard and risk (c.f. Varnes 1984 for definitions of hazard and risk). A large number of rock fall events that most likely originated in permafrost areas have been inventoried for the Alps (Deline, 2002; Noetzli et al., 2003). In glacial environments in particular, rock falls have the potential to trigger down-slope cascades of hazardous events (Huggel et al., 2004) with especially long runout distances (Evans and Clague, 1988; Noetzli et al., 2006). An example that illustrates the potential scale of such events was the rock/ice avalanche of 2002 at Kolka/Karmadon (Haeberli et al., 2004; Huggel et al., 2005) that travelled 19 km down a sparsely populated valley in the Russian Caucasus and claimed the lives of 140 (see Section 12).

Research into relationships between permafrost and the stability of Alpine rock faces was initiated in the 1990s (Haeberli et al., 1997; Wegmann, 1998; Wegmann et al., 1998) and renewed impetus has come from improved measurement strategies and technology in combination with more sophisticated models (Gruber et al., 2003a,b; Gruber et al., 2004a). The extreme summer in 2003, when the months of June, July and August were the hottest on record in the Alps (Schär et al., 2004), led to significantly deeper active layers than normal (see Section 3.3) and greatly increased rock fall activity (Schiermeier, 2003; Gruber et al., 2004b). Measurements (Fig. 5) and model experiments (Gruber et al., 2004b) confirmed the extraordinary response in active layer thickening during 2003. Careful observation of detachment surfaces located within the permafrost zone immediately following failure often revealed the presence of ice that formerly occupied, and probably cemented, the discontinuities along which failure occurred (Fig. 28).

In steep, cold mountain ranges such as the European Alps, where permafrost in bedrock slopes makes up a large proportion of the total permafrost area, the presence of ice-bonded discontinuities is likely to be a decisive factor in the stability of rock faces Haeberli and Gruber, 2008). Unlike slope geometry, structure and rock mass properties, the presence of permafrost constitutes a transient element that responds rapidly to climate change or human disturbance. Recently Gruber and
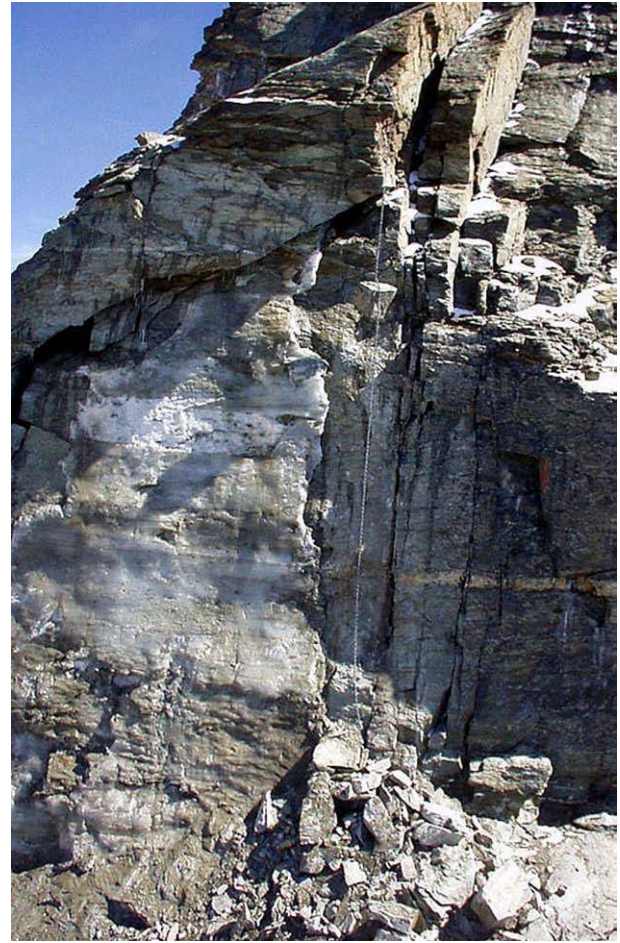

Fig. 28. Ice-covered detachment surface exposed by release of a rock fall in 2003 on the Matterhorn Lion ridge. Photo: L. Trucco.

Haeberli (2007) have provided an overview of warming-induced destabilization in steep bedrock and highlighted the followinge evidence for the importance of permafrost:

a) the high proportion of rock fall events originating in permafrost areas;
b) ice observed on fresh detachment surfaces immediately after several events;
c) the presence of wide ice-filled fissures in bedrock;
d) the potential temperature-dependent loss of stability in permafrost (see below);
e) recent research demonstrating physical processes that actively widen frozen rock joints; and
f) observed warming of both atmospheric and rock temperatures.

7.3. Mechanisms leading to rock fall

Permafrost rock walls in general only present a hazard when they are jointed. Loss of strength of ice-bonded joints during warming or thaw is likely to be related to changes in ice/rock interlocking (Davies et al., 2001), ice-rock adhesion (Ryzhkin and Petrenko, 1997), pore water pressure, ice crystal geometry (Voytkovskiy and Golubev, 1973) and presence of impurities (Hooke et al., 1972; Paterson, 1994). It is well known that the shear strength of ice is usually higher at lower temperatures and decreases toward the bulk-melting temperature (e.g. Fish and Zaretsky, 1997). This has been demonstrated in laboratory direct shear tests and centrifuge experiments (Davies et al., 2001, 2003) where the shearing resistance of a frozen ice-bonded bedrock slope was shown to fall during warming. Direct shear

tests and centrifuge modelling of ice-filled joints in an instrumented model rock slope imply that where the direction of dip of the joint planes is appropriate, the stability of a steep, jointed rock slope may be maintained by the ice (Davies et al., 2000, Davies et al., 2001). In all cases, the factor of safety reduces when the temperature increases.

Thus, many processes (operating at different temperatures and time scales) may translate warming or thaw of permafrost into reduced rock slope stability. In view of current understanding and results of laboratory experiments (see Section 6.1), it appears plausible that very slow growth of segregation ice over a long period during permafrost aggradation and stability might actively widen joints in their frozen state and thus contribute to a reduction in stability when permafrost subsequently warms and thaws (Gruber and Haeberli, 2007). Warming may result from changes in snow and ice cover ice during the retreat of glaciers (c.f. Fischer et al., 2006), as well as the direct effects of atmospheric temperatures.

7.4. Modelling near-surface rock temperature response to changing boundary conditons

Surface temperatures are mainly controlled by the surface energy balance that depends on climatologic variables, topographical factors and surface characteristics (see Section 4) (Hoelzle et al., 2001; Mittaz et al., 2000). Since snow and soil cover are sparse or absent, the surface temperatures of steep rock walls mainly change with aspect (shortwave radiation), altitude (sensible heat and longwave incoming radiation) and lithology. In complex high mountain topography these factors can change significantly over very short distances leading to spatially highly variable surface temperatures.

Several researchers report rock surface or near-surface temperature measurements (e.g. Coutard and Francou, 1989; Hall, 1997; Matsuoka et al., 1997; Wegmann, 1998; Matsuoka and Sakai, 1999; Hall and André, 2001; Lewkowicz, 2001) but a coherent spatial pattern can usually not be deduced. A combination of systematic measurements and modelling was used by Gruber et al. (2003a,b, 2004a) to investigate spatial (mainly related to topography), regional (related to climate) and temporal variations in rock surface temperatures. Fourteen time series of daily near-surface rock temperatures from rock faces in the Alps between 2500 and 4500 m a.s.l, with different exposure to solar radiation (aspect) were used to further develop and validate an energy-balance model that simulates surface temperatures over alpine topography. The validated model was then used to perform 21-year forward model runs based on meteorological data (Fig. 29). The high temporal and spatial variability of simulated mean annual ground temperatures during those 21 years demonstrated the importance of a combination of measurements and modelling. Surface conditions such as the presence of snow or ice in the rock wall can have a strong effect on surface temperatures, but currently little is known of their influence.

Salzmann et al. (2007a,b) have assessed a possible range of changes in ground surface temperatures in steep rock. Surface temperature scenarios were calculated based on an energy balance model and climate time series that were downscaled from output of Regional Climate Models (RCM). In order to account for the uncertainties associated with RCM output, a set of 12 different scenario climate time series were applied to simulate the average change in ground surface temperatures for 36 different topographical situations. Results show a significant influence of topography on the temperature changes because it modifies the amount of solar radiation received at the surface. In addition, north-facing surfaces show a higher sensitivity to the climate scenario used while the uncertainty for south-facing surfaces is generally higher.

In alpine environments, most topographic features such as mountain peaks or steep ridges are 3-dimensional in nature and geothermal responses to change in ground surface temperatures are similarly strongly three dimensional. Such three dimensional complexity in the ground thermal field influences the heat flow density and generates strong lateral heat fluxes (Wegmann, 1998; Gruber et al., 2004c). In order to describe these effects, Noetzli et al. (2007) conducted a series of numerical experiments using idealised test cases. Subsurface temperatures were calculated for simplified ridges, peaks and spurs that were identified as the most typical topographic features found in high mountains. For this purpose, a modelling chain that combines the processes in the atmosphere (climate), at the surface (energy balance) and in the subsurface (heat conduction) has been developed. Surface temperatures were calculated using an energy balance model driven by climate time series. These were then used as upper boundary conditions in a numerical 3D heat conduction scheme that determines temperatures at depth. Climate time series gained from RCMs and generated in the scope of a study by Salzmann et al. (2007a,b) were used for time-dependent model runs.

Results indicate complex 3-dimensional patterns of temperature distribution and heat flow density below mountainous topography for equilibrium conditions, that are additionally perturbed by transient effects. The steady state temperature field below complex topography is basically controlled by the spatially varying surface temperature of different mountain sides and is little influenced by the geothermal heat flux (Fig. 30). Isotherms are nearly vertical and a strong heat flux is directed from the warmer to the colder sides of a mountain. This leads to permafrost occurrence at many locations where temperatures at the surface do not indicate it, e.g., on the south face of ridges or below the edges of a peak. Permafrost degradation in steep topography takes places from different sides, affecting both the permafrost table and the permafrost base leading to an increase in the pace of permafrost degradation as compared to flat terrain, where warming penetrates vertically into the ground. For the investigation of permafrost occurrence in complex terrain and its response to climate forcing, it is therefore important to account for 3-dimensional effects
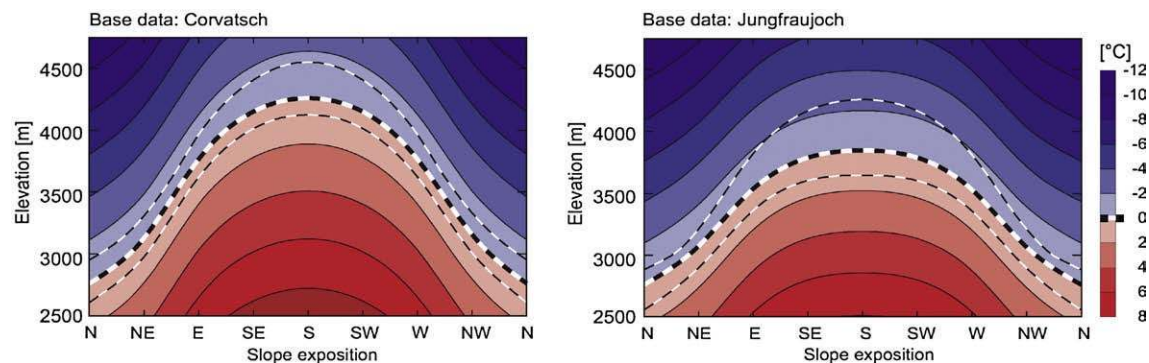

Fig. 29. Mean simulated annual rock surface temperature for 70° slope steepness and two locations, 1982–2002. The thick dashed line indicates the elevation of the mean 0 °C isotherm during this period. The thin dashed lines indicate the highest and lowest positions of the mean annual 0 °C isotherm. From Gruber et al. (2004b).
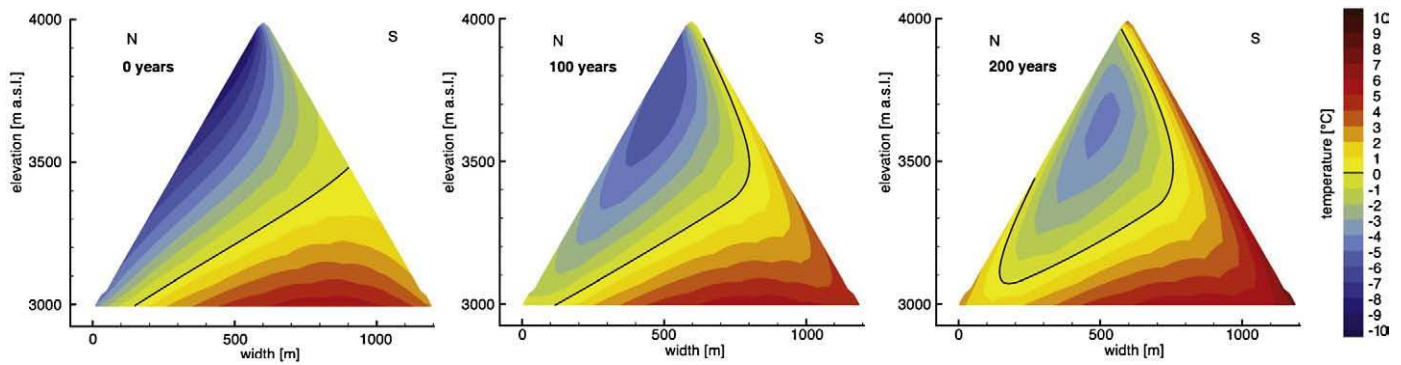
Fig. 30. Distribution and evolution of subsurface temperatures in a simplified ridge with a gradient of 60° for steady state (0 years) and after time periods of 100 and 200 years.The warming at the surface was set to +3.5 °C for north slopes, +2.5 °C for south slopes and +3 °C for east and west slopes over a time period of 100 years The black line corresponds to the 0 °C.

(caused by geometry and variable surface temperatures) and transient effects (Noetzli et al., 2007). This type of artificial geometry is suitable for the investigation and understanding of thermal effects at depth, and the modelling chain applied in Fig. 30 (Noetzli et al., 2007; Salzmann et al., 2007a,b) can easily be applied to study the distribution and evolution of mountain permafrost temperatures in response to extreme events (e.g., warmer than average summer periods), or to investigate transient states of thermal fields in real topography.

7.5. The significance of scale in a warming climate

The thermal response of permafrost to atmospheric warming generally takes place at different scales of time and depth (Haeberli et al., 1997; Haeberli and Beniston, 1998; Lunardini, 1996), that correspond to frequency and magnitude of potential rock slope destabilisation (Fig. 31). Following increases in surface temperature, with a delay of only months or years, the active layer thickens, and thus, new volumes of rock will be subject to critical temperature ranges or thaw. This rapid and immediate response corresponds to events observed in the hot summer of 2003. A longer timescale response relates to the temperature profile within the permafrost, which is displaced towards the warmer side as the warming propagates downwards (See Section 3.4). Eventually, the lower permafrost boundary (up to several hundred metres depth) will rise, potentially causing large and deep-seated instabilities delayed by decades or centuries. The Brenva Glacier rock avalanche (Deline, 2002) that occurred in January 1997 in the Mont Blanc East face, Italy, may be related to such deep-reaching and long-term changes of the subsurface thermal conditions. Ice content additionally influences the response time by the uptake of latent heat (Wegmann, 1998; Noetzli et al., 2007) and can influence the time scales of permafrost degradation by about an order of magnitude. Clearly, the assessment of hazard and risk arising from future climate-related changes in rock fall magnitude and frequency must take account of the complex transient thermal fields within high mountain permafrost.

8. Creeping permafrost: rock glaciers and climate

8.1. Rock glacier thermal condition

Creeping perennially frozen debris streams, or rock glaciers (Fig. 32) are widely reported in cold mountains (e.g. Barsch, 1992) and are fundamentally characterised by their thermal state (Haeberli, 2000). The rock glacier surface layer consists of debris with typical diameters ranging from several centimetres, decimetres, to metres, depending on the geological setting, weathering conditions, and processes of debris reworking. If this layer is at least as thick as the local active layer, summer thawing cannot reach the underlying

ground-ice containing permafrost body, which therefore persists. The difference between rock glaciers, dead glacier ice, and debris-covered glaciers can thus be defined by the thermal state of the material, since rock glaciers by definition require the presence of permafrost. The debris on and within rock glaciers may be derived from periglacial and glacial processes, and the rock glacier ice content may originate from refreezing rain and meltwater, glacier ice, buried ice, avalanche snow, and snow patches, etc., or combinations thereof (Haeberli and Vonder Mühll, 1996; Humlum et al., 2007). Temporal transformations and spatial transitions between rock glaciers, debris-covered glaciers or dead ice, ice-cored moraines, etc., are certainly possible, and indeed often found in nature.

Rock glaciers provide a clear topographic expression of the presence of perennially frozen ground. Rock glaciers may, however, end above the regional permafrost limit due to topographic conditions, the lack of sufficient material supply, or insufficient time to fully develop. On the other hand, the coarse debris cover on top of a rock glacier favours ground cooling due to enhanced heat transfer to the atmosphere and rock glaciers may therefore extend below the regional permafrost limit when the surrounding terrain cover causes relatively higher ground temperatures.

8.2. Rock glacier dynamics

The basic concept of mass transport within a rock glacier can be derived from the characteristic thermal and kinematic conditions. Frozen ice-rich debris is transported down-slope by gravitational creep, with the highest rates at the surface. The advected surface material then falls over the steep rock glacier front. The grain-size
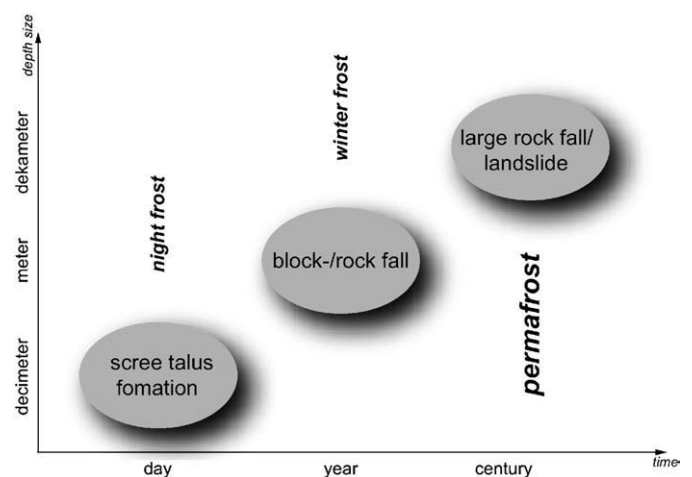

Fig. 31. Time and depth scales involved in slope stabilities in high-mountain areas.

Fig. 32. Muragl rock glacier, Upper Engadine, Swiss Alps.

sorting along the frontal slope occurring during this process leads to the typical appearance of rock glacier fronts. The surface debris that accumulates at the front is then overridden by the advancing rock glacier and again incorporated into its base ("caterpillar" or "conveyor belt" effect) (Kääb and Reichmuth, 2005).

In the case of a total cessation of mass supply, a rock glacier would continue to advance as long as sufficient ice is present, and shear stresses are sufficient to make creep possible. Loss of interstitial ice would lead to stagnation of the rock glacier, but not retreat. The main process of mass loss is the melt-out of ice at the rock glacier front where the thermally protecting debris cover becomes thinner than the thaw depth due to frontal erosion. In addition, the frontal grain-size sorting leads to smaller grain sizes in the upper part of the front, reducing the insulation effect in comparison to the coarser debris at the rock glacier surface. Due to the melt-out of ice, the potential loss of solids, and the decrease of horizontal speeds with depth, the advance rate of rock glaciers is significantly smaller than their surface speed. Advance rates measured so far range from a few centimetres to decimetres per year (Kääb, 2005).

8.3. Geotechnical properties of coarse frozen soils in relation to permafrost creep

Arenson et al. (2007) present a detailed overview of the geotechnical properties of coarse frozen soils, characterised by high ice and air content. The behaviour of frozen finer-grained soils is discussed by Andersland and Ladanyi (2004) and Esch (2004). The strength and the deformation behaviour of frozen soils is mainly a function of i) ice and air content, ii) temperature, iii) loading rate (Goughnour and Andersland, 1968; Ting, 1983; Arenson et al., 2003a; Arenson and Springman, 2005a). Laboratory investigations suggest that dispersed soil particles within dirty ice change the failure mechanism, so that strength is slightly lower than in pure ice (e.g. Hooke et al., 1972; Yasufuku et al., 2003; Arenson and Springman, 2005a). As the volumetric ice content decreases, structural hindrance between the solid particles develops and dilation occurs, increasing the strength and reducing creep deformation significantly.

At high relative soil densities, the ice cements the matrix, and the resulting increase in strength over the same soil in its unfrozen state may be quantified as cohesion at zero stress (e.g. Arenson et al., 2004). However, at large strains, ice-bonding fails, destroying the cohesive

effect and the large strain strength of the frozen material is tending towards a similar strength to that of the equivalent unfrozen soil. In other words, the thawed large strain strength can be considered as a lower boundary for the frozen state. Since the strength of ice decreases as the temperature increases, so does the strength of the frozen soil.

8.4. Measurement of rock glacier creep

Technological advances have resulted in the rapid introduction of new methods for quantifying small-scale ground movements and today a range of ground-based, airborne and spacebourne methods are applied in monitoring temporal and spatial trends in rock glacier creep rates. Terrestrial surveying techniques such as polar survey and global navigation satellite system (Zick, 1996; Berthling et al., 1998; Kääb et al., 2003b; Kääb and Weber, 2004; Lambiel and Delaloye, 2004) have provided time series of rock glacier movement with comparable high temporal resolution and thus revealed inter-annual and seasonal speed variations (Schneider and Schneider, 2001; Kääb et al., 2005a,b). Terrestrial laserscanning (Bauer et al., 2003) and perhaps also terrestrial radar interferometry are likely to become increasingly important in resolving small spatio-temporal variations of rock glacier surfaces.

Photogrammetry, based on repeat optical data (mostly air-photos), has been used to measure entire surface velocity fields on rock glaciers or groups of rock glaciers, and also to measure spatio-temporal variations of rock glacier velocity (Kääb and Vollmer, 2000; Kaufmann and Ladstädter, 2003; Kääb and Weber, 2004; Roer et al., 2005) (Fig. 33). Repeat airborne laserscanning, though not yet applied to rock glaciers, has a large potential to measure rock glacier volume changes and, to some extent, horizontal displacements (Geist and Stötter, 2003). Spaceborne radar interferometry is being applied to detect and quantify rock glacier surface deformation over large areas (Rott and Siegel, 1999; Rignot et al., 2002; Kenyi and Kaufmann, 2003; Strozzi et al., 2004). Due to the millimetre-accuracy of this technique even small displacements can be detected.

More traditional approaches to rock glacier movement monitoring have included repeat slope indicator measurements in boreholes to investigate the vertical variation of velocities within rock glaciers (Arenson et al., 2002) and occasionally, ground-based mechanical techniques designed to measure surface deformation (Haeberli, 1985; White, 1987). Finally, qualitative investigation of rock glacier creep has
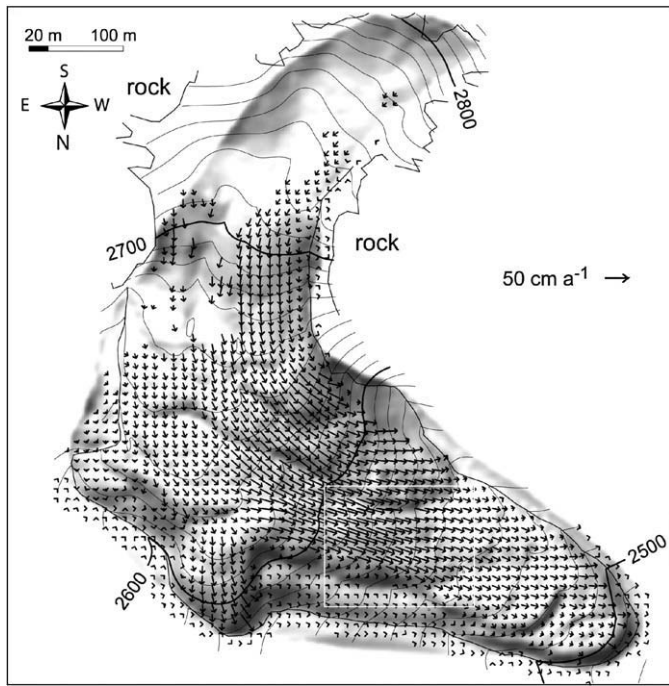
Fig. 33. Average horizontal surface velocities on Muragl rock glacier measured from aerial photography of 1981 and 1994. The white rectangle marks the section shown in Fig. 36.

been attempted through absolute and relative dating methods, geomorphodynamic indicators, vegetation mapping, etc. (e.g. Strozzi et al., 2004).

8.5. Observed creep rates

Surface creep rates of up to several metres per year are common in rock glaciers (Kaufmann and Ladstädter, 2002; Kääb et al., 2003b; Haeberli et al., 2006), transporting talus or glacial debris downslope. Permafrost creep within the high mountain context is localised by the distribution of sufficient ground ice to promote creep movements. In high arctic lowlands, where ground ice is often more extensive within the continuous permafrost, creep is generally much slower (e.g. Dallimore et al., 1996; Foriero et al., 1998), and does not generate such clear surface landforms as in mountain terrain.

Rock glacier creep rates depend among other things on surface slope, composition and internal structure, thickness of the ice-rich body, and ground temperature (Haeberli, 1985). The observation of minimum surface speeds is limited by the detection level of available measurement techniques (see above). A coherent ice content within rock glaciers leads to the lateral transfer of stresses, and thus to a coherent velocity field (Figs. 33 and 36). A number of factors, including the distribution of stress, the effects of lateral friction, and variations in shear modulus, usually result in the highest downslope creep rates on a rock glacier being along its centreline. In the few rock glacier boreholes available, the downslope deformation was concentrated in sub-horizontal layers some decimetres to metres in thickness, rather than being distributed through the body of the rock glacier with a parabolic variation in creep rate with depth, as is found for glacier ice (Arenson et al., 2002).

8.6. Spatial modelling of rock glacier distribution and its response to changing climate

It is generally accepted that several conditions must be fulfilled in order for a rock glacier to form. There must exist (a) a headwall composed of weathering-susceptible rock, (b) a relief permitting the accumulation of talus, (c) a climate cold enough to allow the build-up

and preservation of ground ice (super-saturation) over typical time scales of millennia and dry enough to inhibit the formation of glaciers, (d) hydrological and lithological preconditions that allow the formation of a cohesive debris-ice matrix, and (e) angle and thickness of accumulated talus sufficient to generate sufficient shear stress to cause deformation. To enable the further development, ground temperatures must remain in a range enabling creep, and talus thickness must be maintained by continuous debris supply to allow mass conservation. Stabilisation and formation of relict rock glaciers results either from climatic or dynamic inactivation processes.

Statistical modelling by Brenning (2004, 2005) in the Chilean Andes suggested key factors in rock glacier formation include slope profile, elevation, convergence index, and vertical extent of the contributing area, plus the ratio of potential solar radiation to global radiation, the 'northexposedness' (the cosine of terrain aspect), and their interaction. Studies by Morris (1981) in the in the Sangre de Cristo Mountains, Southern Colorado and Frauenfelder et al. (2003) in the Eastern Swiss Alps showed interaction between altitude, radiation and rock wall jointing, rather than additive independent effects, determined the development of rock glaciers. The relation between rock-wall extent and rock glacier size was complex, involving factors such as cliff recession rates and subsequent talus input variations. Flow rates apparently respond predominantly to non-linear thermal influences on strain rates rather than effects from stress-related geometry (slope-dependent thickness).

Recent dynamic modelling of rock glacier evolution (Frauenfelder et al., 2008) considers both external and internal processes in the spatial and temporal domain. Climate inputs are key external variables, together with rock-debris accumulation, hydrology, and glacier extent. The internal processes considered are creep initiation, advance rate, and creep termination. Field validation shows that the dynamic model enables the simulation of spatio-temporal creep processes on a regional scale, but that the model is highly dependent on the accuracy of the relevant input parameters.

8.7. Environmental change and rock glacier dynamics

The altitudinal belts where active, inactive and relict rock glaciers are found, suggest that atmospheric and ground temperatures are important drivers of rock glacier activity through their influence on debris supply from rockfalls and rock glacier ground ice (Olyphant,
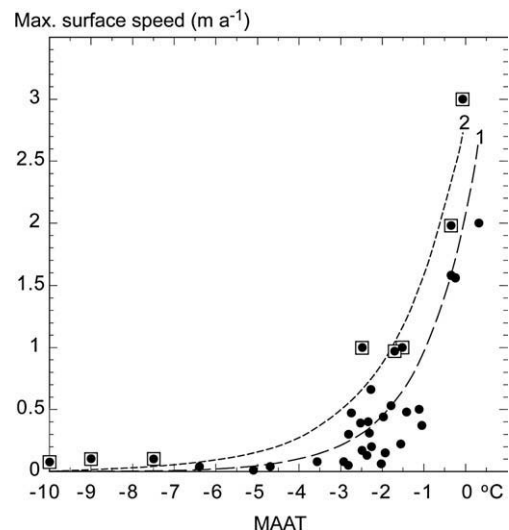

Fig. 34. Maximum surface speed of a global sample of rock glaciers as a function of mean annual air temperature (MAAT) at the rock glacier front (black dots). For data sources see Frauenfelder et al. (2003). Curve 1 is an exponential fit through all points, curve 2 an exponential fit through the upper maximum points only (points marked with rectangles). (For details see also Kääb et al., 2007).

1987; Frauenfelder et al., 2001; Frauenfelder, 2005). Warming trends since the end of the Little Ice Age may be largely responsible for recent reduction in activity of rock glaciers in certain areas. Significantly less well investigated, but potentially of similar importance, is the influence of long-term changes in precipitation, especially snow cover, on mass supply and ground temperatures. Climate change may also lead to overriding of rock glaciers by expanding glaciers, or initiation of rock glaciers in locations vacated by retreating glaciers (Maisch et al., 2003; Kääb and Kneisel, 2005).

Geostatistical investigations of surface velocity measurements and climatic parameters, together with laboratory data and numerical modelling show that the deformation rate of a rock glacier with a given slope, composition, or thickness, is largely dependent on the ground temperature. The increase of rock glacier surface speed with ground temperature seems to be approximately exponential (Frauenfelder et al., 2003; Kääb et al., 2007) (Fig. 34). Consequently, ground temperature warming due to rising air temperatures or changes in snow cover, is expected to increase rock glacier deformation, especially in rock glaciers with ground temperatures of close to 0 °C. Indeed, early investigations confirm a significant recent acceleration of many rock glaciers in the European Alps, where an air temperature increase of close to +1 ° C was observed since the 1980s (Kääb et al., 2007) (Figs. 35 and 36). However, once mean ground temperatures begin to rise above 0 °C, decline in creep activity is likely, so that the response of rock glaciers to prolonged warming might be an an initial acceleration, followed eventually by stagnation.

The high thermal responsiveness of permafrost creep rates at ground temperatures close to 0 °C has apparently led to increased sensitivity to short-term seasonal temperature cycles, ground water influences, impacts from snow cover variations, etc. and in some locations may lead to the initiation of permafrost creep (Kääb et al., 2007; Ikeda et al., 2008).
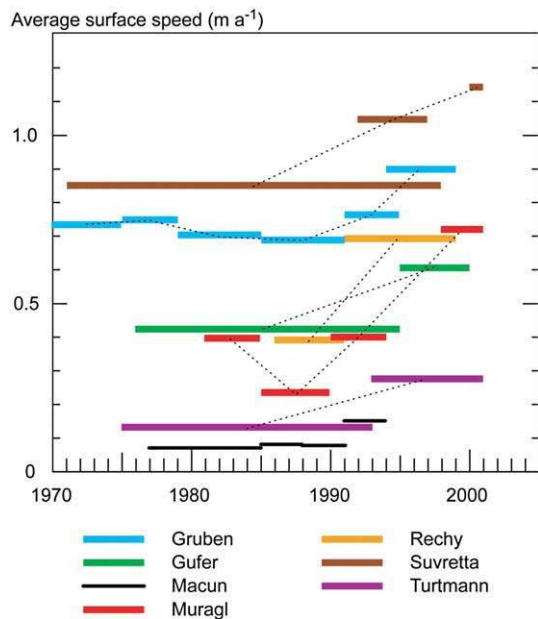

Fig. 36. Horizontal surface velocities on Muragl rock glacier (see Fig. 33). The vectors 1981–1994 represent average velocities derived from airphotos of 7.9.1981 and 23.8.1994. The bold vectors are average velocities between 24.10.1998 and 21.9.2001 derived from repeat terrestrial survey of a set of surface markers. Speed seems to have nearly doubled for 1998–2001 compared to 1981–1994. It is, however, important to keep in mind that Muragl rock glacier showed significant seasonal and pluriannual (Fig. 35) speed variations (Kääb et al., 2007).

9. Thaw-related mass movement processes: solifluction and debris flows

European permafrost areas are generally characterised by a landscape assemblage of steep bedrock slopes, coarse-grained scree slopes with gradients close to the angle of repose where rock glaciers are often initiated, and lower gradient footslopes mantled by finer-grained sediments. Screes and coarser sandy soils are not frost susceptible and where such materials contain significant ice it is likely to have accrued through burial of snow, freezing of groundwater or possibly the burial of residual cold glacial ice (see section 8). Although susceptible to creep when frozen, ice-rich coarse-grained frozen soils will drain rapidly on thawing, so that raised pore pressures leading to large-scale slope failures are unlikely. However, thawing of ice-rich fine-grained soils causes thaw consolidation, raised pore pressures, reduced effective stresses, and in consequence, lowered soil shear strength (e.g. Morgenstern and Nixon, 1971; Harris, 2007). As a result of this, mass movement processes are particularly important.

Periglacial mass movements include slow perennial solifluction (e.g. Washburn 1967, 1999; Harris, 1981; Matsuoka, 2001b) and more localised shallow translational landslides and debris flows. Shallow slope failures may occur when soil thawing is rapid and soil ice content is high or when heavy rainfall leads to rapid saturation of shallow active layers. Thus, many soil-covered periglacial slopes consist of a slowly moving solifluction mantle that from place to place and from time to time is disrupted by rapid mass movement events.

9.1. Slow mass movements (solifluction)

Two processes have been identified as contributing to slow downslope active-layer movement; frost creep, the downslope settlement of near-surface soil particles disturbed by frost action, and gelifluction, the slow gravitational shear deformation of a thawing active layer (Washburn, 1967; Harris, 1981, 2007). Since both frost creep and gelifluction are associated with frost heaving and thaw settlement, in practice they are often impossible to differentiate in field measurements and the term solifluction is commonly used to include all such processes contributing to slow (several mm to several

Fig. 35. Average rock glacier surface speeds in the Swiss Alps as measured for different periods since 1970. Most of the data are from photogrammetry, some from geodesy. The Macun data are from Zick (1996), all other data from Kääb et al., 2007. All horizontal bars represent average speeds over the individual measurement periods. The measurement periods for Suvretta overlap because they refer to different methods (photogrammetry vs. terrestrial survey). The dotted lines connect the average values for individual rock glaciers and measurement periods for better readability. Due to the very different time periods compared these dotted lines do not necessary indicate the actual changes in surface speed.
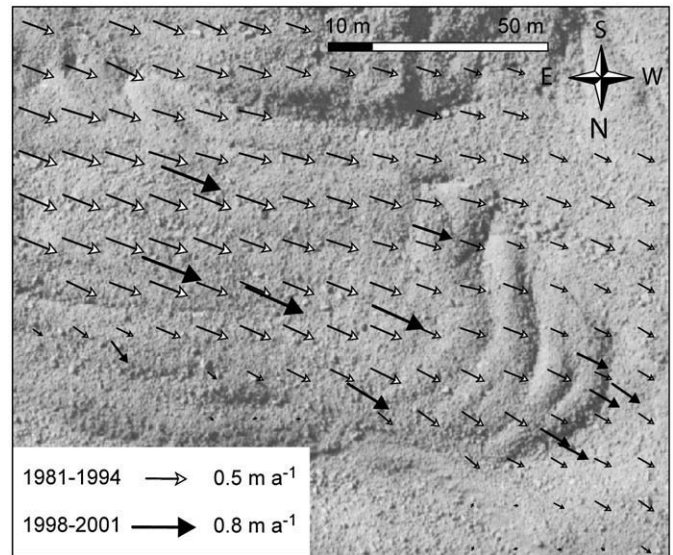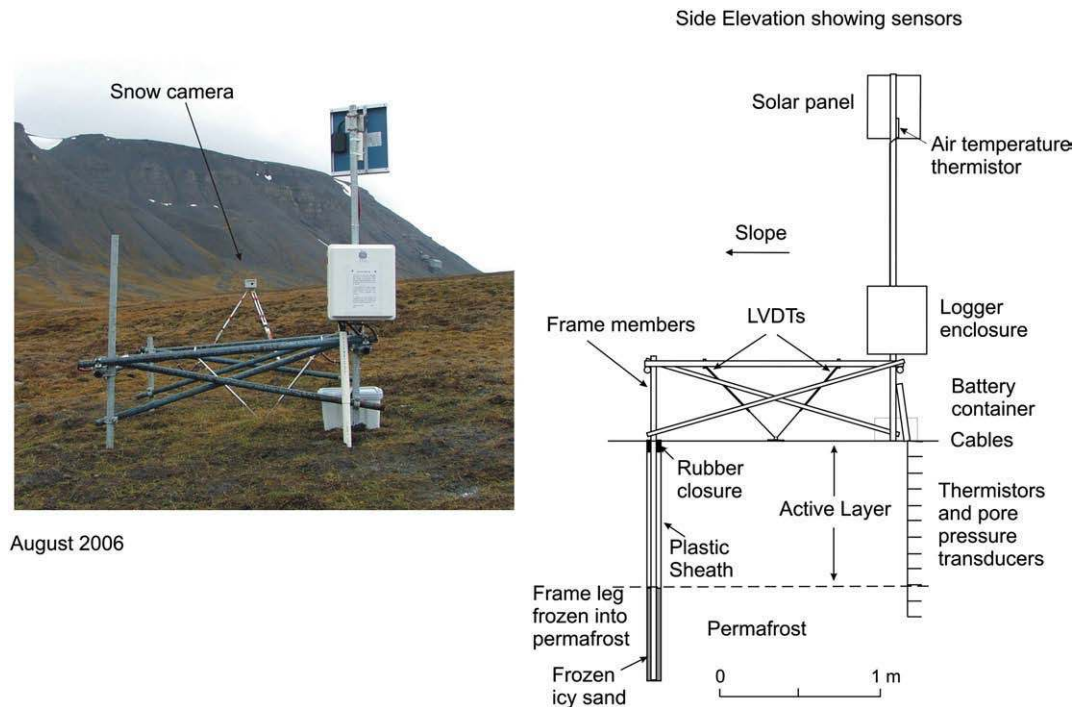
Fig. 37. Solifluction measurement station installed in Endalen, Svalbard in August 2005.

cm per annum) periglacial mass wasting (e.g. Ballantyne and Harris, 1994). The process is commonly the dominant mechanism of sediment transport on periglacial slopes (Matsuoka, 2001b) and occurs both in permafrost areas and in non-permafrost areas with deep seasonal ground freezing.

9.2. Field and laboratory studies of solifluction processes

Recent field studies have focused on continuous monitoring of environmental conditions (air and soil temperatures, snow fall, soil moisture status, frost heave, thaw settlement, and downslope soil movements). Field measurements of slope movements (frost heave, thaw settlement and downslope displacements) require a stable reference datum, and this is often provided by a metal frame anchored in a stable substrate (e.g. Lewkowicz, 1992, Matsuoka 1994; Matsuoka et al., 1997, Jaesche et al., 2003) although technological advances are now allowing surface motion to be resolved at high spatial and temporal resolution using carrier-phase differential GPS (Berthling et al., 2000). Continual measurement of soil temperatures, pore water pressures and ground surface movements was developed by Harris et al. (1997, 2008a) during laboratory simulations of solifluction processes using thermistors, pore pressure transducers, and pairs of linear variable differential transformers (LVDTs), and this instrument package has recently been transferred from the laboratory to two field sites, one in southern Norway and the second in Svalbard (Fig. 37) (Harris et al., 2007, 2008c), allowing direct comparisons to be made between observations in the field and in laboratory simulations.

In Alpine, non-permafrost sites, freezing and thawing is from the surface downwards and ice segregation and soil movement rates are greatest near the surface and decrease with depth (Matsuoka, 2001b; Harris, 2007). Drier steeper slopes are often dominated by frost creep associated with short-term freeze-thaw cycles (Matsuoka, 2005; Matsuoka et al., 1997)., while gelifluction is generally more important than frost creep at snow-rich sites with deep seasonal ground freezing (Jaesche et al., 2003; Harris et al., 2008c).

In permafrost regions, the active layer is likely to freeze from the surface downwards and the permafrost table upwards. The upward advance of a freezing front from the permafrost table causes water migration towards it from the unfrozen soil above, leading to enhanced ice segregation in the lowermost parts of the active layer. In many cases a particularly ice-rich transition zone, termed the "transient layer" (Shur et al., 2005), is present within the lowest parts of the active layer the upper one or two metres of permafrost (Fig. 38). Here ice segregation is enhanced by downward percolation and refreezing of meltwater during active-layer thaw (Mackay, 1983). During two-sided freezing, the active layer may become effectively a hydraulically closed system, so that migration of water towards the advancing freezing fronts leaves the central zone relatively dry and ice poor. During active layer thaw, thaw-settlement and associated solifluction occurs early in the thaw period as near-surface ice-rich soil thaws, and then again later in the summer when the ice-rich basal zone begins to thaw. In late summer, therefore, the active layer above moves down slope en-masse across a soft deforming basal layer

Fig. 38. Borehole core sample taken from within the uppermost 0.5 m of permafrost in Endalen, Svalbard. Thick lenses of segregation ice indicate a volumetric ice content of between 40 and 50%. Photograph F.W. Smith.
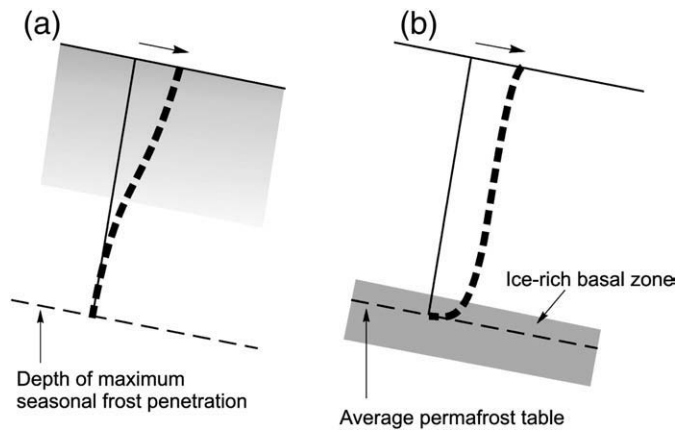
Fig. 39. Distribution of segregation ice and associated solifluction profiles in (a) seasonally frozen ground with one-sided freezing, and (b) permafrost, with two-sided active layer freezing.

(Fig. 39) where thaw consolidation is concentrated (Matsuoka and Hirakawa, 2000; Lewkowicz and Clark, 1998; Mackay, 1981).

In Svalbard, Matsuoka and Hirakawa (2000) emphasized the importance of ice distribution within the active layer. They observed no ice-rich zone at the base of the active layer in a solifluction sheet at Kapp Linné, due to the absence of two-sided freezing at this relatively warm site (mean annual temperature −4.9°) and the presence of non-frost susceptible marine sands beneath the solifluction sheet. Summer thawing was associated with solifluction in the upper 10-50 cm only, with no soil deformation at depth. In contrast, at a site in Adventdalen (mean annual air temperature −7° to −8 °C), continuous monitoring throughout an annual cycle in 2005–2006 at a site with frost susceptible soil revealed two-sided freezing with soil deformation during summer thaw concentrated within the basal ice-rich zone, giving plug-like active layer movement (Harris et al., 2006).

The influence of climate change is likely to differ markedly between the alpine non-permafrost environments with deep seasonal ground freezing, and colder regions (higher altitudes or higher latitudes) with ice-rich permafrost. In the former, the link between atmospheric temperatures and the near-surface thermal regime may be weak, depending largely on the depth and duration of snow and its date of arrival and clearance. Sediment transport by solifluction, reflecting rates of surface movement and the profile of soil movement with depth, is therefore likely to respond in a complex and site-specific manner to changes in snowfall regime that may accompany future climate change. In permafrost areas, particularly the continuous permafrost of high latitudes, warming air temperatures and an increase in frequency of warm years are likely to cause increasing active layer depths and increasing frequency of extreme thaw events, leading to thawing of the ice-rich zone at the base of the active layer and in the upper layers of permafrost. The consequence is likely to be a marked increase in both rates of solifluction and the volume of sediment transported annually (Matsuoka, 2001b).

Long-term (1973–2003) monitoring of annual surface displacement rates at Kapp Linné, Svalbard by Åkerman (2005) appears to illustrate such trends. Summer mean air temperatures are shown to have increased fairly consistently from around +3.5 °C in the early 1980s to around 5.5 °C in 2004, and this has been accompanied by increasing values of degree days thaw and increasing active layer depth. A highly significant correlation between average annual surface movement rates of solifluction sheets and the depth of active-layer thawing can be demonstrated (Fig. 40).

The advantages of laboratory physical modelling in, which soil properties and boundary conditions are well-controlled, have recently been exploited in full-scale modelling (e.g. Harris et al., 1997; 2008a;

Harris and Davies, 2000) and reduced scale geotechnical centrifuge modelling (Harris et al., 2003a, 2008b, Kern-Luetschg et al., 2008) of solifluction processes. Harris et al. (2003a,b) demonstrated that gelifluction is the elasto-plastic deformation of saturated thawing soils in, which shear strengths are reduced by high pore pressures, rather than viscosity-controlled flow as was suggested in some early definitions of the process. Both full-scale modelling and scaled centrifuge modelling have established a clear relationship between the amount of frost heave (and hence thaw settlement) and the observed rate of solifluction (e.g. Harris and Smith, 2003).

9.3. Debris flows and related phenomena on thawing soil-covered slopes

Extreme events such as deeper than normal thaw penetration during very warm summers, or intense summer rainstorms that rapidly saturate the active layer, may cause high pore water pressures sufficient to release rapid slope failures (e.g. Larsson, 1982; Chandler, 1972; Harris and Lewkowicz, 2000; Lewkowicz and Harris, 2005a,b). On steep mountain slopes, by far the most common mode of failure is debris flow. The mechanisms of debris flow initiation and displacement were reviewed by Iverson et al. (1997), who showed that most are triggered by high pore pressures often associated with transient very high groundwater levels. Initial slope failure is followed by soil liquefaction as the soil fabric is disturbed during movement. At this stage, a pore-pressure induced upward component of seepage enhances the potential for debris flow mobilisation. Mechanisms of thaw-related mass movement, including mudflows, flow-slides and detachment slides, were recently simulated in scaled centrifuge experiments by Harris et al. (2008b) who showed that initial instability arose from thaw consolidation of ice-rich soils giving excess pore pressures and upward seepage away from the thaw front, the subsequent displacement process (flow or slide) depending largely on soil properties.

A well-documented example of debris flow initiation in permafrost is from the Longyear Valley, Svalbard, where 30.8 mm rainfall fell in a 12 h period in July 1972 and caused some 80 debris flows and slides (Larsson, 1982). Many debris flows were initiated as translational slides over the permafrost table and developed into debris flows as water contents and slope gradients increased. Clearly climate change associated with an increase in frequency of extreme summer rainfall events would lead to greater debris flow activity. A lack of long-term
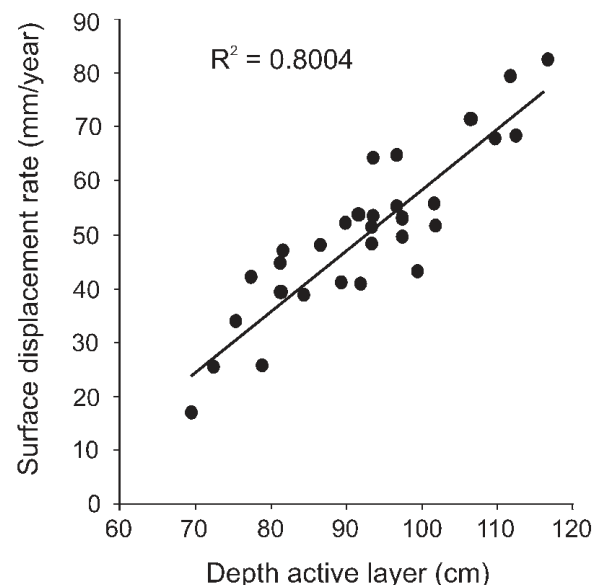

Fig. 40. Relationship between average surface movement rates and average active layer depths at Kapp Linné over the period 1973 to 2003. Data from Åkerman (2005).

data makes accurate assessment of recurrence intervals difficult, but there is evidence for increasing annual precipitation in Svalbard through the latter part of the 20th century (Larsson, 1982). Debris flows elsewhere also result from intense summer rainfall. In Northern Sweden, for instance, debris flow initiation by extreme rainfall has been described by Jonasson and Nyberg (1999) and Beylich and Sandberg (2005). In the latter study, a rainstorm in the Abisko region in July 2004 was shown to have initiated debris flows, shallow translational landslides and fluvial erosion that generated sediment transfers in one day that exceeded average annual sediment transfers by several times.

In the Swiss Alps, evidence has been presented that the number of extreme rainfall events capable of triggering debris flows in summer has increased. Analysis of climatic data for the last decades of the 20th century in the region of Ritigraben, Valais, Switzerland, suggested an increasing frequency of such events (Rebetez et al., 1997). The rise in atmospheric temperatures observed through the latter part of the 20th Century, and the early years of the 21st Century (see Section 2) is associated with permafrost degradation and glacier retreat, both factors tending to increase the sediment supply during debris flow events (Zimmermann and Haeberli, 1992; Haeberli, 1992, 1994; Rikenmann and Zimmermann, 1993). However, a longer-term perspective on debris flow activity in the Ritigraben Valley based on tree ring analysis (Stoffel et al., 2005) showed that debris flows actually occurred more frequently in the nineteenth century than they do today.

Jomelli et al., (2004) have demonstrated that in the French Alps the frequency of debris flows has decreased significantly at low altitudes (<2200 m) since the 1950s, whereas no significant variation has been observed at high altitude (>2200 m). The zone from, which debris flows are triggered also appears to have moved toward higher elevations. Over this period, air temperatures have risen and the number of freezing days fallen, and there has been a significant increase in summer rains higher than 30 mm/d. Jomelli et al. (2004) suggested that climate changes may have reduced the rate of sediment production at lower altitudes, so that debris flow transport may be limited by sediment supply rather than rainstorm frequency.

The limitation of debris flow activity by debris supply rather than the frequency of extreme rainfall events was also emphasised in the context of hazard assessment by Glade (2005) in a study of debris flow frequency in the Westfjords of Iceland. Here supply rates by rock weathering and solifluction were less than potential debris flow transport rates by a factor of 6.2–8.5, so that replenishment of debris storage was not always fast enough to supply the next potential debris flow triggering rainfall event. Thus debris flow initiation may depend as much on the stochastic variation in timing of extreme rainfall events as the overall statistical recurrence interval.

10. Ground ice phenomena

This section reviews the geomorphological significance of ground ice in the arctic and sub-arctic zones of Europe (Svalbard, Iceland and Fennoscandia) in the context of changing climate. Thus, the focus is on lowland areas rather than the mountain permafrost realm. Ground ice is classified according to its principal transfer process (Mackay, 1972) into wedge ice, intrusive ice and segregated ice.

10.1. Ice wedge formation and climate

It is likely that ice wedges are the most widespread periglacial landform in lowland continuous permafrost areas. Settlements located in arctic lowlands or valleys must take account of the likely presence of ice wedges within the substrate. Svalbard airport, Longyearbyen, for example, is located on a raised marine terrace with a large-scale polygonal network of ice wedges. Since its opening in 1975, the runway has suffered from unevenness of the surface due to thaw settlement in the spring/summer, and frost-heave during

autumn/winter causing significant maintenance problems and costs (Humlum et al., 2003).

Pleistocene distribution of permafrost in Europe has been mapped largely through identification of ice wedge casts (e.g. Svensson, 1988, Huijzer and Vandenberghe, 1998; Huissteden et al., 2003). The presence of ice wedge casts has been interpreted as indicating maximum mean annual air temperature at the time of formation of −6 °C in Alaska (Péwé, 1966), −4 °C in Yukon (Burn, 1990) and up to −2.5 °C in Siberia if formed in clay (Romanovskii, 1985). Péwé also concluded that periodic winter cooling of the permafrost down to −15 °C to −20 °C is necessary. In the Canadian arctic, Mackay (1993) demonstrated that sharp falls in air temperature lasting for at least 4 days, with a cooling rate of 1.8 °C/day, were necessary to cause ice wedge cracking, and this was prevented by snow depths above 60 cm (Mackay, 1986). Cooling rates of −0.5 °C to −0.9 °C/day at the surface and −0.1 °C to −0.4 °C/day at the permafrost table were reported by Mackay (1993) and similar threshold conditions were reported by Fortier and Allard (2005) and Allard and Kasper (1998). In temperate southern Sweden, Svensson (1996) showed that in the winter of 1966 a rapid fall in air temperature of 3–4 °C/h to −15 °C to −20 °C caused opening of thermal contraction fissures and associated ground shaking.

The use of ice wedge casts to reconstruct palaeotemperatures was questioned by Murton and Kolstrup (2003) because of the limited knowledge of the frequency of ice wedge cracking in modern permafrost environments, the lack of understanding of the natural controls on cracking, the difference between former mid latitude permafrost environments and modern high latitude permafrost environments, and the limited understanding of ice wedge casting.

10.1.1. Thermal conditions for present-day ice wedge activity in Svalbard

The modern high arctic continuous permafrost landscape in Svalbard (Fig. 41) provides the opportunity to study the frequency of ice wedge cracking, and its climatic controls in a maritime climatic setting that may differ only a little from much of central Europe during the last glacial maximum. Investigations have included morphology, isotope variation, age and process (e.g. Christiansen, 2005; Svensson, 1969a,b, 1976). The year-round field access from the University Centre in Svalbard, UNIS, has enabled continuous or high frequency ice wedge process monitoring since 2002, including cracking events recorded by miniature shock recorders, at a field site in Adventdalen, 10 km east of Longyearbyen (Christiansen, 2005). Some initial results of the first three years are presented below. A more detailed analysis is presented in Matsuoka and Christiansen (2008).
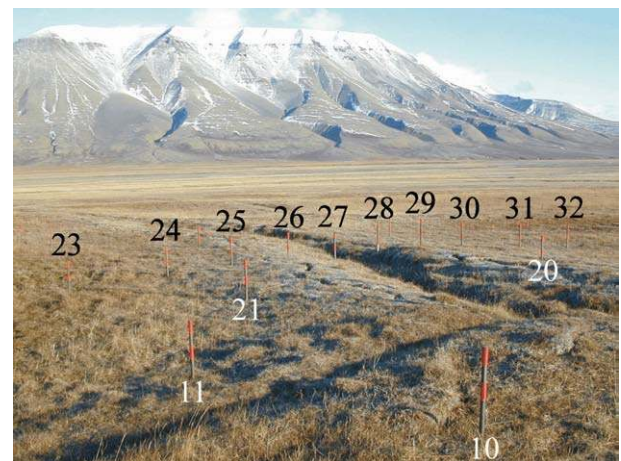

Fig. 41. Ice wedge research site in Adventdalen, Svalbard, September 2003. In the foreground, benchmark poles on the ramparts each side of ice wedge troughs are numbered below the poles. In the background benchmark poles, numbered above the poles, cross a first order ice wedge through and ramparts. Photo Hanne H. Christiansen.

The mean annual air temperature measured at the official meteorological station closest to the field site ranged from −5.1 to −3.7 °C for the period 2002–2005. Winter air temperature was below −30 °C for shorter or longer periods each year. In the centre of the ice wedge, below the deepest part of the ice wedge trough, and also in the ice wedge periphery below the rampart, temperatures at the top of the permafrost were below −15 °C for a period each winter. Ice wedge polygon ramparts were mainly blown free of snow, with only up to 5 cm snow accumulating for short periods, while the troughs contained up to 35 cm snow each winter.

The relationship between air and ground temperature and the incidence of ice wedge cracking has been investigated through thermal measurements and the installation of one-dimensional miniature accelerators with dataloggers (Tinytag Plus High Sensitivity Shock (0–5 g) and Sensitivity Shock (0–120 g)). These record hourly maximum ground acceleration and are placed in the ground surface, measuring acceleration perpendicular to the ice wedge orientation. In the winter of 2004–2005, nine such shock loggers were distributed around an ice wedge polygon in Adventdalen. Fig. 42 shows data from four of these shock loggers located along a 6.5 m section of the large ice wedge in the polygon seen in Fig. 41. Ground acceleration was only registered shortly after or during significant temperature falls. The largest acceleration of 6.3 m/s^2 occurred at the end of a 20 °C fall in air temperature on 14 January 2005, when all the nine loggers registered acceleration during the same hour. When the air temperature dropped from +1 °C to −24 °C from 23 to 27 February, and again when the air temperature dropped further from −16 °C to −31 °C from 7 to 9 March, small-scale ground accelerations of up to 2 m/s^2 were recorded over a period of several days. It was not until the end of this last period of activity that the permafrost temperature fell to −15 °C and the vertical temperature gradient reached −15 °C/m. The maximum cooling rate of −0.4 °C/h occurred just after this period (Fig. 43).

Excavation of snow profiles across the ice wedge troughs on 20 February 2005 revealed no open cracks in the ground surface. Cracks were present in the snow cover over a short distance in the ice wedge trough and in the top of the ramparts on 9 March. Seven snow pits were dug at shock logger locations on 16 April 2005, and open cracks were found in only two of them. During early July 2005, no cracks were seen along the 5.6 m section of the ice wedge where the shock loggers had registered small-scale movement (Fig. 42). However, open cracks were found in most of the ice wedge troughs elsewhere in the polygon, where shock loggers registered acceleration maxima of 4–5 m/s^2, significantly above the level recorded by the loggers in Fig. 42. Thus the data presented in Figs. 42 and 43 are thought to lie close to the thermal limit for ground thermal contraction cracking to occur.

10.1.2. Ice wedge formation and decay in relation to climate change

From the data reported above it is clear that ice wedge cracking depends on the occurrence of significantly cold winter periods, with rapid cooling of the near-surface permafrost to below −15 °C, as suggested by Mackay (1993, 2000). In Svalbard, such cold periods occur during high pressure conditions. The data from Svalbard also demonstrate that cracking can occur at MAAT up to −3.7 °C in this maritime area, where the substrate comprises fine-grained silt-rich frozen sediments. In contrast, it has been suggested that frozen sand and gravel require a maximum MAAT of −6 °C for cracking to occur (e.g. Murton and Kolstrup, 2003).

Climate warming leading to thicker active layers will cause degradation of ice wedges in the upper permafrost. In most cases, ice wedges thaw from above (Harry and Gozdzik, 1988) due to increasing active layer thickness or because of local geomorphological activity such as alas lake development. Since ice wedge growth and decay are slow, little is known of the nature of the thaw transformation process both in different materials, geomorphological settings
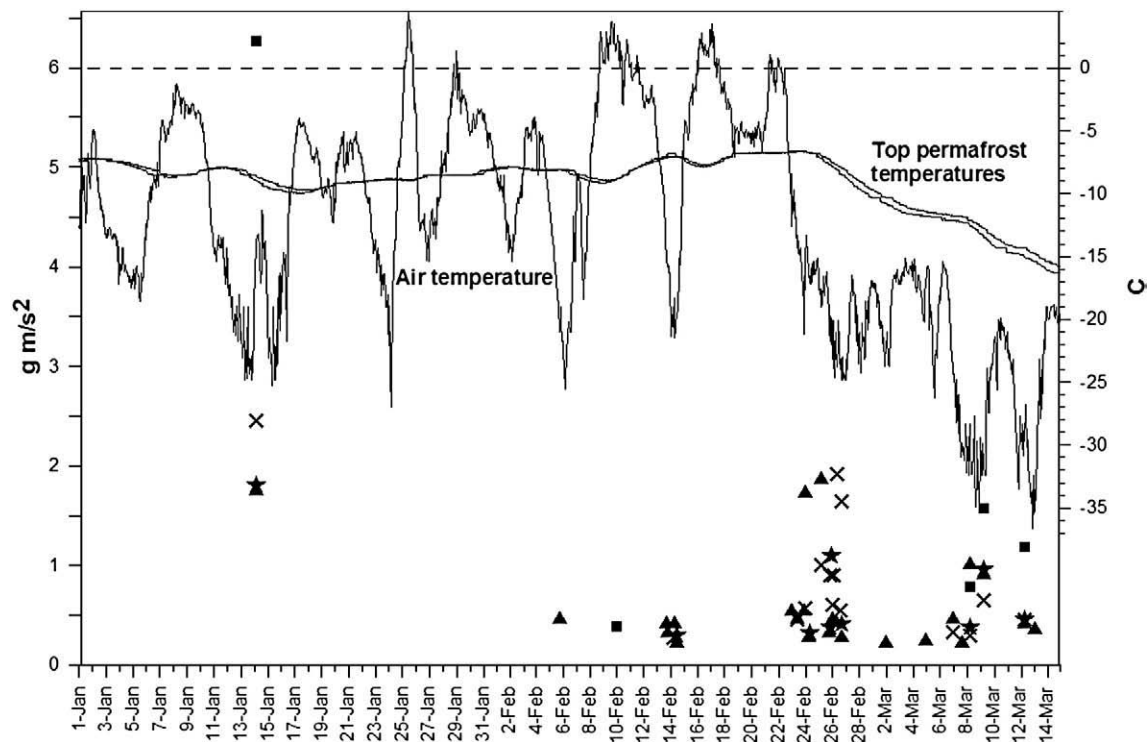

Fig. 42. Air and ground temperatures plotted with ground acceleration data measured in the top of the active layer at three places along a 6.5 m section of a first order ice wedge trough during winter 2005. The ground temperature graphs are from 68 cm depth below the centre of the ice wedge trough, at the top of the ice wedge, and from the permafrost table 100 cm below the rampart crest, adjacent to the ice wedge trough. Ground acceleration is measured by 3 High Sensitivity Shock loggers (0–5 g) and one Sensitivity logger (0–120 g), each represented by a different symbol.
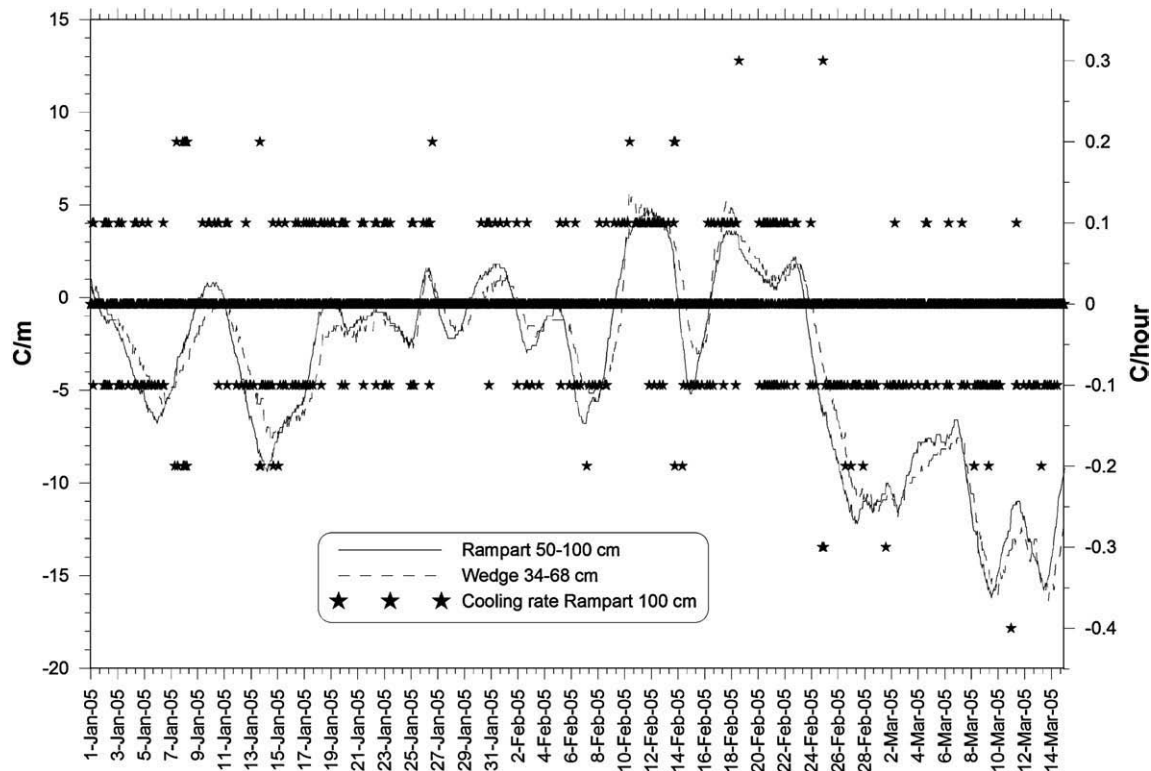
Fig. 43. Vertical temperature gradients (°C/m) in the lower half of the active layer of the rampart and ice wedge trough during winter 2005 (lines). Cooling (negative) and warming (positive) rates (°C/h) for the permafrost table below the rampart is also shown (stars).

and relationships to climatic change. Most studies of partial thaw of ice wedges are based on stratigraphical sections (Harry and Gozdzik, 1988), and they indicate small-scale faulting with subsidence and slumping in the thawed zone above the ice wedge, affecting the stability of the terrain surface. This situation can lead to development of thermokarst terrain. Rapid backwards niveo-fluvial erosion of ice wedges has been demonstrated to create small valleys or large gullies in polygonal terrain (Svensson, 1982, 1988; Harry and Gozdzik, 1988). In Svalbard such small valleys are up to 20–30 m long and 4–5 m deep and have developed relatively rapidly in sediments deposited during the last 3000 years.

Harris and Murton (2005) modelled ice wedge thawing and found that the degree of deformation during casting increases as the host sediments become finer-grained and more ice-rich. Thus, well-preserved ice wedge casts that replicate the original ice wedge form are common in coarse-grained ice-poor sediments, but in silts and clays, casts may be poorly preserved and significantly smaller than the original ice wedges. Temperature reconstructions where casts in coarser sediments are over-represented may therefore be on the cold side (Harris and Murton, 2005).

10.2. Palsa formation in relation to climate

Palsas are peat covered permafrost mounds containing segregation ice, surrounded by wet mires in, which permafrost is absent (French, 1996). Palsas develop where the dry surface peat layer provides sufficient insulation to preserve the frozen palsa core during summer, but is moist enough and has a sufficiently high thermal conductivity in winter to allow deep frost penetration. Winter snow is generally thin, so that mean annual air temperature and mean annual ground surface temperatures are closely coupled. Because of the special combination of vegetation and snow cover, palsa mires may fall beyond the limits of discontinuous mountain permafrost predicted by spatial modelling (see Section 4). However, the location of palsa mires in areas close to

the limits of permafrost development makes them highly sensitive to climatic fluctuations (e.g. Seppälä, 1988). The limiting MAAT for palsa formation is between 0 °C and −1.5 °C, though the ideal areas for palsa formation have mean annual air temperature between −3° and −5 °C and low annual precipitation (<450 mm) (Luoto et al., 2004b).

Both aggradation and degradation of palsas has been shown to occur contemporaneously on the same mires (Seppälä, 1986; Matthews et al., 1997), due to cyclic palsa development. Frost heave caused by ice segregation raises the palsa surface above the mire, but cracking eventually releases peat blocks, that slide from the edges of the mound into the surrounding mire. In this way the frozen core looses its insulation (Seppälä, 1988). In winter, the insulating peat layer becomes thinner as wind abrades the surface, again leading to palsa degradation. During the last few years, wind erosion associated with winter storms in northern Finland has caused heavy abrasion of palsas (Seppälä, 2003b).

In Fennoscandia, palsas are mainly located north of 68° 30' N latitude, but on the high fells of Norway palsas occur north of about 62°N (Fig. 44). From Fennoscandia the palsa area continues to the central Kola Peninsula north of the Arctic Circle, and towards northern Russia also south of the Arctic Circle (Oksanen, 2005). Palsas are particularly abundant in northern Finland at altitudes between 180 m and 390 m asl (Luoto & Seppälä, 2002b) where peat thicknesses are in excess of 40 −50 cm. In Scandinavia, the extent of subarctic palsa mires appears to be decreasing (e.g. Luoto and Seppälä, 2003; Luoto et al., 2004a), but some expansion of areas with palsa formation has been reported in Finnish Lapland (Seppälä, 1998; Luoto and Seppälä, 2002a). Degradation of palsas in southern Norway and in northern Sweden may be related to rising air temperatures (Sollid and Sørbel, 1998; Zuidhoff and Kolstrup, 2000), but new permafrost formation observed in places in Finland might be due to stronger winter deflation of snow (Seppälä, 2003b, 2004). In the winter 1992–93, frost penetration was deeper than normal, and in places the ground was
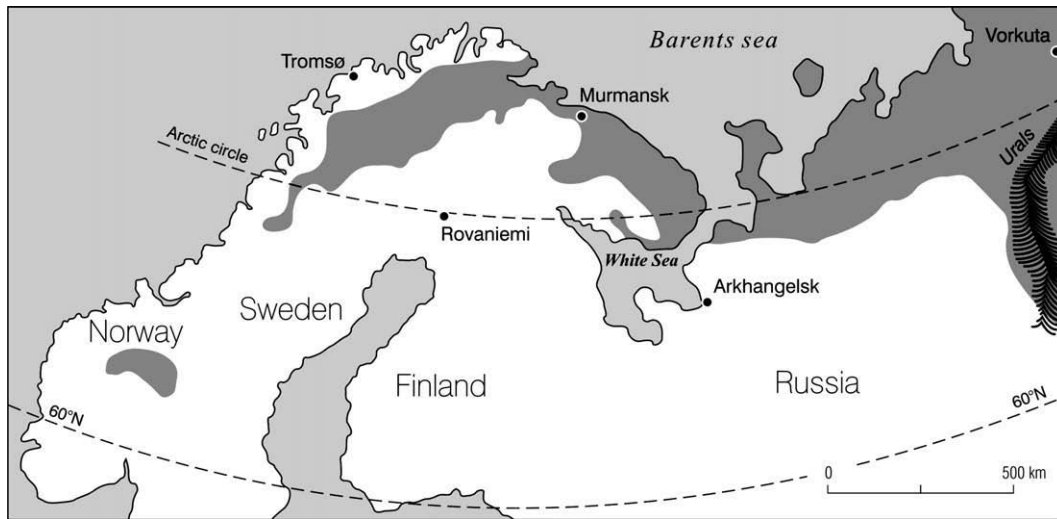
Fig. 44. The area of permafrost with palsas in northern Europe compiled from different sources (based on Oksanen, 2005).

still frozen in September 2005, with new small palsas between 2 and 6 m in diameter, and elevation 20–30 cm above the wet mire surface. The active layer of these new features was around 30 cm in September 2005.

Measurements in Finnish Lapland since 1974 (Seppälä, 1983; Rönkkö & Seppälä, 2003) indicate active layer thickness on palsas to range from 30–75 cm, tending to be thickest where palsa relief is greatest and beneath lichen-covered surfaces, and thinnest under low shrubs such as *Betula nana* (dwarf birch). Recent very warm summers have caused drying of surface peat, leading to greater insulation of the soil below and no increase in active layer thickness. In contrast, during wet summers, the surface peat stays wetter and its thermal conductivity is higher, leading to increasing active layer thicknesses.

Removal of snow from a mire surface several times during three winters between 1976–78 caused the depth of frost penetration to almost double, and a frozen layer to survive for several subsequent thawing seasons (Seppälä, 1982). Conversely, artificial thickening of snow cover by approximately 50 cm between 1997 and 2002, raised mid-winter ground surface temperatures by several degrees (Seppälä, 2003a), but summer thaw penetration was slower. In August 1999 the experimental active layer was 10 to 13 cm thinner than in an adjacent

control palsa but by 2002, the active layers were essentially the same (Seppälä, 2003a). Thus, changes in snow cover may have complex impacts on palsa thermal regime, causing surface warming in winter but slowing summer active layer thaw. The date of arrival and duration of snow may be as important as changes in snow thickness.

Radiocarbon dating of the more xerophilous peat layer that develops on palsa mounds above the general palsa mire surface allows investigation of the timing of palsa iniatiation (e.g. Vorren, 1972; Vorren and Vorren, 1975; Seppälä, 1988). However, wind abrasion may make precise dating more problematic (Seppälä, 2004). In Fennoscandia, palsa mires seem to have developed to approximately their present extent by about 2000 yr BP, though most modern palsas are less than 1000 years old (Seppälä, 2005).

11. Permafrost engineering in a changing climate

11.1. Introduction

Construction and maintenance of mountain infrastructure in permafrost terrain is an engineering challenge. Ground ice is the main problem directly affecting infrastructure, with its susceptibility
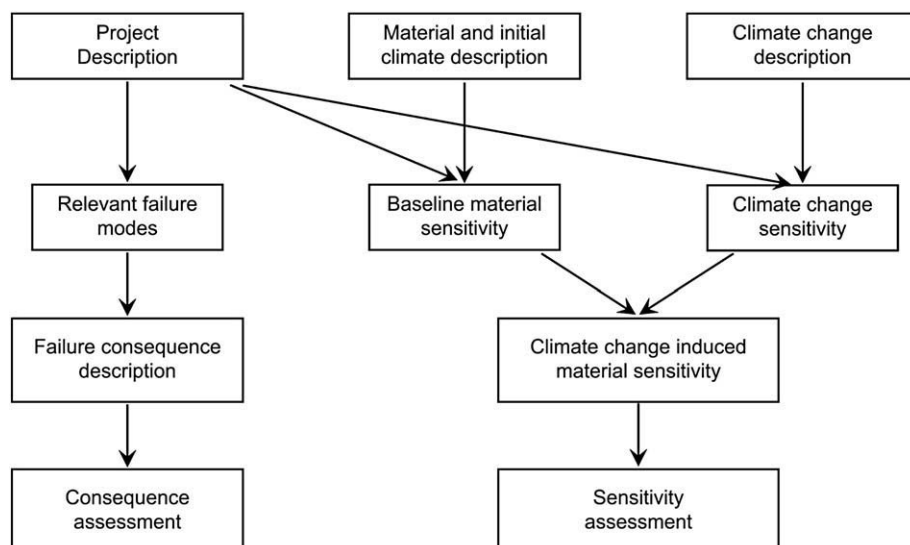
Fig. 45. Schematic of climate change screening process (PERD, 1998).

to creep, accrete and melt. Specially adapted construction and maintenance techniques are necessary in this environment, to ensure the longevity of the infrastructure. Climate change may lead to progressive modification of the permafrost thermal regime, and hence its physical properties and distribution. The rates and magnitudes of changes are difficult to predict, but since the stability and service-ability of structures may be compromised, the impacts of future climate change must be taken into account in the design of infra-structure (Instanes et al., 2005; Springman and Arenson, 2008).

In contrast to arctic regions, where infrastructure in permafrost includes entire communities (Instanes et al., 2005), there are no large permanently inhabited settlements constructed on European moun-tain permafrost. However, densely populated settlements and trans-portation routes at lower altitudes may be severely affected by processes occurring in permafrost terrain (see Section 12), requiring engineering solutions such as retention dams (Keller et al., 2002) and the establishment of hazard maps for improved land-use management (Götz and Raetzo, 2002, and see Bommer et al., 2008; Springman and Arenson, 2008). Much of the infrastructure located directly on or in mountain permafrost pertains either to tourism, communication or power-related industries and is of high economic and social significance.

11.2. Characteristics of alpine permafrost soils

Typically alpine soils are coarse, though glacial tills and rock glaciers often show well graded grain size distributions (Barsch, 1996; Arenson, 2002; Arenson et al., 2002; Springman et al., 2003; Nater et al., 2008.). The characteristics of the soil particles and their distribution affect the strength and deformation response of the frozen soil and its frost susceptibility. Although permafrost is defined by temperature, geotechnical properties are a function of both temperature and ice content. The mineralogy, particle size and pore water chemistry may change the freezing point and the unfrozen water content, so that even at temperatures some degrees below 0 °C, part of the pore water may not be frozen (e.g. Williams, 1967a,b; Anderson and Tice, 1972; Fish, 1985). Alpine permafrost may consist of solid rock with ice-filled joints, fine grained soils containing segregation ice, ice supersaturated gravels, where not all particles are in contact, or dirty ice with some dispersed solid particles distributed within the ice. Recent sampling from triple cored, air cooled drilling has shown that air contents of over 20% by volume can exist (Arenson and Springman, 2005b). The geotechnical properties and stress–strain relationships in frozen coarse grained alpine soils are discussed in section 8.3 of this paper.

11.3. Accounting for climate change

Current engineering practice demands the consideration of climate variability to ensure long-term project reliability. Global climate change adds an additional uncertainty to the design. However, statistical approaches based on historical data to predict future magnitudes and frequency of climatically-friven extreme events are no longer reliable (e.g. Bourque and Simonet, 2006; Guillaud, 2006). In 1998, the Canadian Panel on Energy Research and Development published guidelines for permafrost design affected by climate change (PERD, 1998). The report describes a screening process to account for these uncertainties. This process assesses the sensitivity of the project to climate change as well as the consequences associated with failure in a systematic way (Fig. 45). It concludes that the effort required accounting for climate change effects will not exceed what would normally be undertaken, and may possibly be incorporated into an existing design process with little modification. Fig. 46 shows a flow diagram with the questions that need to be addressed regarding climate change when constructing in alpine permafrost. The figure has been adopted and modified from the recommendations made by Instanes et al. (2005) for Arctic environments.
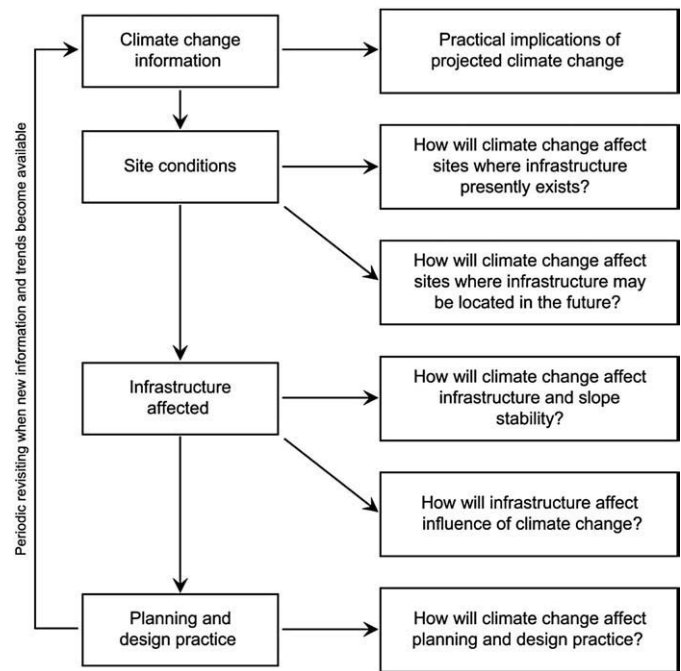

Fig. 46. Flow chart for the design of engineered structures regarding climate change (adapted from Instanes et al., 2005).

In contrast to other regions, the design life of a structure built in a permafrost environment should be planned to be 30 to 50 years, rather than 100 years. In addition, monitoring and adaptation strategies have to be implemented, that will later permit modifications to be made to the structure, as required. Since future climatic trends are difficult to predict, sensitive structures have to be re-assessed on a regular basis, as new trends and better models become available.

11.3.1. Assessing ground conditions

Laboratory and field investigations are essential in order to determine the thermal and geotechnical properties of a particular permafrost soil, in particular its ground ice content and susceptibility to thaw consolidation. The conventional approach is to drill boreholes, generating core material for testing. It is important to test the soil at the boundary conditions that are to be expected in the field. A range of testing procedures is available, such as:

- thermal needle probe measurements for thermal conductivity (ASTM, 2005).
- uniaxial compression tests for creep or strength parameters (ASTM, 2001, 2006).
- triaxial compression tests for deformation and failure mechanisms (e.g. Arenson et al., 2004).
- direct shear tests for strength characteristics of shear interfaces, in the laboratory (Davies et al., 2000, 2001; Yasufuku et al., 2003; Arnold et al., 2005) or in the field (Springman et al., 2003).
- pressuremeter tests for creep properties (Ladanyi, 1993; Arenson et al., 2003b).
- centrifuge modelling for deformation and failure mechanisms (e.g. Davies et al., 2003; Harris et al., 2007).

Clearly information derived from boreholes is specific to each sampling location, and if ground conditions are likely to vary across the site it may be advisable to investigate permafrost characteristics and sensitivity through geophysical approaches (see Section 6 of this paper), using borehole information to calibrate the resulting models.

11.4. Modification of ground thermal conditions

The challenges of construction in permafrost are generally related to thawing of ground ice, and start with a change in the ground thermal regime during or after construction (e.g. Wegmann, 1998, Dätwyler, 2004), or through climatic changes. Excavation of trenches for foundations and removal of surface vegetation may modify the energy balance, and exposure of ground ice can lead to rapid thaw. Thermal disturbance is also possible from frictional heat and water used for flushing during borehole drilling (Haeberli, 1992; Vonder Mühll et al., 2003). Tunnels can also have a disturbing effect, as air or water can warm adjacent frozen rock zones, as was observed during the drilling of access tunnels in Chli Titlis (Haeberli et al., 1997), Klein Matterhorn (Rieder et al., 1980) and in the Jungfrau east ridge (Wegmann, 1998). Measurements below steel snow-supporting structures in Switzerland, however, have shown that despite strong diurnal above ground warming, no discernable heat was conducted into the ground (Phillips et al., 2000; Phillips 2006). The main problem affecting such structures are temperature- and water dependent creep movements of the ice rich permafrost soils in, which they are anchored (Rieder et al., 1980; Phillips et al., 2003a).

Hydration heat generated during curing of concrete or grout can melt large quantities of permafrost ice. For instance, during construction of the midway station for a chairlift in Grächen (Swiss Alps) in 1997 at 2450 m a.s.l., severe permafrost ice degradation occurred, with, as a consequence, settlement, cracking of the concrete and pronounced creep of the structure, that had to be replaced completely in 2003 (Phillips et al., 2007). Subzero ground temperatures can also cause freezing of concrete or grout, impairing the curing process before the appropriate bearing capacity is attained. Anti-freeze additives (Moser, 1999) or warm water (SLF/BUWAL, 2000; Thalparpan, 2000) may be used to delay freezing and ensure that the curing process can be achieved successfully but will disturb the thermal regime of the permafrost. These aspects must therefore be considered carefully in terms of the effect on the ice content and long term stability of the ground.

Infrastructure in snowy, windy areas, including avalanche defence structures, may modify snow cover distribution (Hestnes, 2000; Thiis and Jaedicke, 2000) and thus affect the thermal regime of the ground. The use of technical snow in modern ski piste preparation can lead to long-term lowering of ground temperature due to the higher density and thermal conductivity of technical snow (Fauve et al., 2002). Indeed, Rixen et al. (2004) suggest that at Alpine sites where mean ground temperature is close to 0 °C, the additional temperature reduction may suffice to induce permafrost formation.

11.5. Technical solutions

In order to reduce the risk of failure of a structure or a slope in a permafrost environment, thermal stability of the ground has to be the main goal. Even during pre-construction activities, thermal disturbances should be minimised through the use of insulation materials (Thalparpan 2000) and drilling using chilled air flushing rather than fluids (Arenson, 2002; Vonder Mühll et al., 2003). Passive cooling systems such as thermosyphons, thermoprobes, air-duct cooling systems and gravity-driven air convection offer another possibility (Smith et al., 1991; McKenna and Biggar, 1998; Goering et al., 2000; Goering, 1998; Cheng, 2005; Wen et al., 2005; Arenson et al., 2006; Ma et al., 2006), but their efficiency in alpine environments is still to be tested.

Adaptable systems that have no stiff connection to their foundations, or structures on point bearings, are designed to accommodate terrain movements such as creep and settlement since their geometry can be subsequently corrected (Phillips et al., 2003b). The new chairlift midway station in Grächen, Switzerland, is an example of this type of structure: the two concrete supports are carried by a T-shaped girder with three point bearings (two upslope and one downslope), all of, which can slide horizontally to enable the entire midway station to find its optimal equilibrium position (Phillips et al., 2007). Adaptable systems need to be monitored at regular intervals to allow timely geometrical corrections to be made.

11.6. Long term monitoring of structures and substrates in mountain permafrost

Thermal monitoring is an essential contribution toward the longevity of infrastructure in mountain permafrost. If the thermal regime of the undisturbed site is known in advance in combination with its geotechnical characteristics, the impact of construction activities and climate can be predicted more precisely (Haeberli et al., 1997; Delaloye et al., 2000) and ground deformations foreseen (Steiner et al., 1996). Thermal monitoring should extend through pre-construction (providing baseline data), construction and operational phases at various depths on the site and in the surrounding terrain. Failure to carry out adequate thermal analysis can have serious consequences, such as complete structure replacement after a few years (Phillips et al., 2007). Post construction instrumentation is possible, but the effects of earlier construction activity cannot be construed and it may also be difficult to drill boreholes near or under existing infrastructure. During construction, thermistors can be installed between the structure and the ground, in intermediate insulating materials or air spaces and within the structure itself. Mobile miniature data loggers can be placed in strategic positions and moved whenever necessary (Hoelzle et al., 1999).

Monitoring ground and structural deformation is also crucial for the serviceability of any structure in an alpine permafrost environment. Adaptation strategies have to be designed in advance and have to be applied as critical deformation thresholds are reached. Ground based surveying is the easiest approach to detecting surface deformation, but a range monitoring techniques is available, depending on the structure and situation. Measurement of borehole deformation using inclinometers and extensiometers allow monitoring of ground movements (e.g. Arenson et al., 2002). Time domain reflectometry (TDR) can be used to locate shear zones at depth with more precision than inclinometers (Kane et al., 1996; Arenson, 2002), but the direction and magnitude of strain can only be estimated. Seasonal and long-term changes in pore water pressure have a fundamental effect on the shear strength of soil and measurements of water pressures and moisture contents within the active layer using TDR technologies (O'Connor and Dowding, 1999) or pore pressure transducers (Harris et al., 2008b), allow potential ground deformation processes to be recognised in a timely fashion.

11.7. Engineering in mountain permafrost: the challenge of climate change

In future, infrastructure design, construction methods and monitoring systems in mountain permafrost regions must be adapted to observed trends in climate. Designs should therefore allow for such future adaptations. Before optimum construction techniques can be achieved, further knowledge about the thermo-mechanical behaviour of ice-rich permafrost in response to warming (natural or artificial) is needed. There is a particularly urgent need for the development of guidelines that include risk assessment procedures and economic impact analyses for the construction and maintenance of infrastructure in mountain permafrost. Geotechnical risk assessment requires input from geothermal modelling of permafrost distribution in a changing climate, and from geomorphological process studies that may improve prediction of the nature, magnitude and frequency of permafrost related geohazards. Not only are the structures in mountain permafrost environments endangered, but also those buildings and infrastructure located below any permafrost occurrences. Rock falls,

debris flows and other forms of slope instabilities triggered within the permafrost environment may have severe consequences on infrastructure situated at lower altitudes. Periodic risk assessment and re-evaluation of existing hazard zoning have to be carried out, while incorporating knowledge and understanding of all the diverse but interconnected aspects of climate impact on permafrost.

12. Permafrost hazards

A key issue regarding the assessment of mountain permafrost hazards is the degree to, which climate change may influence the future magnitude and probability of potentially hazardous events. Permafrost hazards generally arise from thawing of ice-bonded frozen debris and rock walls (Harris et al., 2001c), and pose a risk to people and infrastructure. Construction works may be damaged by thaw settlement and slope failures (debris flows, landslides or rockfalls), and serviceability of installations on creeping permafrost may also be compromised (see Section 11). A greater frequency of extreme summers, such as that experienced in Europe in 2003, is likely to lead to significant increases in seasonal thaw depths (see Section 3.3) and problems related to permafrost may become an increasing cost factor in the maintenance or construction of high-mountain infrastructure (Kääb et al., 2005a).

12.1. Creeping frozen debris

Rock glaciers are able to displace debris volumes of the order of 10^3 to 10^4 m^3 per millennium, and the current trend towards higher ground temperatures may be responsible for an apparent increase in creep rates in many Alpine rock glaciers (see Section 8.7). Structures, such as cableways constructed where permafrost creep is active, clearly run the risk of increased maintenance costs and in the absence of appropriate engineering solutions (see Section 11.5) may eventually become unserviceable.

Rock glaciers also act as reservoirs of potentially unstable debris within debris flow initiation zones (Holzle et al., 1998; Frauenfelder, 2006; Roer et al., 2008). An analysis by Arnold et al. (2005) of the stability of the active layer of a rock glacier in Switzerland showed that interlocking in the coarse, elongated and angular particles causes significant dilatancy and hence generates extremely high shear strength parameters. However, sliding over a possible massive ice layer at the permafrost table might be of concern if the interface angle of friction reduces to about half the peak internal angle of friction of the rock glacier materials. Field data relating to hydrothermal processes developing within the active layer (ground temperatures, water contents and deformation rates) have confirmed this concern (Rist and Phillips, 2005).

Ground temperatures have been shown to increase rapidly during snow melt because of convective heat fluxes, and latent heat release during refreezing of water onto the permafrost table. Meltwater seepage will also tend to reduce the effective stresses, while refreezing enhances the ice layer, providing a potential sliding surface. Where a rock glacier has advanced onto steeper ground, debris falls along the steep rock glacier front (Bauer et al., 2003; Kääb and Reichmuth, 2005) may increase the local hazard, and if the ground falls steeply away below the rock glacier, slides and debris flows may affect much greater areas (Kaufmann and Ladstädter, 2003; Kääb et al., 2007; Roer et al., 2005, 2008).

12.2. Warming permafrost on soil-covered slopes

Increasing ground temperatures in ice-rich permafrost is likely to cause extensive thaw settlement and thermokarst processes in arctic lowlands, and thaw-related slope instability in both arctic and lower latitude mountain areas (Harris et al., 2001b; Nelson et al., 2001; Haeberli and Burn, 2002) (see Section 9.3). The latent heat effects of an
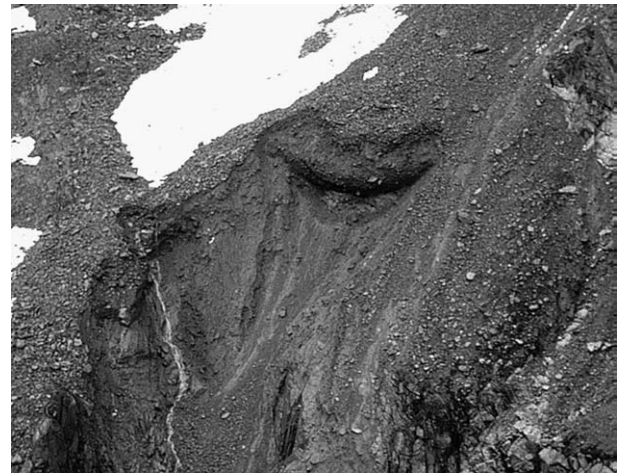
Fig. 47. Debris flow source area in the front of a frozen debris body. Here, groundwater concentration and active layer thickening provide an important trigger. Photo: W. Haeberli, 1987.

ice-rich transient layer immediately below the permafrost table reduces thaw penetration (Shur et al., 2005) but also increases the volume of meltwater released, increasing the risk of landsliding in areas with finer-grained soils. Greater active layer thicknesses associated with climate change will also tend to increase the likelihood of slope failure (e.g. Lewkowicz and Harris, 2005b) and increase the volume of displaced material, while the loss of cementing ground ice is likely to increase retrogressive erosion caused by debris flows (Fig. 47) (Haeberli, 1992; Zimmermann and Haeberli, 1992).

In cold mountainous regions, ground thermal conditions in moraines are often a crucial factor in the damming of moraine lakes (see below). Permafrost or near-permafrost conditions support the long-term preservation of dead ice bodies, but ice melting may leave cavities (Richardson and Reynolds, 2000). Sudden release of meltwater stored in such cavities may lead to significant hazard. Differential thaw settlement is frequently associated with the formation of thermokarst lakes that continue to develop through positive feedback mechanisms of water convection and latent heat effects, leading to further ground ice melt (Kääb and Haeberli, 2001). In such unstable terrain, sudden lake drainage is likely. Glaciers and permafrost often coexist in close spatio-temporal proximity. For instance, permafrost may aggrade in recently deglaciated glacier forefields, thereby altering the thermal, hydrological and dynamic conditions of glacial deposits, and influencing related hazards. These effects are of increasing importance in the light of the current pronounced worldwide glacier retreat.

12.3. Warming permafrost in rock walls

The significance of warming permafrost to the stability of rock walls is reported in detail in Section 7 of this paper, but the role of partially glacierised alpine rock faces where complex thermomechanical conditions are found (Kääb et al., 2004; Fischer et al., 2006) has not been discussed. Through advection of temperate firn, steep glaciers may not be frozen to their beds for much of their lengths, but enhanced heat flux near the lower margin leads to cold frontal sections that have a stabilising influence. Though little understood, it is clear that changes in surface temperatures can cause complicated feedback mechanisms and chain reactions both for rock and glacier stability. In that context, the retreat of steep glaciers and the resulting exposure of rock surfaces might have even more drastic and rapid consequences than a rise in mean annual air temperature itself. Beside the thermally-governed impacts, retreat of steep glaciers leads to de-stressing of the underlying and surrounding

rock wall. It appears that increasing rockfall activity and a number of large rock avalanche disasters might have been influenced by thermo-mechanical changes.

12.4. Glacier-permafrost interactions

Widespread melting of glaciers and rising permafrost temperatures provide an early indication of the environmental and societal significance of global warming (Haeberli and Beniston, 1998; Reiersen, 2005). In both high latitude and high altitude mountains, glaciers commonly interact with permafrost, leading to potentially hazardous geomorphological processes at the temporal and spatial interface between them. A dramatic example, though geographically peripheral to the European sphere of mountain permafrost, was on the north-northeast face of Dzhimarai–Khokh (4780 m a.s.l.), North Ossetia, Russian Caucasus, where on 20 September 2002, 10 million m^3 of rock and ice broke away, falling onto the the underlying Kolka glacier, which in turn sheared off (Fig. 48). As a result, a sledge-like rock-ice avalanche with a volume of about 100 million m^3 and speeds of up to 300 km/h overran parts of the village of Karmadon. Subsequently, the moving mass was blocked by the narrow Genaldon gorge, damming rivers and ejecting a mudflow with devastating effects (Fig. 49). The catastrophic event travelled over a total distance of 33 km, leaving over 100 people killed, and buildings and the main access roads in the valley completely destroyed (Haeberli et al., 2004; Kotlyakov et al., 2004). The resulting damage added up to a total of nearly 20 million EURO. Subsequent risk assessment was based on an integral approach for hazard analysis that implies the reconstruction of the event and all processes involved (cf. Petak and Atkisson, 1982).

Bedrock surface temperatures in the detachment zone were estimated at about −5 to −10 °C (Haeberli et al., 2003, 2004), indicating permafrost within the source area of the rockfall that triggered the event (Haeberli et al., 2003; Frauenfelder et al., 2005).

Fig. 49. ASTER false colour imagery from before (left) and after (right) the 20 September 2002 Kolka–Karmadon disaster. A large rock/ice avalanche from the north face of the Dzhimarai–Khokh peak (bottom) sheared off the entire Kolka glacier tongue. The rock-ice mass filled the valley of Genaldon from the Kolka glacier cirque (lower left) to the gorge of Karmadon (centre). The debris swept through the Genaldon river valley and backed up at the entrance of the narrow gorge of Karmadon (centre), leading to the creation of several large lakes in upstream direction and the ejection of a mudflow trough the gorge far into the lowlands (top). Images: ASTER data.

Prior to the rock fall, the slope had been covered by hanging glaciers that introduced deep-seated thermal anomalies within the bedrock (Haeberli et al., 1997). It is likely, therefore, that the detachment zone at Dzhimarai–Khokh was thermally complex with relatively cold and thick permafrost adjacent to much warmer, if not unfrozen, bedrock within, which meltwater could flow (Haeberli, 2005). Though similar events have apparently occurred in the region before (e.g. Kolka Glacier ice avalanches in 1902), it is not clear whether permafrost–glacier interactions had also played a role in these earlier events. The large run-out distance of the event and the difficult access made spaceborne remote sensing an important tool in assessing the damage (Kääb et al., 2003a,b; Huggel et al., 2005).

12.5. Emerging methodologies and challenges

The assessment of glacier and permafrost hazards requires systematic and integrative approaches. Historical data can be used to test spatial models based on new earth observation and geo-informatics techniques. Such modern methodologies provide powerful tools to assist hazard assessments in complex mountain systems that are experiencing increasing change and divergence from equilibrium conditions (Kääb et al., 2005a). Currently, the most successful strategy is based on the combination of remote sensing, modelling with Geographical Information Systems (GIS), geophysical soundings and other local field surveys and intrusive sampling

Fig. 48. Starting zone of the devastating 20 September 2002 rock-ice avalanche in Kolka-Karmadon, Caucasus (North Ossetia, Russia). The rock-ice avalanche broke off the north-northeast face of Dzhimarai-Khokh, a rock face with complex thermal and mechanical interactions between steep glaciers and frozen rock. Photo: Igor Galushkin, 25.09.2002.

techniques. These methods are best structured in a downscaling approach from area-wide first-order assessments for systematically detecting hazard potentials (i.e. the domain of space-borne remote sensing and GIS-techniques) to detailed ground-based or airborne local investigations in high-risk areas (i.e. the domain of geophysics, surveying, and air-borne and close-range remote sensing) (Kääb et al., 2005a).

12.6. Mapping

A pre-condition for precise hazard mapping is the availability of up-to-date and accurate topographic maps. Since such publicly available data are lacking in many areas, air- and space-borne optical imagery (e.g. Corona, Landsat series, Aster, Ikonos, QuickBird) and microwave data (e.g. ERS, Radarsat, Envisat, Shuttle Radar Topography Mission) can be used instead. Such data can be used to inventory and classify glaciers, lakes, areas prone to mass movements, and debris and other terrain types relevant to glacier and permafrost hazards (e.g. Leber et al., 1999; Kääb et al., 2005b, Kääb 2008). Remotely sensed data can also be used to derive digital elevation models (DEM), a fundamental prerequisite for analysing hazard potential in high-mountains and for related GIS-modelling (Huggel et al., 2003; Kääb et al., 2005b). Even ice flow and terrain displacements can be measured with high accuracy from repeated remote sensing data (Kääb et al., 2005b, Kääb 2008). Using these methods, terrain cover, geometry and dynamics of an area can be investigated without direct access.

12.7. Modelling

A further step towards an integrative hazard assessment consists in the application of GIS and other numerical models for simulating complex processes that are undetectable by remote monitoring. Glacier lake outburst floods, ice avalanches or debris flows can be modelled with a GIS (e.g. Huggel et al., 2003, Kneisel et al., 2007; Salzmann et al., 2004). Also, permafrost distribution, approximate ground-, firn- and ice-temperatures, or various other terrain parameters that have an impact on natural hazards can be computed. Integration of remote sensing results and numerical process models provides a particularly promising basis for the assessment of hazard potential (e.g. Huggel et al., 2003; Kääb et al., 2005b).

12.8. Ground-based methodologies

A more detailed analysis of the hazard sources detected by remote sensing often involves ground-based methods. Geophysical investigations, employing electrical resistivity tomography and ground penetrating radar (see Section 5.2 of this paper), in particular, have been used to develop three-dimensional ground models and have provided information on potential causes of instability such as buried ice bodies within moraine dams that could lead to breaches in the dam if the ice were to melt (Richardson and Reynolds 2000; Pant and Reynolds, 2000). High spatial and temporal resolution of terrain dynamics also demands detailed terrestrial surveying using laser technology or Global Navigation Satellite Systems (GNSS).

12.9. Challenges

Climatically-driven changes in the thermal status and spatial distribution of glaciers and permafrost are leading to perturbation of their dynamic equilibria, with transient conditions shifting hazard zones beyond the range of variability documented in historical archives. For instance, modelling suggests that the lower boundary of permafrost distribution in the Swiss Alps rose at an average vertical rate of 1 to 2 m per year between 1850 and the present (Frauenfelder et al., 2001). Current temperature observations in the Alps suggest the

rate is now close to 2 m per year. If, in fact, environmental conditions in high-mountain regions were to evolve beyond the range of Holocene and historical variability, hazard assessments may become increasingly difficult because estimates of hazard potential based on empirical data from the past (historical documents, statistics, geomorphological evidence) will not be directly applicable under new conditions. In future, prediction of hazard and risk is likely to depend on process-based modelling, especially with respect to slope stability problems. The potential of coupling remote sensing with numerical modelling should be fully exploited, and knowledge transferred to vulnerable regions in the second and third world. Downscaling approaches from initial regional-scale assessments of hazard potentials towards high resolution and high precision site-scale observations and simulations are needed as a response to the current environmental changes (Salzmann et al., 2007a,b).

Magnitude-frequency relations of catastrophic events are one of the key parameters required for risk assessment and the design of engineering solutions. Such relationships are particularly difficult to estimate for permafrost and glacier hazards in mountains due to the complex chain reactions involved. In many cases, large magnitude events occur in remote mountain areas, and are often unnoticed and undocumented. This leads to highly non-uniform and incomplete global event documentation, further complicating the estimation of magnitude-frequency relations. Past (e.g. Lateglacial to Holocene) and historic (e.g. end of Little Ice Age) transitions in permafrost and glacier conditions suggest that adjustments in thermal conditions towards a warmer phase are accompanied by intensified mass movement events. For a number of periglacial and glacial processes, both the event frequency and magnitude might temporarily increase until the corresponding sediment reservoir is exhausted and/or new equilibrium conditions are reached (e.g. Ballantyne, 2002; Curry et al., 2006).

13. Conclusions

This paper provides an overview of the status of permafrost within the European sector, from the discontinuous high mountain permafrost zone in the Alps, to the continuous permafrost of Arctic Svalbard. Much of the research in the last decade originated from the European Union PACE project. Assessment of the impacts of climate change in the sensitive permafrost domain requires an infrastructure for monitoring, and this has been a major achievement over the past decade. In addition, new geophysical methods of permafrost characterisation and mapping have been developed, modelling protocols are being refined to allow impact assessments of future climate scenarios, geomorphologic studies have improved understanding of processes and their likely responses to climate change, and research outcomes have been integrated to provide better understanding of potential permafrost-related hazards and engineering solutions in the context of a changing climate. Data arising from this on-going research will become increasingly valuable as time series become longer, and we report here a snapshot of one decade of progress. The major conclusions to be drawn may be summarised as follows.

1. Palaeoclimate reconstructions provide a critical context for assessing current trends and their potential impacts in permafrost regions. In Europe, Holocene climate fluctuations apparently increased in amplitude with increasing latitude, so that during the climatic optimum, mean annual air temperatures in the Alps were only a degree or so higher than the late 20th Century, while in northern Scandinavia the difference was up to 2 °C and in the arctic archipelago of Svalbard, temperatures between 3–4 °C higher than recent norms. Similarly, during the Little Ice Age in Svalbard, mean annual air temperatures are inferred to have been 4–6 °C below late 20th century values, and in the Arctic Maritime Zone generally, around 3 °C cooler, while in the Alps the difference was less than one degree Celcius.
2. During the 20th Century, air temperatures have tended to increase across mainland Europe, though with greater warming in

Scandinavia than elsewhere during the early part of the century. Since 1975 warming has been more marked during autumn and winter in Scandinavia, but greatest in spring and summer in central Europe.

3. Change in active-layer thickness is a key response of permafrost to climate forcing. In the PACE bedrock boreholes, maximum inter-annual variation has been 20% at Janssonhaugen (Svalbard) and Juvvasshøe (southern Norway), 30% at Stockhorn and 100% at Schilthorn (Swiss Alps). This contrasts with the ice-rich Murtèl–Corvatsch borehole (Swiss Alps) where although the active-layer has increased in thickness by around 16% since 1987, inter-annual variations are less than 4%. Latent heat exchanges dominate the thermal response at Murtèl–Corvatsch, while heat conduction is dominant in the bedrock examples.

4. The extreme summer of 2003 led to warming of near-surface permafrost and thaw penetrating some 4.5 m deeper than in previous years on Schilthorn, and around 1 m deeper on Stockhorn. Across steep Alpine slopes containing ice-bonded discontinuities, this scale of active-layer thickening significantly increased the risk of rockfall events.

5. Consistent warm-side deviations are observed in all the PACE borehole thermal profiles, but in the Alps, the complex topography and variable ground surface interface makes derivation of the climate signal from a given thermal profile a very difficult problem. In contrast, the three boreholes in Svalbard and Scandinavia are located in subdued topography, and permafrost temperatures are strongly coupled to atmospheric temperatures. Here thermal profiles have been interpreted as indicating surface warming of ~1.4 °C, ~1.1 °C and ~1.0 °C over the past few decades at Janssonhaugen (Svalbard), Tarfalaryggen (northern Sweden) and Juvvasshøe (southern Norway) respectively (Isaksen et al., 2007a,b).

6. Time series data from the three northernmost PACE boreholes suggest rapid recent warming, rates at the permafrost table being estimated as 0.04–0.07 °C yr^{-1}, warming being greater at Janssonhaugen and Tarfalaryggen than at Juvvasshøe. In the Swiss Alpine bedrock boreholes time series are shorter and strongly affected by short term seasonal extremes such as the cold winter of 2001–2002 and the hot summer of 2003. However, at depth there is evidence for warming, at Stockhorn, for instance, rates are around 0.01 °C yr^{-1} at 48.3 m depth, and at Schilthorn, similar or slightly higher warming rates are indicated. Trends observed in the ice-rich frozen debris at Murtèl–Corvatsch indicate significant warming over the past 20 years, but the record is dominated by the influence of snow depth and duration rather than atmospheric temperatures.

7. Mapping permafrost distribution and forecasting change is generally based on numerical modelling. The scale of the modelling is critically important, with atmospheric/oceanic circulation patterns and latitude dominating at a global and continental scale, topography appearing as a major factor at regional and local scales, and surface and subsurface properties becoming increasingly important at finer resolutions. A major problem remains in bridging between continental and local scales and this is particularly important when the outputs from Regional Climate Models (RCMs) are downscaled to meet the needs of local scale permafrost models.

8. Two permafrost modelling approaches have been developed, firstly, regionally calibrated empirical-statistical models, and secondly, more physically based process-oriented models. The former may not be applicable in other regions, are limited by assumptions of steady-state conditions, and neglect complex three dimensional topographic effects. Since process-oriented approaches compute surface temperatures and thermal conditions at depth, they are better suited to estimating transient effects in complex topography.

9. The modelling sequence Global Circulation Models–Regional Circulation Models–Energy Balance Models–Heat Transfer Models within three-dimensional topography is identified as a key approach in the future, with emphasis on transient effects that require coupling of time-dependent surface and subsurface ground thermal conditions.

10. Three geophysical properties; electrical resistivity, the dielectric permittivity and the seismic compressional wave velocity, are sensitive to permafrost temperature and ice content. Diffusive electromagnetic, geoelectric, seismic and ground-penetrating radar (georadar) techniques have therefore proved most suitable for determining the distribution and internal structure of frozen ground, and through use of fixed electrode arrays, monitoring of changing permafrost conditions. However, in all cases, accurate calibration of geophysical models against borehole information is required.

11. Recent developments have included the combination of information from several geophysical data sets, using for instance, a fuzzy-logic approach to delineate areas where the occurrence of ground ice is most likely, or the so-called 4-phase model to estimate volumetric fractions of rock, soil matrix, unfrozen water, ice, and air within the ground.

12. The distinctive suite of permafrost geomorphologic processes are intimately related to the presence of, or changes in, ground ice. Understanding these processes is a critical element in formulating adequate assessments of geological hazards and risks in permafrost regions, and to the development of suitable engineering strategies.

13. Monitoring has shown that near-surface freeze-thaw rock weathering is limited by the availability of water, but is responsible for generation of small-scale rock debris. Laboratory studies have emphasised the potential for ice-segregation to occur in porous rocks, and shown that ice volume and frequency of cracking are highest in the upper parts of the permafrost profile. Ice lenses and their bedrock discontinuities form parallel to the isotherms, which are generally parallel to the ground surface. Thus, ice segregation may play a key role in generating rock masses that are susceptible to major rock falls during permafrost warming and active layer thickening.

14. In the Alps the rapid increase in active layer thickness during the extreme summer of 2003 was associated with greatly increased rock fall activity within the permafrost zone and many detachment surfaces revealed ice that formerly cemented the discontinuities along, which failure occurred. Thus, there is good circumstantial evidence that warming and melting of near-surface permafrost during such extreme events will generate a significant increase rockfall frequency.

15. Over much longer timescales, permafrost warming may lead to a rise in the lower permafrost boundary, decreasing permafrost thickness by bottom-upward thawing, and hence increasing the risk of large, deep-seated landslides. The Brenva Glacier rock avalanche (Deline, 2002) that occurred in January 1997, may be related to such deep-reaching and long-term changes of the subsurface thermal conditions. Thus, the probability of large-scale rock falls (millions of cubic meters and more) is likely to increase with time in a period of climate warming.

16. Rock glaciers develop due to permafrost creep where ground ice content in frozen debris is high. Since creep is largely dependent on the ground temperature, warming is expected to increase rock glacier deformation, especially where ground temperatures are close to 0 °C. Investigations confirm a significant recent acceleration of many rock glaciers in the European Alps, where an air temperature increases of close to +1 °C have occurred since the 1980s.

17. Seasonal thawing of ice-rich fine-grained soils leads to solifluction and shallow debris flows or landslides. In Alpine regions, changes in solifluction rates in response to future changes in atmospheric thermal conditions and snow fall regime are likely to be complex and site specific. In the continuous permafrost terrain of Svalbard, however, rising air temperatures and an increase in frequency of warm years are likely to cause greater active layer depths and a marked increase in both rates of solifluction and the volume of sediment transported annually.

18. Debris flows require an unfrozen sediment source area, and are usually triggered by high intensity summer rainfall events. Recent evidence suggests that in the Alps, debris flow starting zones are migrating to higher elevations, but there is no clear indication of increased debris flow activity in these zones, despite the likely increase in potentially unstable sediment as glaciers retreat and permafrost degrades.

19. In the continuous permafrost of Svalbard, monitoring of thermal contraction cracking and formation of vein ice has suggested that the thermal limit for significant cracking to occur corresponds to a fall in winter air temperatures of at least 15–25 °C over one or two days. Climate warming might therefore reduce the frequency of cracking, and through active layer thickening, lead to an overall reduction in the volume vein ice by reducing the length of existing ice wedges.

20. Palsas occur across subarctic Europe, from Iceland, across Scandinavia to Russia, and represent outliers of sporadic permafrost that form isolated lenses in peat-covered mires. Deflation of snow is critical for their formation. Changes in winter snow regime therefore strongly modulate the effects of atmospheric warming, but there is evidence that palsa mires are shrinking across northern Europe.

21. Just as many of the geomorphological processes specific to permafrost regions relate to ground ice, so ground ice is the main problem directly affecting engineering and infrastructure. Thus, detailed ground investigations of the site and its hinterland prior to any construction work should focus not only on geotechnical characteristics, but also on establishing ground ice content and composition and ground thermal conditions. Ground ice is susceptibile to creep and may accrete or melt, all of, which may adversely affect the longevity of engineering stuctures. Frost heaving, thaw settlement, and on sloping ground, thaw-induced slope instability may directly affect structural integrity. An additional threat is at lower elevations that lie within the run-out zones of rock falls, landslides and debris flows.

22. A range of engineering solutions are available, but the importance of monitoring should not be forgotten, and in view of uncertainties relating to future climate impacts, design lifetimes of no more than 30–50 years may be appropriate for many structures in permafrost areas.

23. Permafrost hazards generally arise from ground instability caused by thawing of ice-bonded frozen debris and rock walls, and pose a risk to people and infrastructure. Instability of rock walls is considered in conclusions 14 and 15, above, but in addition to permafrost effects, hazardous ground conditions may also arise from glacier-permafrost interactions. Rapid decay of glacier ice on steep bedrock slopes may lead to ice falls, complex geothermal conditions in bedrock may trigger unforeseen rock fall events, and decay of buried ground ice may cause catastrophic proglacial lake drainage.

24. Assessment of permafrost hazard in the context of changing climate should be based on the combination of remote sensing, modelling with Geographical Information Systems (GIS), and field investigations using geophysics and intrusive sampling approaches. Area-wide first-order assessments to detect hazard potentials (i.e. the domain of space-borne remote sensing and GIS-techniques) should be followed by progressively more detailed ground-based or airborne local investigations in high-risk areas, including permafrost modelling approaches to assess potential change, and the establishment of monitoring strategies to provide early warnings.

25. Finally, risk assessment strategies require accurate information on the future magnitude and frequency of hazardous events. Data may be derived from forecasting changes in occurrence and intensity of extreme climatic events, but information on hazard occurrence, magnitude and frequency may be difficult to aquire in remote and sparsely populated regions. For this reason, prediction of hazard and risk is likely to depend on process-based modelling, demanding a better understanding of geomorphological process-response systems. Thus there remains a need for continued integrative research in permafrost regions between atmospheric scientists, permafrost scientists, geomorphologists and geotechnical engineers.

References

Akagawa, S., Fukuda, M., 1991. Frost heave mechanism in welded tuff. Permafrost and Periglacial Processes 2, 301–309.

Åkerman, H.J., 2005. Relations between slow slope processes and active-layer thickness 1972–2002. Kapp Linné, Svalbard Norsk Geografisk Tidsskrift 59, 116–128.

Allard, M., Kasper, J.N., 1998. Temperature conditions for ice-wedge cracking: field measurements from Salluit, Northern Quebec. In: Lewkowicz, A.G., Allard, M. (Eds.), Permafrost, Proceedings, 7th International Conference, Yellowknife, Canada, Centre d'etudes nordiques, Universite Laval, Collection Nordicana 57, Quebec, pp. 5–11.

Andersland, O.B., Ladanyi, B., 2004. An introduction to frozen ground engineering. John Wiley & Sons, Inc., Hoboken, New Jersey. xii, 363 pp.

Anderson, D.M., Tice, A.R., 1972. Predicting unfrozen water content in frozen soils from surface area measurements. No. 393. Highway Research Record.

Archie, G.E., 1942. The electrical resitivity log as an aid in determining some reservoir characteristics. American Institute of Mining and Metallurgical Engineers, pp. 55–62.

Arcone, S., Lawson, D., Delaney, A., Strasser, J.C., Strasser, J.D., 1998a. Ground-penetrating radar reflection profiling of groundwater and bedrock in an area of discontinuous permafrost. Geophysics 63 (5), 1573–1584.

Arcone, S.A., Lawson, D.E., Delaney, A.J., Strasser, J.C., Strasser, J.D., 1998b. Ground-penetrating radar reflection profiling of groundwater and bedrock in an area of discontinuous permafrost. Geophysics 63, 1573–1584.

Arenson, L.U. 2002. Unstable alpine permafrost: a potentially important natural hazard. Ph.D. dissertation, Institute for Geotechnical Engineering ETH, Zurich. Available from http://e-collection.ethbib.ethz.ch/show?type=diss&nr=14801.

Arenson, L.U., Springman, S.M., 2005a. Mathematical description for the behaviour of ice-rich frozen soils at temperatures close to zero centigrade. Canadian Geotechnical Journal 42 (2), 431–442.

Arenson, L.U., Springman, S.M., 2005b. Triaxial constant stress and constant strain rate tests on ice-rich permafrost samples. Canadian Geotechnical Journal 42 (2), 412–430.

Arenson, L., Hoelzle, M., Springman, S., 2002. Borehole deformation measurements and internal structure of some rock glaciers in Switzerland. Permafrost and Periglacial Processes 13 (2), 117–135.

Arenson, L.U., Almasi, N., Springman, S.M., 2003a. Shearing response of ice-rich rock glacier material. In: Phillips, M., Springman, S.M., Arenson, L.U. (Eds.), Eighth International Conference on Permafrost. A.A. Balkema, Zurich, Switzerland, pp. 39–44.

Arenson, L.U., Springman, S.M., Hawkins, P.G., 2003b. Pressuremeter tests within an active rock glacier in the Swiss Alps. In: Phillips, M., Springman, S.M., Arenson, L.U. (Eds.), Eighth International Conference on Permafrost. A.A. Balkema, Zurich, Switzerland, pp. 33–38.

Arenson, L.U., Johansen, M.M., Springman, S.M., 2004. Effects of volumetric ice content and strain rate on shear strength under triaxial conditions for frozen soil samples. Permafrost and Periglacial Processes 15 (3), 261–271.

Arenson, L.U., Sego, D.C., Newman, G., 2006. The use of a convective heat flow model in road designs for Northern regions. Climate Change Technology Conference, Ottawa, Ontario, Canada. CD-ROM.

Arenson, L.U., Springman, S.M., Sego, D.C., 2007. The rheology of frozen soils. Applied Rheology 17 (1), 12147–1–12147–14.

Arnold, A., Thielen, A., Springman, S.M., 2005. On the stability of active layers in alpine permafrost. 11th International Conference and Field Trip on Landslides (ICFL). Taylor & Francis, Netherlands, Trondheim, Norway, pp. 19–25.

ASTM, 2001. D 5520, Standard test method for laboratory determination of creep properties of frozen soil samples by uniaxial compression.

ASTM, 2005. D 5334, Standard test method for determination of thermal conductivity of soil and soft rock by thermal needle probe procedure.

ASTM, 2006. WK10696, New standard test method for laboratory determination of strength properties of frozen soil at a constant rate of strain.

Ballantyne, C.K., 2002. Paraglacial geomorphology. Quaternary Science Reviews 21 (18–19), 1935–2017.

Ballantyne, C.K., Harris, C., 1994. The Periglaciation of Great Britain. Cambridge University Press, Cambridge. 330p.

Barber, K.E., Chambers, F.M., Maddy, D., Stoneman, R., Brew, J.S., 1994. A sensitive high resolution record of late Holocene climatic change from a raised bog in northern England. The Holocene 4, 198–205.

Barnekow, L., Sandgren, P., 2001. Palaeoclimate and tree-line changes during the Holocene based on pollen and plant macrofossil records from six lakes at different altitudes in northern Sweden. Review of Palaeobotany and Palynology 117, 109–118.

Barsch, D., 1992. Permafrost creep and rockglaciers. Permafrost and Periglacial Processes 3, 175–188.

Barsch, D., 1996. Rockglaciers: indicators for the present and former geoecology in high mountain environments. . Springer Series in Physical Environment, vol. 16. New York, Springer. 331 pp.

Bartelt, P., Lehning, M., 2002. A physical SNOWPACK model for the Swiss avalanche warning. Part I: numerical model. Cold Regions Science and Technology 35 (3), 123–145.

Bauer, A., Paar, G., Kaufmann, V., 2003. Terrestrial laser scanning for rock glacier moni-
toring. In: Phillips, M., Springman, S., Arenson, L. (Eds.), 8th International Conference
on Permafrost, Proceedings 1. Zurich. Swets & Zeitlinger, Lisse, pp. 55–60.

Beltrami, H., Harris, R.N. (Eds.), 2001. Inference of climate change from geothermal data.
Global and Planetary Change, vol. 29, pp. 149–348 (Special Issue).

Berger, A., Loutre, M.F., 1991. Insolation values for the climate of the last 10 million years.
Quaternary Science Reviews 10, 297–317.

Berthling, I., Etzelmüller, B., Eiken, T., Sollid, J.L., 1998. Rock glaciers on Prins Karls
Forland, Svalbard, I: internal structure, flow velocity and morphology. Permafrost
and Periglacial Processes 9 (2), 135–145.

Berthling, I., Etzelmüller, B., Isaksen, K., Sollid, J.L., 2000. Rock glaciers on Prins Karls
Forland. II: GPR soundings and the development of internal structures. Permafrost
and Periglacial Processes 11 (4), 357–369.

Beylich, A.A., Sandberg, O., 2005. Geomorphic effects of the extreme rainfall event of
20–21 July, 2004 in the Latnjavagge catchment, northern Swedish Lapland.
Geografiska. Annaler 87 A, 409–419.

Birks, H.H., 1991. Holocene vegetational history and climatic change in West Spitsbergen
based on plant macrofossils from Skardtjørna. The Holocene 1, 209–218.

Blikra, L.H., Selvik, S.F., 1998. Climate signals recorded in snow avalanche-dominated
colluvium in western Norway: depositional facies successions and pollen records.
The Holocene 8, 631–658.

Bommer, C., Keusen, H.R., Phillips, M., 2008. Engineering solutions for foundations and
anchors in mountain permafrost. In: Kane, D.L., Hinkel, K.M. (Eds.), Ninth Inter-
national Conference on Permafrost.Fairbanks, Fairbanks Alaska, 29 June–3 July
2008, vol. 1. Institute of Northern Engineering, University of Alaska, pp. 159–163.

Bourque, A., Simonet, G., 2006. Impacts of climate change on infrastructures and
implications on engineering. EIC Climate Change Technology Conference, Ottawa,
ON Canada. CD-ROM.

Bradley, R.S., 1990. Holocene paleoclimatology of the Queen Elizabeth Islands, Canadian
high Arctic. Quaternary Science Reviews 9, 365–384.

Bradley, R.S., 1999. Paleoclimatology; Reconstructing climates of the Quaternary.
Academic Press, San Diego, CA. 613 p.

Brenning, A., 2004. Statistical estimation and logistic regression modelling of rock
glacier distribution in the Andes of Santiago, Central Chile, European Geosciences
Union 2004, Nice, France. SRef-ID: 1607-7962/gra/EGU04-A-01032.

Brenning, A., 2005. Climatic and geomorphological controls of rock glaciers in the Andes
of Central Chile – combining statistical modelling and field mapping. PhD Thesis,
Humboldt-Universität zu Berlin, Berlin, 137 pp.

Brenning, A., Gruber, S., Hoelzle, M., 2005. Sampling and statistical analysis of BTS
measurements. Permafrost and Periglacial Processes 16 (3), 231–240.

Briffa, K.R., Osborn, T.J., Schweingruber, F.H., Harris, I.C., Jones, P.D., Shiyatov, S.G.,
Vaganov, E.A., 2001. Low-frequency temperature variations from a northern tree
ring density network. Journal of Geophysical Research 106 (d3), 2929–2941.

Brown, J., Ferrians, O., Heginbottom, J.A. and Melnikov, E.S. 1997. Circum-arctic map of
permafrost and ground-ice conditions. 1:10,000,000 Map CP-45. Circum-Pacific
map series, USGS.

Brown, J., French, H.M., Cheng, G., 2008. The International Permafrost Association:
1983–2008. In: Kane, D.L., Hinkel, K.M. (Eds.), Ninth International Conference on
Permafrost, University of Alaska Fairbanks, 29 June–3 July 2008. Institute of
Northern Engineering, University of Alaska Fairbanks, pp. 199–204.

Bucki, A.K., Echelmeyer, K.A., MacInnes, S., 2004. The thickness and internal structure of
Fireweed rock glacier, Alaska, U.S.A., as determined by geophysical methods.
Journal of Glaciology 50 (168), 67–75.

Büdel, J., 1977. Klima-Geomorphologie. Gebrüeder Borntraeger, Berlin. 304 pp.

Büdel, J., 1982. Climatic Geomorphology. Princeton University Press, Princeton.

Burga, C.A., 1991. Vegetation history and paleoclimatology of the middle Holocene —
pollen analysis of Alpine peat bog sediments, covered formerly by the Rutor
Glacier, 2510 m Aosta Valley, Italy. Global Ecology and Biogeography Letters 1 (5),
143–150.

Burga, C.A., 1993. Swiss alpine palaeoclimate during the Holocene: pollen analytical
evidence and general features. In: Frenzel, B. (Ed.), Solifluction and Climatic Variation
in the Holocene. European Science Foundation, Verlag, Stuttgart, pp. 11–22.

Burn, C.R., 1990. Implications for palaeoenvironmental reconstruction of recent ice-wedge
development at Mayo, Yukon Territory. Permafrost and Periglacial Processes 1, 3–14.

Burn, C.R., 2007. Permafrost. In: Elias, S.A. (Ed.), Encyclopedia of Quaternary Science,
vol. 3. Elsevier, Oxford. 2191–2199.

Cannone, N., Guglielmin, M., Hauck, C., Vonder Mühll, D., 2003. The impact of recent
glacier fluctuation and human activities on the permafrost distribution: a case
study from Stelvio Pass (Italian Central-Eastern Alps). In: Phillips, Springman,
Arenson (Eds.), Permafrost. Swets & Zeitlinger, Lisse, pp. 125–130.

Cermak, V., Safanda, J., Kresl, M., Dedecek, P., Bodri, L., 2000. Recent climate warming:
surface air temperature series and geothermal evidence. Studia geophysica et
geodaetica 44, 430–441.

Chandler, R.J., 1972. Periglacial mudslides in Vestspitsbergen and their bearing on the
origin of fossil "solifluction" shears in low angled clay slopes. Quaterterly Journal of
Engineering Geology 5, 223–241.

Cheng, G., 2005. A roadbed cooling approach for the construction of Qinghai–Tibet
Railway. Cold Regions Science and Technology 42 (2), 169–176.

Cheng, G., 1983. The mechanism of repeated segregation for the formation of thick-
layered ground ice. Cold Regions Science and Technology 8, 57–66.

Christiansen, H.H., 2005. Thermal regime of ice-wedge cracking in Adventdalen.
Svalbard. Permafrost and Periglacial Processes 16, 87–98.

Christiansen, H.H., Humlum, O., 2008. Interannual variations in active layer thickness in
Svalbard. In: Kane, D.L., Hinkel, K.M. (Eds.), Proceedings Ninth International
Conference on Permafrost, June 29-July 3, Fairbanks Alaska, vol. 1. Institute of
Northern Engineering, University of Alaska Fairbanks, pp. 257–262.

Cihlar, J., Barry, T.G., Ortega Gil, E., Haeberli, W., Kuma, K., Landwehr, J.M., Norse, D.,
Running, S., Scholes, R., Solomon, A.M., Zhao, S., 1997. GCOS/GTOS plan for
terrestrial climate related observation.

Coutard, J.P., Francou, B., 1989. Rock temperature measurements in two alpine environ-
ments: implications for frost shattering. Arctic and Alpine Research 21 (4), 399–416.

Curry, A.M., Cleasby, V., Zukowkyj, P., 2006. Paraglacial response of steep, sediment-
mantled slopes to post-'Little Ice Age' glacier recession in the central Swiss Alps.
Journal of Quaternary Science 21 (3), 211–225.

Dahl, S.O., Nesje, A., 1996. A new approach to calculating Holocene winter precipitation
by combining glacier equilibrium line altitudes and pine-tree limits: a case study
from Hardangerjökulen, central south Norway. The Holocene 6, 381–398.

Dallimore, S.R., Davis, J.L., 1987. Ground probing radar investigations of massive ground
ice and near surface geology in continuous permafrost. Geological Survey of
Canada, Paper 87–1A, 913–918.

Dallimore, S.R., Nixon, F.M., Eggington, P.A., Bisson, J.G., 1996. Deep-seated creep of massive
ground ice, Tuktoyaktuk, N.W.T., Canada. Permafrost and Periglacial Processes 7, 337–347.

Daniels, J.J., Keller, G.V., Jacobson, J.J., 1976. Computer-assisted interpretation of
geomagnetic soundings over a permafrost section. Geophysics 41, 752–765.

Dätwyler, T., 2004. SAC-Hütten und Jahrhundertsommer 2003. Die Alpen, vol. 1.
Stämpfli, Bern, pp. 46–49.

Davies, M.C.R., Hamza, O., Lumsden, B.W., Harris, C., 2000. Laboratory measurements of
the shear strength of ice-filled rock joints. Annals of Glaciology 31, 463–467.

Davies, M.C.R., Hamza, O., Harris, C., 2001. The effect of rise in mean annual temperature
on the stability of rock slopes containing ice-filled discontinuities. Permafrost and
Periglacial Processes, 12, 137–144.

Davies, M.C.R., Hamza, O., Harris, C., 2003. Physical modelling of permafrost warming in
rock slopes. In: Phillips, M., Springman, S.M., Arenson, L.U. (Eds.), Proceedings of the
8th International Conference on Permafrost, Zurich. Lisse, Netherlands, Balkema,
pp. 169–173.

Davis, B.A.S., Brewer, S., Stevenson, A.C., Guiot, J., data contributors, 2003. The
temperature of Europe during the Holocene reconstructed from pollen data.
Quaternary Science Reviews 22, 1701–1716.

de Pascale, G.P., Williams, K.K., Pollard, W.H. 2008. Geophysical mapping of ground ice
using a combination of capacitive coupled resistivity and ground penetrating radar,
NWT, Canada. Journal of Geophysical Research – Earth Surface, in press.

Delaloye, R., Reynard, E., Lambiel, C., 2000. Pergélisol et construction de remontées
mécaniques: l'exemple des Lapires (Mont-Gelé, Valais). Publication de la Société
Suisse de Mécanique des Sols et des Roches, Le gel en géotechnique, Réunion
d'automne, 10 novembre 2000, pp. 103–113.

Deline, P. 2002. Etude géomorphologique des interactions écroulement rocheux/
glaciales dans la haute montagne alpine (versant sud-est du massif Mont Blanc),
PhD thesis, Savoie, Savoie.

Delisle, G., Allard, M., Fortier, R., Calmels, F., Larrivée, É., 2003. Umiujaq, Northern
Québec: innovative techniques to monitor the decay of a lithalsa in response to
climate change. Permafrost and Periglacial Processes 14, 375–385.

Duchesne, C., Wright, J.F., Côté, M.M., Nixon, F.M., 2003. An enhanced vegetation
classification for permafrost modelling, NWT, Canada. In: Phillips, M., Springman,
S.M., Arenson, L. (Eds.), Proceedings 8th International Conference on Permafrost.
Swets and Zeitlinger, Lisse, pp. 217–221.

Einarsson, T.H., 1975. Um myndunarsögu íslensks mýrlendis. In: Gardarso, A. (Ed.),
Votlendi. Reykjavík, Landvernd, pp. 15–21.

Eronen, M., Zetterberg, P., 1996. Climatic changes in Northern Europe since late glacial
times, with special reference to dendroclimatological studies in northern Finnish
Lapland. Geophysica 2, 35–60.

Esch, D.C. (Ed.), 2004. Thermal analysis, construction, and monitoring methods for
frozen ground. Technical Council on Cold Regions Engineering monograph.
American Society of Civil Engineers, Reston, VA. 492 pp.

Etzelmüller, B., Hagen, J.O., 2005. Glacier-permafrost interaction in Arctic and alpine
mountain environments with examples from southern Norway and Svalbard. In:
Harris, C., Murton, J.M. (Eds.), Cryospheric Systems: Glaciers and Permafrost.
Geological Society of London Special Publication, vol. 242, pp. 11–28.

Etzelmüller, B., Berthling, I., Sollid, J.L., 1998b. The distribution of permafrost in
Southern Norway; a GIS approach. In: Lewkowicz, A.G., Allard, M. (Eds.), Seventh
International Conference on Permafrost, Proceedings. Collection Nordicana. Centre
d'Etudes Nordiques, Universite Laval, Quebec, PQ, Canada, pp. 251–257.

Etzelmüller, B., Berthling, I., Sollid, J.L., 2003. Aspects and concepts on the
geomorphlogical significance of Holocene permafrost in southern Norway.
Geomorphology 52, 87–104.

Etzelmüller, B., Hoelzle, M., Heggem, E.S.F., Isaksen, K., Mittaz, C., Vonder Mühll, D.,
Ødegård, R.S., Haeberli, W., Sollid, J.L., 2001a. Mapping and modelling the occur-
rence and distribution of mountain permafrost. Norwegian Journal of Geography
55, 186–194.

Etzelmüller, B., Ødegård, R.S., Berthling, I., Sollid, J.L., 2001b. Terrain parameters and
remote sensing data in the analysis of permafrost distribution and periglacial
processes: principles and examples from Southern Norway. Permafrost and
Periglacial Processes 12 (1), 79–92.

Etzelmüller, B., Heggem, E.S.F., Sharkhuu, N., Frauenfelder, R., Kääb, A., Goulden, C.E.,
2006. Mountain permafrost distribution modelling using a multi-criteria approach
in the Hövsgöl area, Northern Mongolia. Permafrost and Periglacial Processes 17,
91–104.

Etzelmüller, B., Farbrot, H., Guðmundsson, Á., Humlum, O., Tveito, O.E., Björnsson, H.,
2007. The regional distribution of mountain permafrost in Iceland. Permafrost and
Periglacial Processes 18, 185–199.

Etzelmüller, B., Schuler, T.V., Farbrot, H., Gudmundsson, A., 2008. Permafrost in Iceland —
distribution, ground temperatures and climate change impact. In: Kane, D.L.,
Hinkel, K.M. (Eds.), Proceedings Ninth International Conference on Permafrost,

June 29–July 3, Fairbanks Alaska, vol. 1. Institute of Northern Engineering, University of Alaska Fairbanks, pp. 421–426.

Evans, S.G., Clague, J.J., 1988. Catastrophic rock avalanches in glacial environment. Proceedings of the fifth International Symposium on Landslides, Lausanne, 10–15 July 1988, vol. 2, pp. 1153–1158.

Farbrot, H., Isaksen, K., Eiken, T., Kääb, A., Sollid, J.L., 2005. Composition and internal structures of a rock glacier on the strandflat of western Spitsbergen, Svalbard. Norsk Geografisk Tidsskrift 59 (2), 139–148.

Farbrot, H., Etzelmüller, B., Gudmundsson, A., Schuler, T.V., Eiken, T., Humlum, O., Björnsson, H., 2007. Thermal characteristics and impact of climate change on mountain permafrost in Iceland. Journal of Geophysical Research 112. doi:10.1029/2006JF000541.

Farbrot, H., Isaksen, K., Etzelmüller, B., 2008. Present and past distribution of mountain permafrost in Gaissane Mountains, Northern Norway. In: Kane, D.L., Hinkel, K.M. (Eds.), Proceedings volume 1, Ninth International Conference on Permafrost, University of Alaska Fairbanks, 29 June–3 July 2008. Institute of Northern Engineering, University of Alaska Fairbanks, pp. 427–432.

Fauve, M., Rhyner, H., Schneebeli, M., 2002. Pistenpräparation und Pistenpflege: Das Handbuch für den Praktiker. Davos, Eidg. Institut für Schnee- und Lawinenforschung.

Fierz, C., Lehning, M., 2001. Assessment of the microstructure-based snow-cover model SNOWPACK: thermal and mechanical properties. Cold Regions Science and Technology 33, 123–131.

Filippi, M.L., Lambert, P., Hunziker, J., Kubler, B., Bernasconi, S., 1999. Climatic and anthropogenic influence on the stable isotope record from bulk carbonates and ostracodes in Lake Neuchatel, Switzerland, during the last two millennia. Journal of Paleolimnology 21, 19–34.

Fischer, L., Kääb, A., Huggel, C., Nötzli, J., 2006. Geology, glacier retreat and permafrost degradation as controlling factors of slope instabilities in a high-mountain rock wall: the Monte Rosa east face. Natural Hazards and Earth System Sciences 6, 761–772. www.nat-hazards-earth-syst-sci.net/6/761/2006/.

Fish, A.M., 1985. Creep strength, strain rate, temperature and unfrozen water relationship in frozen soil. In: Kinosita, S., Fukuda, M. (Eds.), Fourth International Symposium on Ground Freezing. A.A. Balkema, Rotterdam, Sapporo, pp. 29–36.

Fish, A.M., Zaretsky, Y.K., 1997. Ice strength as a function of hydrostatic pressure and temperature. Cold Regions Research and Engineering Laboratory (CRREL), Hanover NH, USA. 14pp.

Foriero, A., Ladanyi, B., Dallimore, S.R., Egginton, P.A., Nixon, F.M., 1998. Modelling of deep seated hill slope creep in permafrost. Canadian Geotechnical Journal 35, 560–578.

Forman, S.L., Lubinski, D.J., Ingolfsson, O., Zeeberg, J.J., Snyder, J.A., Siegert, M.J., Matishov, G.G., 2004. A review of postglacial emergence on Svalbard, Franz Josef Land and Novaya Zemlya, northern Eurasia. Quaternary Science Reviews 23 (11–13), 1391–1434.

Fortier, D., Allard, M., 2005. Frost-cracking Conditions, Bylot Island, Eastern Canadian Arctic Archipelago. Permafrost and Periglacial Processes 16, 145–161.

Frauenfelder, R. 2005. Regional-scale modeling of the occurrence and dynamics of rockglaciers and the distribution of paleopermafrost. Department of Geography, University of Zurich, Physical Geography Series. 45, 70 p. plus Annex. ISBN 3 85543 241 4.

Frauenfelder, R., 2006. Debris transport by rockglacier — a quantitative estimate for an Alpine study site. NGF - Abstracts and Proceedings of the Geological Society of Norway 4, 40–41.

Frauenfelder, R., Kääb, A., 2000. Towards a palaeoclimatic model of rock glacier formation in the Swiss Alps. Annals of Glaciology 31, 281–286.

Frauenfelder, R., Haeberli, W., Hoelzle, M., Maisch, M., 2001. Using relict rockglaciers in GIS-based modelling to reconstruct younger dryas permafrost distribution patterns in the Err-Julier area, Swiss Alps. Norwegian Journal of Geography 55 (4), 195–202.

Frauenfelder, R., Haeberli, W., Hoelzle, M., 2003. Rockglacier occurrence and related terrain parameters in a study area of the Eastern Swiss Alps. In: Phillips, M., Springman, S.M., Arenson, L.U. (Eds.), Proceedings 8th International Conference on Permafrost. Swets and Zeitlinger, Lisse, pp. 253–258.

Frauenfelder, R., Zgraggen-Oswald, S., Huggel, C., Kääb, A., Haeberli, W., Galushkin, I., Polkvoy, A., 2005. Permafrost distribution assessments in the North-Ossetian Caucasus: first results. Geophysical Research Abstracts, vol. 7. 01619, SRef-ID: 1607-7962/gra/EGU05-A-01619.

Frauenfelder, R., Schneider, B., Kääb, A., 2008. Using dynamic modelling to simulate the distribution of rockglaciers. Geomorphology 93, 130–143.

French, H.M., 1996. The Periglacial Environment. Longman, Harlow, 341pp.

French, H.M., Bennett, L., Hayley, D.W., 1986. Ground ice conditions near Rea Point and on Sabine Peninsula, eastern Melville Island. Canadian Journal of Earth Sciences 23, 1389–1400.

Furrer, G. 1994. Zur Gletschergeschichte des Liefdefjords/NW-Spizbergen. Zeitschrift für Geomorphologie, N.F., Suppl.-Bd. 97, 43–47.

Gamper M.W., 1993. Holocene solifluction in the Swiss Alps: dating and climatic implications. In: Frenzel, B. (Ed.), Solifluction and Climatic Variation in the Holocene. European Science Foundation, Verlag, Stuttgart, pp. 1–10.

Geist, T., Stötter, H., 2003. First results of airborne laser scanning technology as a tool for the quantification of glacier mass balance. EARSel eProceedings 2 (1), 8–14.

Glade, T., 2005. Linking debris-flow hazard assessments with geomorphology. Geomorphology 66, 189–213.

Goering, D.J., 1998. Experimental investigation of air convection embankments for permafrost-resistant roadway design. In: Lewkowicz, A.G., Allard, M. (Eds.), Seventh International Conference on Permafrost. Collection Nordicana, vol. 57. Yellowknife, NWT, Canada, pp. 319–326.

Goering, D.J., Instanes, A., Knudsen, S., 2000. Convective heat transfer in railway embankment ballast. International Symposium on Ground Freezing and Frost Action in Soils. Louvain-la-Neuve, Belgium, pp. 31–36.

Gold, L.W., Lachenbruch, A.H., 1973. Thermal conditions in permafrost — a review of North American literature. Permafrost: The North American Contribution to the Second International Conference, 13–28 July 1973, Yakutsk, U.S.S.R. National Academy of Science, Washington, DC, pp. 3–25.

Goodrich, L.E., 1978. Efficient numerical technique for the one-dimensional thermal problems with phase change. International Journal of Heat and Mass Transfer 21, 615–621.

Goodrich, L.E., 1982. The influence of snow cover on ground thermal regime. Canadian Geotechnical Journal 19, 421–432.

Götz, A., Raetzo, H., 2002. Permafrost — mit dem Risiko umgehen. TEC 21 (17), 7–10.

Gross, R., Green, A.G., Horstmeyer, H., Holliger, K., Baldwin, J., 2003. 3-D georadar images of an active fault: efficient data acquisition, processing and interpretation strategies. Subsurface Sensing Technique and Application 4 (1), 19–40.

Goughnour, R.R., Andersland, O.B., 1968. Mechanical properties of a sand-ice system. Journal of the soil mechanics and foundations division. ASCE 94 (SM 4), 923–950.

Gruber, S., 2005. Mountain Permafrost: Transient spatial modelling, model verification and the use of remote sensing. PhD Thesis, Universität Zürich, Zürich, 121 pp.

Gruber, S., Hoelzle, M., 2001. Statistical modelling of mountain permafrost distribution: local calibration and incorporation of remotely sensed data. Permafrost and Periglacial Processes 12 (1), 69–77.

Gruber, S., Haeberli, W., 2007. Permafrost in steep bedrock slopes and its temperature-related destabilization following climate change. Journal of Geophysical Research 112, F02S18. doi:10.1029/2006JF000547.

Gruber, S., Peter, M., Hoelzle, M., Woodhatch, I., Haeberli, W., 2003a. Surface tempera-tures in steep alpine rock faces — a strategy for regional-scale measurement and modelling. In: Phillips, M., Springman, S.M., Arenson, L.U. (Eds.), Proceedings 8th International Conference on Permafrost. Swets and Zeitlinger, Lisse, pp. 325–330.

Gruber, S., Peter, M., Hoelzle, M., Woodhatch, I., Haeberli, W., 2003b. Surface temperatures in steep alpine rock faces — a strategy for regional-scale measurement and modelling. In: Phillips, M., Springman, S.M., Arenson, L.U. (Eds.), Proceedings of the 8th International Conference on Permafrost, vol. 1. Swets & Zeitlinger, Lisse, pp. 325–330.

Gruber, S., Hoelzle, M., Haeberli, W., 2004a. Rock-wall temperatures in the Alps: modelling their topographic distribution and regional differences. Permafrost and Periglacial Processes 15, 299–307.

Gruber, S., Hölzle, M., Haeberli, W., 2004b. Permafrost thaw and destabilization of Alpine rock walls in the hot summer of 2003. Geophysical Research Letters 31, L13504. doi:10.1029/2004GL020051.

Gruber, S., King, L., Kohl, T., Herz, T., Haeberli, W., Hoelzle, M., 2004c. Interpretation of geothermal profiles perturbed by topography: the Alpine permafrost boreholes at Stockhorn Plateau, Switzerland. Permafrost and Periglacial Processes 15, 349–357.

Gudmundsson, H., 1997. A review of the Holocene environmental history of Iceland. Quaternary Science Reviews 16, 81–92.

Guglielmin, M., Cannone, N., Dramis, F., 2001. Permafrost — glacial evolution during the Holocene in the Italian Central Alps. Permfrost and Periglacial Processes 12 (1), 111–124.

Guillaud, C., 2006. Coping with uncertainty in the design of hydraulic structures: climate change is but one more uncertain parameter. EIC Climate Change Technology Conference, Ottawa, ON Canada. CD-ROM.

Haas, J.N., Rischoz, I., Tinner, W., Wick, L., 1998. Synchronous Holocene climatic oscillations recorded on the Swiss Plateau and at the timberline in the Alps. The Holocene 8 (3), 301–309.

Haeberli, W., 1973. Die Basis-Temperatur der winterlichen Schneedecke als möglicher Indikator für die Verbreitung von Permafrost in den Alpen. Zeitschrift für Gletscher-kunde und Glazialgeologie. Universitätsverlag Wagner - Innsbruck, pp. 221–227.

Haeberli, W., 1975. Untersuchungen zur Verbreitung von Permafrost zwischen Flüelapass und Piz Grialetsch (Graubünden). Mitteilung der Versuchsanstalt für Wasserbau. Hydrologie und Glaziologie der ETH Zürich 17, 221.

Haeberli, W., 1985. Creep of mountain permafrost. Mitteilungen der Versuchsanstalt für Wasserbau. Hydrologie und Glaziologie der ETH Zürich 77.

Haeberli, W., 1992. Construction, environmental problems and natural hazards in periglacial mountain belts. Permafrost and Periglacial Processes 3 (2), 111–124.

Haeberli, W., 1994. Accelerated glacier and permafrost changes in the Alps. In: Beniston, M. (Ed.), Mountain Environments in Changing Climates. Routledge Publishing Company, London and New York, pp. 91–107.

Haeberli, W., 2000. Modern research perspectives relating to permafrost creep and rock glaciers. Permafrost and Periglacial Processes 11, 290–293.

Haeberli, W., 2005. Investigating glacier/permafrost-relations in high-mountain areas: historical background, selected examples and research needs. In: Harris, C., Murton, J.B. (Eds.), Cryospheric Systems: Glaciers and Permafrost, 242. Geological Society, London, Special Publications, pp. 29–37.

Haeberli, W., Vonder Mühll, D., 1996. On the characteristics and possible origins of ice in rock glacier permafrost. Zeitschrift für Geomorphologie 104, 43–57.

Haeberli, W., Wegmann, M., Vonder Mühll, D., 1997. Slope stability problems related to glacier shrinkage and permafrost degradation in the Alps. Eclogae Geologicae Helvetiae 90, 407–414.

Haeberli, W., Beniston, M., 1998. Climate change and its impacts on glaciers and permafrost in the Alps. Ambio 27 (4), 258–265.

Haeberli, W., Burn, C., 2002. Natural hazards in forests — glacier and permafrost effects as related to climate changes. In: Sidle, R.C. (Ed.), Environmental Change and Geomorphic Hazards in Forests. IUFRO Research Series, 9, pp. 167–202.

Haeberli, W., Gruber, S., 2008. Research challenges for permafrost in steep and cold terrain: an Alpine perspective. Plenary paper. In: Kane, D.L., Hinkel, K.M. (Eds.), Proceedings Ninth International Conference on Permafrost, June 29–July 3, Fairbanks Alaska, vol. 1. Institute of Northern Engineering, University of Alaska Fairbanks, pp. 597–605.

Haeberli, W., Hohmann, R., 2008. Climate, glaciers and permafrost in the Swiss Alps 2050: scenarios, consequences and recommendations. In: Kane, D.L., Hinkel, K.M.

(Eds.), Proceedings Ninth International Conference on Permafrost, vol. 1. Institute of Northern Engineering, University of Alaska Fairbanks, pp. 607–612.

Haeberli, W., Kääb, A., Vonder Mühl, D., Teysseire, Ph., 2001. Prevention of outburst floods from periglacial lakes at Grubengletscher, Valais, Swiss Alps. Journal of Glaciology 47 (156), 111–122.

Haeberli, W., Huggel, C., Kääb, A., Polkvoj, A., Zotikov, I., Osokin, N., 2003. Permafrost conditions in the starting zone of the Kolka–Karmadon rock/ice slide of 20 September 2002 in North Osetia (Russian Caucasus). In: Haeberli, W., Brandova, D. (Eds.), 8th International Conference on Permafrost, Extended Abstracts, Zurich, pp. 49–50.

Haeberli, W., Huggel, C., Kääb, A., Zgraggen-Oswald, S., Polkvoj, A., Galushkin, I., Zotikov, I., Osokin, N., 2004. The Kolka–Karmadon rock/ice slide of 20 September 2002: an extraordinary event of historical dimensions in North Ossetia, Russian Caucasus. Journal of Glaciology 50, 533–546.

Haeberli, W., Hallet, B., Arenson, L., Elconin, R., Humlum, O., Kääb, A., Kaufmann, V., Ladanyi, B., Matsuoka, N., Springman, S., Vonder Mühl, D., 2006. Permafrost creep and rock glacier dynamics. Permafrost and Periglacial Processes 17 (3), 189–214.

Hall, K., 1997. Rock temperatures and implications for cold region weathering I: New data from Viking Valley, Alexander Island, Antarctica. Permafrost and Periglacial Processes 8, 69–90.

Hall, K., André, M.-F., 2001. New insights into rock weathering as deduced from high-frequency rock temperature data: an Antarctic study. Geomorphology 41, 23–35.

Hall, K., Thorn, C.E., Matsuoka, N., Prick, A., 2002. Weathering in cold regions: some thoughts and perspectives. Progress in Physical Geography 26, 577–603.

Hallet, B., Walder, J.S., Stubbs, C.W., 1991. Weathering by segregation ice growth in microcracks at sustained sub-zero temperatures: verification from an experimental study using acoustic emissions. Permafrost and Periglacial Processes 2, 283–300.

Hallsdóttir, M., 1995. On the pre-settlement history of Icelandic vegetation. Icelandic Agricultural Science 9, 17–29.

Hamilton, S.J., Whalley, W.B., 1995. Preliminary results from the lichenometric study of Hanson S., Hoelzle M. 2004. The thermal regime of the active layer at the Murtèl rock glacier based on data from 2002. Permafrost and Periglacial Processes 15, 273–282.

Harada, K., Wada, K., Fukuda, M., 2000. Permafrost mapping by the transient electromagnetic method. Permafrost and Periglacial Processes 11, 71–84 2000.

Harris, C., 1981. Periglacial mass-wasting: a review of research. BGRG Research Monograph, 204. Geobooks, Norwich.

Harris, C., 2007. Slope deposits and forms. In: Elias, S.A. (Ed.), Encyclopedia of Quaternary Science, vol. 3. Elsevier, Amsterdam, pp. 2207–2216.

Harris, C., Davies, M.C.R., 2000. Gelifluction: observations from large-scale laboratory simulations. Arctic, Antarctic and Alpine Research 32 (2), 202–207.

Harris, C., Lewkowicz, A.G., 2000. An analysis of the stability of thawing slopes, Ellesmere Island, Nunavut, Canada. Canadian Geotechnical Journal 37 (2), 465–478.

Harris, C., Haeberli, W., 2003. Warming permafrost in the mountains of Europe. WMO Bulletin 52/3, 252–257.

Harris, C., Smith, J.S., 2003. Modelling gelifluction processes: the significance of frost heave and slope gradient. In: Phillips, M., Springman, S.M., Arenson, L.G. (Eds.), Proceedings 8th International Conference on Permafrost, Zurich. Swets and Zeitlinger, Lisse, pp. 355–360.

Harris, C., Murton, J.B., 2005. Experimental simulation of ice-wedge casting: processes, products and palaeoenvironmental significance. In: Harris, C., Murton, J.B. (Eds.), Cryogenic Systems: Glaciers and Permafrost. Geological Society, London, Special Publication, vol. 242, pp. 131–143.

Harris, C., Isaksen, K., 2008. Recent warming of European permafrost: evidence from borehole monitoring. In: Kane, D.L., Hinkel, K.M. (Eds.), Proceedings vol. 1, Ninth International Conference on Permafrost, University of Alaska Fairbanks, 29 June–3 July 2008. Institute of Northern Engineering, University of Alaska Fairbanks, pp. 655–661.

Harris, C., Davies, M.C.R., Coutard, J.-P., 1997. Rates and processes of periglacial solifluction: an experimental approach. Earth Surface Processes and Landforms 22, 849–868.

Harris, C., Haeberli, W., Vonder Mühl, D., King, L., 2001a. Permafrost monitoring in the high mountains of Europe: the PACE project in its global context. Permafrost and Periglacial Processes 12 (1), 3–11.

Harris, C., Rea, B., Davies, M.C.R., 2001b. Scaled physical modelling of mass movement processes on thawing slopes. Permafrost and Periglacial Processes 12 (1), 125–136.

Harris, C., Davies, M.C.R., Etzelmüller, B., 2001c. The assessment of potential geotechnical hazards associated with mountain permafrost in a warming global climate. Permafrost and Periglacial Processes 12 (1), 145–156.

Harris, C., Davies, M.C.R., Rea, B.R., 2003a. Gelifluction: viscous flow or plastic creep? Earth Surface Processes and Landforms 28, 1289–1301.

Harris, C., Vonder Mühl, D., Isaksen, K., Haeberli, W., Sollid, J.L., King, L., Holmlund, P., Dramis, F., Guglielmin, M., Palacios, D., 2003b. Warming permafrost in European mountains. Global and Planetary Change 39, 215–225.

Harris, C., Luetschg, M., Murton, B., Smith, F.W., Davies, M.C.R., Christiansen, H.H., Ertlen-Font, M., 2006. Solifluction processes in Arctic permafrost: results of laboratory and field experiments. Eos Trans. AGU 87 (52) Fall Meeting Supplement, Abstract C43A-03.

Harris, C., Luetschg, M.A., Davies, M.C.R., Smith, F.W., 2007. Field instrumentation for real-time monitoring of periglacial solifluction. Permafrost and Periglacial Processes 18 (1), 105–114.

Harris, C., Kern-Luetschg, M., Murton, J.B., Font, M., Davies, M.C.R., Smith, F.W., 2008a. In: Kane, D.L., Hinkel, K.M. (Eds.), Full-scale physical modelling of solifluction processes associated with one-sided and two-sided active layer freezing. Proceedings Ninth International Conference on Permafrost, June 29–July 3, Fairbanks Alaska, vol. 1. Institute of Northern Engineering, University of Alaska Fairbanks, pp. 663–668.

Harris, C., Smith, J.S., Davies, M.C.R., Rea, B., 2008b. An investigation of periglacial slope stability in relation to soil properties based on physical modelling in the geotechnical centrifuge. Geomorphology 93, 437–459. doi:10.1016/j.geomorph.2007.03.009.

Harris, C., Kern-Luetschg, M.A., Smith, F.W., Isaksen, K., 2008c. Solifluction processes in an area of seasonal ground freezing, Dovrefjell, Norway. Permafrost and Periglacial Processes 19, 31–47. doi:10.1002/ppp.609.

Harris, S.A., Corte, A.E., 1992. Interactions and relations between mountain permafrost, glaciers, snow and water. Permafrost and Periglacial Processes 3, 103–110.

Harry, D.G., Gozdzik, J.S., 1988. Ice wedges: growth, thaw transformation, and palaeoenvironmental significance. Journal of Quaternary Science 3, 39–55.

Hauck, C., 2002. Frozen ground monitoring using DC resistivity tomography. Geophysical Research Letters 29 (21), 2016.

Hauck, C., Guglielmin, M., Isaksen, K., Vonder Mühl, D., 2001. Applicability of frequency-domain and time-domain electromagnetic methods for mountain permafrost studies. Permafrost and Periglacial Processes 12 (1), 39–52.

Hauck, C., Vonder Mühl, D., 2003a. Evaluation of geophysical techniques for application in mountain permafrost studies. Z. Geomorph. vol. 132, 159–188 N.F., Suppl.-

Hauck, C., Vonder Mühl, D., 2003b. Inversion and interpretation of 2-dimensional geoelectrical measurements for detecting permafrost in mountainous regions. Permafrost and Periglacial Processes 14 (4), 305–318.

Hauck, C., Wagner, U., 2003. Combining and interpreting geoelectric and seismic tomographies in permafrost studies using fuzzy logic. Extended abstract, 8th Int. Conf. on Permafrost, Zurich 2003, pp. 57–58.

Hauck, C., Kneisel, C., 2006. Application of capacitively-coupled and DC electrical resistivity imaging for mountain permafrost studies. Permafrost and Periglacial Processes 17 (2), 169–177.

Hauck, C., Kneisel, C. (Eds.), 2008. Applied geophysics in periglacial environments. Cambridge University Press.

Hauck, C., Isaksen, K., Vonder Mühl, D., Sollid, J.L., 2004. Geophysical surveys designed to delineate the altitudinal limit of mountain permafrost: an example from Jotunheimen, Norway. Permafrost and Periglacial Processes 15 (3), 191–205.

Hauck, C., Vonder Mühl, D., Hoelzle, M., 2005. Permafrost monitoring in high mountain areas using a coupled geophysical and meteorological approach. In: de Jong, C., Collins, D., Ranzi R. (Eds.), Climate and Hydrology of Mountain Areas. Wiley, London, pp. 59–71.

Hauck, C., Bach, M., Hilbich, C., 2008. A 4-phase model to quantify subsurface ice and water content in permafrost regions based on geophysical data sets. In: Kane, D.L., Hinkel, K.M. (Eds.), Proceedings Ninth International Conference on Permafrost, June 29–July 3, Fairbanks Alaska, vol. 1. Institute of Northern Engineering, University of Alaska Fairbanks, pp. 675–680.

Heggem, E., Juliussen, H., Etzelmüller, B., 2005. Mountain permafrost in Central-Eastern Norway. Norsk Geografisk Tidsskrift 59 (2), 94–108.

Heggem, E.S.F., Etzelmüller, B., Sharkhuu, N., Goulden, C.E., Nandinsetseg, B., 2006. Spatial empirical modelling of ground surface temperature in the Hövsgöl area, Northern Mongolia. Permafrost and Periglacial Processes 17 (4), 357–369.

Hestnes, E. 2000. Impact of rapid mass movement and drifting snow on the infrastructure and development of Longyearbyen, Svalbard. Proceedings of the International Workshop on Permafrost Engineering, 259-282, Longyearbyen, Svalbard, Norway, 18-21 June 2000. Ed. K. Senneset.

Hilbich, C., Hauck, C., Hoelzle, M., Scherler, M., Schudel, L., Völksch, I., Vonder Mühl, D., Mäusbacher, R., 2008a. Monitoring mountain permafrost evolution using electrical resistivity tomography: a 7-year study of seasonal, annual, and long-term variations at Schilthorn, Swiss Alps. J. Geophys. Res. 113, F01S90. doi:10.1029/2007JF000799.

Hilbich, C., Hauck, C., Delaloye, R., Hoelzle, M., 2008b. A geoelectric monitoring network and resistivity-temperature relationships of different mountain permafrost sites in the Swiss Alps. In: Kane, D.L., Hinkel, K.M. (Eds.), Proceedings Ninth International Conference on Permafrost, June 29–July 3, Fairbanks Alaska, vol. 1. Institute of Northern Engineering, University of Alaska Fairbanks, pp. 699–704.

Hjort, C., 1997. Glaciation, climate history, changing marine levels and the evolution of the Northeast Water Polynia. Journal of Marine Systems 10, 23–33.

Hodgson, D.A., St-Onge, D.A., Edlund, S.A., 1991. Surficial materials of Hot Weather Creek basin, Ellesmere Island, Northwest Territories. Current Research, Part E: Geological Survey of Canada, Paper 91–1E, pp. 157–163.

Hoelzle, M., 1996. Mapping and modelling of mountain permafrost distribution in the Alps. Norwegian Journal of Geography 50, 11–15.

Hoelzle, M., Haeberli, W., 1995. Simulating the effects of mean annual air temperature changes on permafrost distribution and glacier size. An example from the Upper Engadin, Swiss Alps. Annals of Glaciology 21, 400–405.

Hoelzle, M., Wegmann, M., Krummenacher, B., 1999. Miniature temperature data loggers for mapping and monitoring of permafrost in high mountain areas: first experience from the Swiss Alps. Permafrost and Periglacial Processes 10, 113–124.

Hoelzle, M., Mittaz, C., Etzelmüller, B., Haeberli, W., 2001. Surface energy fluxes and distribution models of permafrost in European mountain areas: an overview of current developments. Permafrost and Periglacial Processes 12 (1), 53–68.

Hoelzle, M., Vonder Mühl, D., Haeberli, W., 2002. Thirty years of permafrost research in the Corvatsch-Furtschellas area, Eastern Swiss Alps: a review. Norwegian Journal of Geography 56 (2), 137–145.

Hoelzle, M., Paul, F., Gruber, S., Frauenfelder, R., 2005. Glacier and Permafrost in Mountain areas: different modelling approaches. Projecting Global Change Impact and Sustainable Land use and Natural Resource Management in Mountain Biosphere Reserves (GLOCHAMORE). Global Change Impacts in Mountain Bisophere Reserves. UNESCO, Paris, pp. 28–39.

Hoelzle, M., Gruber, S., 2008. Borehole and ground surface temperatures and their relationship to meteorological conditions in the Swiss Alps. In: Kane, D.L., Hinkel, K.M. (Eds.), Proceedings Ninth International Conference on Permafrost, June 29–July 3, Fairbanks Alaska, vol. 1. Institute of Northern Engineering, University of Alaska Fairbanks, pp. 723–728.

Holzhauser, H., Magny, M., Zumbuhl, H.J., 2005. Glacier and lake-level variations in west-central Europe over the last 3500 years. The Holocene 15, 789–801.

Kenyi, L.W., Kaufmann, V., 2003. Measuring rock glacier surface deformation using SAR interferometry. Eighth International Conference on Permafrost, vol. 1. Balkema, pp. 537–541.

Kern-Luetschg, M., Harris, C., Cleall, P., Li, Y., Thomas, H., 2008. Scaled centrifuge modelling of solifluction in permafrost and seasonally frozen soils. In: Kane, D.L., Hinkel, K.M. (Eds.), Proceedings Ninth International Conference on Permafrost, June 29–July 3, Fairbanks Alaska, vol. 1. Institute of Northern Engineering, University of Alaska Fairbanks, pp. 919–924.

King, L., 1986. Zonation and ecology of high mountain permafrost in Scandinavia. Geografisk Annaler 68 A, 131–139.

King, M.S., Zimmerman, R.W., Corwin, R.F., 1988. Seismic and electrical properties of unconsolidated permafrost. Geophysical Prospecting 36, 349–364.

King, L., Gorbunov, A.P., Evin, M., 1992. Prospecting and mapping of mountain permafrost and associated phenomena. Permafrost and Periglacial Processes 3 (2), 73–81.

King, L., Åkerman, J., 1993. Mountain permafrost in Europe. Proceedings of the Sixth International Conference on Permafrost, July 5–9, Beijing, vol. 2. South China University of Techology Press, pp. 1022–1027.

King, L., Kalisch, A., 1998. Permafrost distribution and implications for construction in the Zermatt area, Swiss Alps. In: Lewkowicz, A.G., Allard, M. (Eds.), 7th International Conference on Permafrost. Proceedings. Collection Nordicana. Centre d'Etudes Nordiques, Université Laval, Yellowknife, Canada, pp. 569–574.

Kneisel, C., 2003. Permafrost in recently deglaciated forefields – measurements and observations in the eastern Swiss Alps and northern Sweden. Zeitschrift für Geomorphologie 47 (3), 289–305.

Kneisel, C., 2004. New insights into mountain permafrost occurrence and characteristics in glacier forefields at high altitude through the application of 2D resistivity imaging. Permafrost and Periglacial Processes 15, 221–227.

Kneisel, C., Haeberli, W., Baumhauer, R., 2000a. Comparison of spatial modelling and field evidence of glacier/permafrost relations in an Alpine permafrost environment. Annals of Glaciology 31, 269–274.

Kneisel, C., Hauck, C., Vonder Mühll, D., 2000b. Permafrost below the timberline confirmed and characterized by geoelectrical resistivity measurements, Bever Valley, eastern Swiss Alps. Permafrost and Periglacial Processes 11, 295–304.

Kneisel, C., Rothenbühler, C., Keller, F., Haeberli, W., 2007. Hazard assessment of potential periglacial debris flows based on GIS-based spatial modelling and geophysical field surveys: a case study in the Swiss Alps. Permafrost and Periglacial Processes 18, 259–268. doi:10.1002/ppp.593.

Kneisel, C., Hauck, C., Fortier, R., Moorman, B., 2008. Advances in geophysical methods of permafrost investigations. Permafrost and Periglacial Processes 19, 157–178. doi:10.1002/pp.616.

Koç, N., Jansen, E., Haflidason, H., 1993. Paleoceanographic reconstructions of surface ocean conditions in the Greenland, Iceland and Norwegian seas through the last 14 ka based on diatoms. Quaternary Science Reviews 12, 115–140.

Koç, N., Jansen, J., 1994. Response of the high-latitude Northern Hemisphere to orbital climate forcing: evidence from the Nordic Seas. Geology 22, 523–526.

Kohl, T., 1999. Transient thermal effects of complex topographies. Tectonophysics 306, 311–324.

Korhola, A., Vasko, K., Toivonen, H.T.T., Olander, H., 2002. Holocene temperature changes in northern Fennoscandia reconstructed from chironomids using Bayesian modelling. Quaternary Science Reviews 21 (16–17), 1841–1860.

Kotlyakov, V.M., Rototaeva, O.V., Nosenko, G.A., 2004. The September 2002 Kolka glacier catastrophe in North Ossetia, Russian Federation. evidence and analysis. Mountain Research and Development 24 (1), 78–83.

Krautblatter, M., Hauck, C., 2007. Electrical resistivity tomography monitoring of permafrost in solid rockwalls. Journal of Geophysical Research 112, F02S20. doi:10.1029/2006JF000546.

Kukkonen, I.T., Safanda, J., 2001. Numerical modelling of permafrost in bedrock in northern Fennoscandia during the Holocene. Global and Planetary Change 29, 259–274.

Kultti, S., Mikkola, K., Virtanen, T., Timonen, M., Eronen, M., 2006. Past changes in the Scots pine forest line and climate in Finnish Lapland: a study based on megafossils, lake sediments, and GIS-based vegetation and climate data. Holocene 16 (3), 381–391.

Lachenbruch, A.H., Marshall, B.V., 1986. Changing climate: geothermal evidence from permafrost in the Alaskan Arctic. Science 234, 689–696.

Ladanyi, B.M., 1993. Determination of creep properties of frozen soils by means of the borehole stress relaxation test. Canadian Geotechnical Journal 30, 170.

Lambiel, C., Reynard, E., 2001. Regional modelling of present, past and future potential distribution of discontinuous permafrost based on a rock glacier inventory in the Bagnes–Hérémence area (Western Swiss Alps). Norwegian Journal of Geography 55 (4), 219–223.

Lambiel, C., Delaloye, R., 2004. Contribution of real-time kinematic GPS in the study of creeping mountain permafrost: examples from the Western Swiss Alps. Permafrost and Periglacial Processes 15 (3), 229–241.

Larsson, S., 1982. Geomorphologica effects on the slopes of Longyear Valley, Spitsbergen, after a heavy rainstorm in July 1972. Geografiska Annaler 64A, 105–125.

Lauritzen, S.-E., Lundberg, J., 1999. Calibration of the speleothem delta function: an absolute temperature record for the Holocene in northern Norway. The Holocene 9 (6), 659–669.

Leber, D., Häusler, H., Morawetz, R., Schreilechner, M., Wangda, D., 1999. GLOF risk assessment in the Northwestern Bhutanese Himalayas based on remote sensing sustained geo-hazard mapping and engineering geophysical methods. Journal of Nepal Geological Society 20, 141–142.

Lehmann, F., Green, A.G., 2000. Topographic migration of georadar data: implications for acquisition and processing. Geophysics 65, 836–848.

Lehning, M., Bartelt, P., Brown, B., Russi, T., Stöckli, U., Zimmerli, M., 1999. SNOWPACK model calculation for avalanche warning based upon a new network of weather and snow stations. Cold Regions Science and Technology 30 (1–3), 145–157.

Lehning, M., Bartelt, P., Brown, B., Fierz, C., Satyawali, P., 2002a. A physical SNOWPACK model for Swiss avalanche warning. Part II. Snow microstructure. Cold Regions Science and Technology 35 (3), 147–167.

Lehning, M., Bartelt, P., Brown, B., Fierz, C., 2002b. A physical SNOWPACK model for Swiss avalanche warning. Part III: meteorological forcing, thin layer formation and evaluation. Cold Regions Science and Technology 35 (3), 169–184.

Lehning, M., Völksch, I., Gustafsson, D., Nguyen, T.A., Stähli, M., Zappa, M., 2006. ALPINE3D: a detailed model of mountain surface processes and its application to snow hydrology. Hydrological Processes 20, 2111–2128.

Lehning, M., Löwe, H., Ryser, M., Raderschall, N., 2008. Inhomogeneous precipitation distribution and snow transport in steep terrain. Water Resources Research. doi:10.1029/2007WR006545.

Lewkowicz, A.G., 1992. A solifluction meter for permafrost sites. Permafrost and Periglacial Processes 3, 11–18.

Lewkowicz, A.G., 2001. Temperature regime of a small sandstone tor, latitude 80°N, Ellesmere Island, Nunavut, Canada. Permafrost and Periglacial Processes 12, 351–366.

Lewkowicz, A.G., Clark, S., 1998. Late summer solifluction and active-layer depths, Fosheim Peninsula, Ellesmere Island, Canada. In: Lewkowicz, A.G., Allard, M. (Eds.), Proceedings of the 6th International Conference on Permafrost. Centre d'études nordiques, Université Laval, pp. 641–666.

Lewkowicz, A.G., Ednie, M., 2004. Probility mapping of mountain permafrost using the BTS method, Wolf Creek, Yukon Territory, Canada. Permafrost and Periglacial Processes 15 (1), 67–80.

Lewkowicz, A.G., Harris, C., 2005a. Frequency and magnitude of active-layer detachment failures in discontinuous and continuous permafrost, northern Canada. Permafrost and Periglacial Processes 16 (1), 115–130.

Lewkowicz, A.G., Harris, C., 2005b. Morphology and geotechnique of active-layer detachment failures in discontinuous and continuous permafrost, northern Canada. Geomorphology 69, 275–297.

Lewkowicz, A.G., Bonnaventure, P.P., 2008. Interchangeability of mountain permafrost probability models, northwest Canada. Permafrost and Periglacial Processes 19, 49–62. doi:10.1002/ppp.612.

Li, X., Cheng, G., Chen, X., 1998. Response of permafrost to global change on the Qinghai–Xizang plateau — a GIS-aided model. In: Lewkowicz, A.G., Allard, M. (Eds.), 7th International Conference on Permafrost. Proceedings. Collection Nordicana. Centre d'Etudes Nordiques, Université Laval, Yellowknife, Canada, pp. 657–661.

Ling, F., Zhang, T., 2004. A numerical Q81 model for surface energy balance and thermal regime of the active layer and permafrost containing unfrozen water. Cold Regions Science and Technology 38, 1–15. doi:10.1016/S0165-232X(03)00057-0.

Lubinski, D.J., Forman, S.L., Miller, G.H., 1999. Holocene glacier and climate fluctuations on Franz Josef Land, Arctic Russia, 80°N. Quaternary Science Reviews 18, 85–108.

Luetschg, M.A., 2005. A model and field analysis of the interaction between snow cover and Alpine permafrost. Schriftenreihe Physische Geographie. Glaziologie und Geomorphologie, vol. 47. 204pp.

Luetschg, M.A., Bartelt, P., Stoeckli, V., Lehning, M., Haeberli, W., 2003. Numerical simulation of the interaction processes between snow cover and alpine permafrost. In: Phillips, M., Springman, S., Arenson, L. (Eds.), 8th International Conference on Permafrost. Proceedings. Swets & Zeitlinger, Lisse, Zürich, pp. 697–702.

Luetschg, M.A., Stoeckli, V., Lehning, M., Haeberli, W., 2004. Temperature studies in two boreholes at Fluela Pass, Eastern Swiss Alps: the effect of snow redistribution on permafrost distribution patterns in high mountain areas. Permafrost and Periglacial Processes 15, 283–297.

Luetschg, M.A., Haeberli, W., 2005. Permafrost evolution in the Swiss Alps in a changing climate and the role of the snow cover. Norwegian Journal of Geography 59 (2), 77–83.

Lugon, R., Delaloye, R., 2001. Modelling alpine permafrost distribution, Val de Rechy, Valais Alps (Switzerland). Norsk Geografisk Tidskrift 55 (4), 224–229.

Lunardini, V.J., 1996. Climatic warming and the degradation of warm permafrost. Permafrost and Periglacial Processes 7, 311–320.

Luoto, M., Seppälä, M., 2002a. Characteristics of earth hummocks (pounus) with and without permafrost in Finnish Lapland. Geografiska Annaler 84A (2), 127–136.

Luoto, M., Seppälä, M., 2002b. Modelling the distribution of palsas in Finnish Lapland with logistic regression and GIS. Permafrost and Periglacial Processes 13, 17–28.

Luoto, M., Seppälä, M., 2003. Thermokarst ponds indicating former distribution of palsas in Finnish Lapland. Permafrost and Periglacial Processes 14, 19–27.

Luoto, M., Heikkilä, R.K., Carter, T.R., 2004a. Loss of palsa mires in Europe and biological consequences. Environmental Conservation 31, 30–37.

Luoto, M., Fronzek, S., Zuidhoff, F.S., 2004b. Spatial modelling of palsa mires in relation to climate in northern Europe. Earth Surface Processes and Landforms 29, 1373–1387.

Luterbacher, J., Dietrich, D., Xoplaki, E., Grosjean, M., Wanner, H., 2004. European seasonal and annual temperature variability, trends, and extremes since 1500. Science 303, 1499–1503.

Ma, W., Shi, C.-H., Wu, Q.-B., Zhang, L.-X., Wu, Z.-J., 2006. Monitoring study on technology of the cooling roadbed in permafrost region of Quinghai–Tibet plateau. Cold Regions Science and Technology 44 (1), 1–11.

Mackay, J.R., 1972. The world of underground ice. Annals, Association of American Geographers 62, 1–22.

Mackay, J.R., 1981. Active layer slope movement in a continuous permafrost environment, Garry Island, Northwest Territories, Canada. Canadian Journal of Earth Sciences 18, 1666–1680.

Mackay, J.R., 1983. Downward water movement into frozen ground, western Arctic coast, Canada. Canadian Journal of Earth Sciences 20, 120–134.

Mackay, J.R., 1986. The first 7 years (1978–1985) of ice wedge growth, Illisarvik experimental drained lake site, western Arctic coast. Canadian Journal of Earth Sciences 23, 1782–1795.

Mackay, J.R., 1993. Air temperature, snow cover, creep of frozen ground, and the time of ice-wedge cracking, western Arctic coast. Canadian Journal of Earth Sciences 30, 1720–1729.

Mackay, J.R., 1999. Cold-climate shattering (1974–1993) of 200 glacial erratics on the exposed bottom of a recently drained arctic lake, Western Arctic Coast, Canada. Permafrost and Periglacial Processes 10, 125–136.

Mackay, J.R., 2000. Thermally induced movements in ice-wedge polygons, western arctic coast: a long-term study. Geographie physique et Quaternaire 54, 41–68.

Maisch, M., Haeberli, W., Frauenfelder, R., Kääb, A., 2003. Lateglacial and Holocene evolution of glaciers and permafrost in the Val Muragl, Upper Engadine, Swiss Alps. In: Phillips, M., Springman, S.M., Arenson, L.U. (Eds.), Proceedings of the 8th International Conference on Permafrost, vol. 2. Swets & Zeitlinger, Lisse, Zürich, pp. 717–722.

Mann, M.E., Bradley, R.S., Hughes, M.K., 1999. Northern Hemisphere temperatures during the last millennium: inferences, uncertainties and limitations. Geophysical Research Letters 26, 759–762.

Marchenko, S.S., 2001. A model of permafrost formation and occurrences in the intracontinental mountains. Norwegian Journal of Geography 55 (4), 230–234.

Marescot, L., Loke, M.H., Chapellier, D., Delaloye, R., Lambiel, C., Reynard, E., 2003. Assessing reliability of 2D resistivity imaging in permafrost and rock glacier studies using the depth of investigation index method. Near Surface Geophysics 1 (2), 57–67.

Matsuoka, N., 1994. Diurnal freeze-thaw depth in rockwalls: field measurements and theoretical considerations. Earth Surface Processes and Landforms 19, 423–435.

Matsuoka, N., 2001a. Microgelivation versus macrogelivation: towards bridging the gap between laboratory and field frost weathering. Permafrost and Periglacial Processes 12, 299–313.

Matsuoka, N., 2001b. Solifluction rates, processes and landforms: a global review. Earth-Science Reviews 55, 107–133.

Matsuoka, N., 2005. Temporal and spatial variations in periglacial soil movements on alpine crest slopes. Earth Surface Processes and Landforms 30, 41–58.

Matsuoka, N., 2008. Frost weathering and rockwall erosion in the eastern Swiss Alps: long-term (1994–2006) observations. Geomorphology 99, 353–368.

Matsuoka, N., Hirakawa, K., 2000. Solifluction resulting from one-sided and two-sided freezing: field data from Svalbard. Polar Geoscience 13, 187–201.

Matsuoka, N., Christiansen, H.H., 2008. Ice wedge dynamics in Svalbard: high resolution monitoring by multiple techniques. In: Kane, D.L., Hinkel, K.M. (Eds.), Proceedings Ninth International Conference on Permafrost, Fairbanks Alaska, 29 June–3 July 2008. Institute of Northern Engineering, University of Alaska Fairbanks, pp. 1149–1154.

Matsuoka, N., Murton, J., 2008. Frost weathering: recent advances and future directions. Permafrost and Periglacial Processes 19, 195–210.

Matsuoka, N., Sakai, H., 1999. Rockfall activity from an alpine cliff during thawing periods. Geomorphology 28, 309–328.

Matsuoka, N., Hirakawa, K., Watanabe, T., Moriwaki, K., 1997. Monitoring of periglacial slope processes in the Swiss Alps: the first two years of frost shattering, heave and creep. Permafrost and Periglacial Processes 8, 155–177.

Matsuoka, N., Hirakawa, K., Watanabe, T., Haeberli, W., Keller, F., 1998. The role of diurnal, annual and millennial freeze-thaw cycles in controlling alpine slope stability. In: Lewkowicz, A.G., Allard, M. (Eds.), Proceedings of the Seventh International Conference on Permafrost. Centre d'etudes nordiques, Universite Laval, pp. 711–718.

Matsuoka, N., Ikeda, A., Hirakawa, K., Watanabe, T., 2003. Contemporary periglacial processes in the Swiss Alps: seasonal, inter-annual and long-term variations. In: Phillips, M. (Ed.), Proceedings of the Eighth International Conference on Permafrost, vol. 2. Balkema, Lisse, pp. 735–740.

Matthews, J.A., 1976. 'Little Ice Age' paleotemperatures from high altitude tree growth in S. Norway. Nature 264, 243–245.

Matthews, J.A., Dahl, S.-O., Berrisford, M.S., Nesje, A., 1997. Cyclic development and thermokarstic degradation of palsas in the mid-alpine zone at Leirpullan, Dovrefjell, southern Norway. Permafrost and Periglacial Processes 8, 107–122.

Matthews, J.A., Berrisford, M.S., Dresser, Q.P., Nesje, A., Dahl, S.O., Bjune, A.E., Bakke, J., John, H., Birks, B., Lie, Ø., Dumayne-Peaty, L., Barnett, C., 2005. Holocene glacier history of Bjørnbreen and climatic reconstruction in central Jotunheimen, Norway, based on proximal glaciofluvial stream-bank mires. Quaternary Science Reviews 24, 67–90.

Maurer, H., Hauck, C., 2007. Geophysical imaging of alpine rock glaciers. Journal of Glaciology 53 (180), 110–120.

McGinnis, L.D., Nakao, K., Clark, C.C., 1973. Geophysical identification of frozen and unfrozen ground, Antarctica. Proceedings 2nd International Conference on Permafrost. Yakutsk, Russia, pp. 136–146.

McKenna, J.K., Biggar, K.W., 1998. The rehabilitation of a passive-ventilated slab on grade foundation using horizontal thermosyphons. Canadian Geotechnical Journal 35, 684– 691.

McNeill, J.D., 1980. Electromagnetic terrain conductivity measurements at low induction numbers.- Technical Note, TN-6. Geonics Ltd.

Meincke, J., 2002. Climate dynamics of the North Atlantic and NW Europe: an observation-based overview. In: Wefer, G., Berger, W., Behre, K.-E., Jansen, E. (Eds.), Climate development and history of the North Atlanticrealm. Springer-Verlag, Berlin, Heidelberg, pp. 25–40.

Mellor, M., 1977. Engineering properties of snow. Journal of Glaciology 19 (81), 15–66.

Mittaz, C., Hoelzle, M., Haeberli, W., 2000. First results and interpretation of energy-flux measurements of Alpine permafrost. Annals of Glaciology 31, 275–280.

Mittaz, C., Imhof, M., Hoelzle, M., Haeberli, W., 2002. Snowmelt evolution mapping using an energy balance approach over an alpine terrain. Arctic. Antarctic and Alpine Research 34 (3), 264–281.

Moberg, A., Jones, P.D., 2005. Trends in indices for extremes in daily temperature and precipitation in central and western Europe, 1901–99. International Journal of Climatology 25, 1149–1171.

Moberg, A., Sonechkin, D.M., Holmgren, K., Datsenko, N.M., Karlén, W., 2005. Highly variable Northern Hemisphere temperatures reconstructed from low- and high-resolution proxy data. Nature 433, 613–617.

Moorman, B.J., Robinson, S.D., Burgess, M.M., 2003. Imaging periglacial conditions with ground-penetrating radar. Permafrost and Periglacial Processes 14, 319–329.

Morgenstern, N.R., Nixon, J.F., 1971. One-dimensional consolidation of thawing soils. Canadian Geotechnical Journal 8, 558–565.

Morris, S.E., 1981. Topoclimatic factors and the development of rock glacier facies, Sangre de Cristo Mountains, Southern Colorado. Arctic and Alpine Research 13 (3), 329–338.

Moser, K., 1999. Ankermörtel im Permafrost. EMPA (Swiss Federal Laboratories for Materials Testing and Research). Technical Report no. 200229.

Munroe, J.S., Doolittle, J.A., Kanevisky, M.Z., Hinkel, K.M., Nelson, F.E., Jones, B.M., Shur, Y., Kimble, J.M., 2007. Application of ground-penetrating radar imagery for three-dimensional visualization of near-surface structures in ice-rich permafrost, Barrow, Alaska. Permafrost and Periglacial Processes, 18 (4), 309–321.

Murton, J.B., Kolstrup, E., 2003. Ice-wedge casts as indicators of palaeotemperatures: precise proxy or wishful thinking? Progress in Physical Geography 27, 155–170.

Murton, J.B., Coutard, J.-P., Ozouf, J.-C., Lautridou, J.-P., Robinson, D.A., Williams, R.B.G., Guillemet, G., Simmons, P., 2000. Experimental design for a pilot study on bedrock weathering near the permafrost table. Earth Surface Processes and Landforms 25, 1281–1294.

Murton, J.B., Coutard, J.P., Lautridou, J.P., Ozouf, J.C., Robinson, D.A., Williams, R.B.G., 2001. Physical modelling of bedrock brecciation by ice segregation in permafrost. Permafrost and Periglacial Processes 12, 255–266.

Murton, J.B., Peterson, R., Ozouf, J.-C., 2006. Bedrock fracture by ice segregation in cold regions. Science 314, 1127–1129. doi:10.1126/science.1132127.

Musil, M., Maurer, H., Green, A.G., Horstmeyer, H., Nitsche, F., Vonder Mühll, D., Springman, S., 2002. Shallow seismic surveying of an Alpine rock glacier. Geophysics 67 (6), 1701–1710.

Musil, M., Maurer, H., Hollinger, K., Green, A.G., 2006. Internal structure of an alpine rock glacier based on crosshole georadar traveltimes and amplitudes. Geophysical Prospecting 54 (3), 273–285.

Mustafa, O., Gude, M., Hoelzle, M., 2003. Modeling permafrost distribution in the northern Alps using global radiation. In: Haeberli, W., Brandova, D. (Eds.), 8th International Conference on Permafrost, Extended Abstracts. University of Zurich, Zürich, pp. 111–112.

Nater, P., Arenson, L.U., Springman, S.M., 2008. Choosing geotechnical parameters for slope stability assessments in alpine permafrost soils. In: Kane, D.L., Hinkel, K.M. (Eds.), Ninth International Conference on Permafrost, University of Alaska Fairbanks, 29 June-3 July 2008. Proceedings, vol. 2. Institute of Northern Engineering, University of Alaska Fairbanks, pp. 1261–1266.

Nelson, F.E., Anisimov, O.A., Shiklomanov, N.I., 2001. Subsidence risk from thawing permafrost — the treat to man-made structures across regions in the far north can be monitored. Nature 410, 889–890.

Nelson, F.E., Anisimov, O.A., Shiklomanov, N.I., 2002. Climate change and hazard zonation in the Circum-Arctic permafrost regions. Natural Hazards 26, 203–225.

Nesje, A., 1992. Younger Dryas and Holocene glacier fluctuations and equilibrium-line altitude variations in the Jostedalsbre region, western Norway. Climate Dynamics 63 (3–4), 221–227.

Nesje, A., Dahl, O.S., Andersson, C., Matthews, J.A., 2000. The lacustrine sedimentary sequence in Sygneskardvatnet, western Norway: a continuous, high-resolution record of the Jostedalsbreen ice cap during the Holocene. Quaternary Science Reviews 19, 1047–1065.

Nesje, A., Kvamme, M., 1991. Holocene glacier and climate variations in western Norway: evidence for early Holocene glacier demise and multiple Neoglacial events. Geology 19, 610–612.

Nesje, A., Matthews, J.A., Olaf Dahl, S., Berrisford, M.S., Andersson, C., 2001. Holocene glacier fluctuations of Flatebreen and winter precipitation changes in the Jostedalsbreen region, western Norway, based on glaciolacustrine sediment records. The Holocene 11 (3), 267–280.

Noetzli, J., Hoelzle, M., Haeberli, W., 2003. Mountain permafrost and recent Alpine rock-fall events: a GIS-based approach to determine critical factors. In: Phillips, M., Springman, S.M., Arenson, L.U. (Eds.), Proceedings of the 8th International Conference on Permafrost, vol. 2. Swets & Zeitlinger, Lisse, Zürich, pp. 827–832.

Noetzli, J., Huggel, C., Hoelzle, M., Haeberli, W., 2006. GIS-based modelling of rock/ice avalanches from Alpine permafrost areas. Computational Geosciences 10, 161–178.

Noetzli, J., Gruber, S., Kohl, T., Salzmann, N., Haeberli, W., 2007. Three-dimensional distribution and evolution of permafrost temperatures in idealized high-mountain topography. Journal of Geophysical Research 112, F02S13. doi:10.1029/2006JF000545.

Noetzli, J., Hilbich, C., Hauck, C., Hoelzle, M., Gruber, S., 2008. Comparison of simulated 2D temperature profiles with time-lapse electrical resistivity data at the Schilthorn crest, Switzerland. In: Kane, D.L., Hinkel, K.M. (Eds.), Ninth International Conference on Permafrost, University of Alaska Fairbanks, 29 June–3 July 2008. Proceedings, vol. 2. Institute of Northern Engineering, University of Alaska Fairbanks, pp. 1293–1298.

Nyenhuis, M., Hoelzle, M., Dikau, R., 2005. Rock glacier mapping and permafrost distribution modelling in the Turtmanntal, Valais, Switzerland. Zeitschrift für Geomorphologie 49 (3), 275–292.

O'Connor, K.M., Dowding, C.H., 1999. Geomeasurements by pulsing TDR cables and probes. CRC Press. 402 pp.

Ødegård, R.S., Hoelzle, M., Johansen, K.V., Sollid, J.L., 1996. Permafrost mapping and prospecting in southern Norway. Norsk geografisk Tidsskrift 50, 41–54.

Ødegård, R.S., Isaksen, K., Eiken, T., Sollid, J.L., 2008. MAGST in Mountain Permafrost, Dovrefjell, Southern Norway, 2001–2006. In: Kane, D.L., Hinkel, K.M. (Eds.), Ninth International Conference on Permafrost, University of Alaska Fairbanks, 29 June–3 July 2008. Proceedings, vol. 2. Institute of Northern Engineering, University of Alaska Fairbanks, pp. 1311–1315.

Oelke, C., Zhang, T., 2003. Comparing thaw depth measured at CALM field sites with estimates from a medium-resolution hemispheric heat conduction model. In:

Haeberli, W., Brandova, D. (Eds.), 8th International Conference on Permafrost, Extended Abstracts. University of Zurich, Zürich, pp. 117–118.

Oksanen, P.O., 2005. Development of palsa mires on the northern European continent in relation to Holocene climatic and environmental changes. Acta Universitatis Ouluensis A446, 50 p + 6 appending papers.

Olyphant, G.A., 1987. Rock glacier response to abrupt changes in talus production. In: Giardino, J.R., Shroder, J.F., Vitek, J.D. (Eds.), Rock Glaciers. Allen & Unwin, pp. 55–64.

Osterkamp, T.E., Romanovsky, V.E., 1999. Evidence for warming and thawing of discontinuous permafrost in Alaska. Permafrost and Periglacial Processes 10, 17–37.

Osterkamp, T.E., 2008. Thermal state of permafrost in Alaska during the fourth quarter of the twentieth century. In: Kane, D.L., Hinkel, K.M. (Eds.), Ninth International Conference on Permafrost, University of Alaska Fairbanks, 29 June–3 July 2008. Proceedings, vol. 2. Institute of Northern Engineering, University of Alaska Fairbanks, pp. 1333–1338.

Otto, J.C., Sass, O., 2006. Comparing geophysical methods for talus slope investigations in the Turtmann valley (Swiss Alps). Geomorphology 76 (3–4), 257–272.

Pandit, B.I., King, M.S., 1978. Influence of pore fluid salinity on seismic and electrical properties of rocks at permafrost temperatures. Proc. 3rd Int. Conf. on Permafrost, vol. 1. Edmonton, Canada, pp. 553–566.

Pant, S.R., Reynolds, J.M., 2000. Application of electrical imaging techniques for the investigation of natural dams: an example from Thulagi Glacier Lake, Nepal. Journal of Nepal Geological Society 22, 211–218.

Paterson, W.S.B., 1994. The Physics of Glaciers. Pergamon Press Ltd. 380 pp.

Pearson, C., Murphy, J., Halleck, P., Hermes, R., Mathews, M., 1983. Sonic and resistivity measurements on Berea sandstone containing tetrahydrofuran hydrates: a possible analog to natural gas hydrate deposits. Proceedings 4th International Conference on Permafrost. Fairbanks, Alaska, pp. 973–978.

PERD, 1998. Climate change impacts on permafrost engineering design. Panel on Energy Research and Development, Environment Canada, Ottawa ON, Canada. 42p.

Permafrost Subcommittee, National Research Council of Canada, 1988. Glossary of Permafrost and Related Ground-ice Terms, National Research Council of Canada Technical Memorandum No. 142. 156pp.

Petak, W.J., Atkisson, A.A., 1982. Natural hazard risk assessment and public policy: anticipating the unexpected. Springer, New York.

Péwé, T.L., 1966. Ice wedges in Alaska — classification, distribution and climatic significance. Proceedings, 1st International Conference on Permafrost, vol. 1287. National Academy of Science: National Research Council of Canada, Publication, pp. 76–81.

Phillips, M., 2006. Avalanche defence strategies and monitoring of two sites in mountain permafrost terrain, Pontresina, Eastern Swiss Alps. Natural Hazards 39, 353–379.

Phillips, M., Bartelt, P., Christen, M., 2000. Anchor temperatures of avalanche defence snow-supporting structures in frozen ground. In: Hjorth-Hansen, E., Holand, I., Løset, S., Norem, H. (Eds.), Proceedings of the Fourth International Conference on Snow Engineering, Trondheim, Norway, 19–21 June 2000. Balkema, pp. 245–250.

Phillips, M., Margreth, S., Ammann, W.J., 2003a. Creep of snow-supporting structures in alpine permafrost. In: Phillips, Springman, Arenson (Eds.), Proceedings of the Eighth International Conference on Permafrost, 21–25 July, Zurich. A.A. Balkema, Zurich, Switzerland, pp. 891–896.

Phillips, M., Margreth, S., Stoffel, L., Ammann, W.J., 2003b. Development of Swiss Guidelines for the construction of snow-supporting structures in creeping Alpine permafrost terrain. In: Culligan, P.J., Einstein, H.H., Whittle, A.J. (Eds.), Proceedings of the 12th Panamerican Conference on Soil Mechanics and Geotechnical Engineering – Soil and Rock America 2003, vol. 2. MIT, Verlag Glückauf, pp. 2603–2610.

Phillips, M., Ladner, F., Müller, M., Sambeth, U., Sorg, J., Teysseire, P., 2007. Monitoring and reconstruction of a chairlift midway station in creeping permafrost terrain, Grächen, Swiss Alps. Cold Regions Science and Technology 47 (1), 32–42.

Polyak, I., 1996. Computational Statistics in Climatology. Oxford University Press, New York and Oxford. 358 pp.

Powers, T.C., Helmuth, R.A., 1953. Theory of volume changes in hardened Portland cement paste during freezing, paper presented at Highway Research Board Proceedings. In: Press, F., Hamilton, R.M. (Eds.), Mitigating natural disasters. Science, vol. 284, p. 1927.

Prick, A., 2003. Frost weathering and rock fall in an arctic environment, Longyearbyen, Svalbard. In: Phillips, M., et al. (Ed.), Proceedings of the Eighth International Conference on Permafrost, vol. 2. Balkema, Lisse, pp. 907–912.

Rapp, A., 1960. Recent development of mountain slopes in Kärkevagge and surroundings, Northern Scandinavia. Geografiska Annaler 42A, 65–200.

Rebetez, M., Lugon, R., Baeriswyl, P.–A., 1997. Climatic change and debris flows in high mountain regions: the case study of the Ritigraben Torrent (Swiss Alps). Climatic Change 36, 3–4.

Rieder, U., Keusen, H.R., Amiguet, J.L., 1980. Geotechnische Probleme beim Bau der Luftseilbahn Trockener Steg–Klein Matterhorn. Schweizer Ingenieur und Architekt 18, 428–431.

Reiersen, L.-O., 2005. Impacts of a warming Arctic. European Geosciences Union, General Assembly 2005, Vienna. EGU05-A-07268 (CD-ROM).

Rempel, A.W., Wettlaufer, J.S., Worster, M.G., 2004. Premelting dynamics in a continuum model of frost heave. Journal of Fluid Mechanics 498, 227–244.

Richardson, S.D., Reynolds, J.M., 2000. Degradation of ice-cored moraine dams: implications for hazard development, debris covered Glaciers. IAHS Publication 264, 187–197.

Riseborough, D.W., 2002. The mean annual temperature at the top of permafrost, the TTOP model, and the effect of unfrozen water. Permafrost and Periglacial Processes 13, 137–143.

Riseborough, D., Shiklamonov, N.I., Etzelmuller, B., Gruber, S., Marchengo, S., 2008. Recent advances in permafrost modeling. Permafrost and Periglacial Processes 19 (2), 137–156.

Rignot, E., Hallet, B., Fountain, A., 2002. Rock glacier surface motion in Beacon Valley, Antarctica, from synthetic-aperture radar interferometry. Geophysical Research Letters 29 (12), 1607.

Rikenmann, D., Zimmermann, M., 1993. The 1987 debris flows in Switzerland: documentation and analysis. Geomorphology 8, 175–189.

Rist, A., Phillips, M., 2005. First results of investigations on hydrothermal processes within the active layer above alpine permafrost in steep terrain. Norwegian Journal of Geography 59, 177–183.

Rixen, C., Haeberli, W., Stoeckli, V., 2004. Ground temperature under ski pistes with artificial and natural snow. Arctic, Antarctic and Alpine Research 36 (4), 419–427.

Rodwell, M.J., Rowell, D.P., Folland, C.K., 1999. Oceanic forcing of the wintertime North Atlantic Oscillation and European climate. Nature 398, 320–323.

Roer, I., Kääb, A., Dikau, R., 2005. Rockglacier kinematics derived from small-scale aerial photography and digital airborne pushbroom imagery. Zeitschrift für Geomorphologie 49 (1), 73–87.

Roer, I., Haeberli, W., Avian, M., Kaufmann, V., Delaloye, R., Lambiel, C., Kääb, A., 2008. Observations and considerations on destabilizing active rock glaciers in the European Alps. In: Kane, D.L., Hinkel, K.M. (Eds.), Ninth International Conference on Permafrost, vol 2. Institute of Northern Engineering, University of Alaska Fairbanks, pp. 1505–1510.

Romanovskii, N.N., 1985. Distribution of recently active ice and soil wedges in the USSR. In: Church, M., Slaymaker, O. (Eds.), Field and theory; lectures in geocryology. University of British Columbia Press, Vancouver, pp. 154–165.

Romanovsky, V.E., Osterkamp, T.E., 1995. Interannual variation of the thermal regime of the active layer and near surface permafrost in northern Alaska. Permafrost and Periglacial Processes 6, 313–335.

Romanovsky, V.E., Osterkamp, T.E., Duxbury, N.S., 1997. An evaluation of three numerical models used in simulations of the active layer and permafrost temperature regime. Cold Regions Science and Technology 26, 195–203.

Romanovsk, V.E., Kholodov, A.L., Marchenko, S.S., Oberman, N.G., Drozdov, D.S., Malkova, G.V., Moskalenko, N.G., Vasiliev, A.A., Sergeev, D.O., Zheleznyak, M.N., 2008. Thermal state and fate of permafrost in Russia: first results of IPY. In: Kane, D.L., Hinkel, K.M. (Eds.), Ninth International Conference on Permafrost, University of Alaska Fairbanks, 29 June–3 July 2008. Proceedings, vol. 2. Institute of Northern Engineering, University of Alaska Fairbanks, pp. 1511–1518.

Rönkkö, M., Seppälä, M., 2003. Surface characteristics affecting active layer formation in palsas, Finnish Lapland. In: Phillips, M., Springman, S.M., Arenson, L.U. (Eds.), Permafrost: Proceedings of the Eighth International Conference on Permafrost. Swets and Zeitlinger, Lisse, pp. 995–1000.

Ross, N., Harris, C., Christiansen, H.H., Brabham, P.J., 2005. Ground-penetrating radar investigations of open system pingos, Adventdalen, Svalbard. Norwegian Journal of Geography 59, 129–138.

Ross, N., Brabham, P.J., Harris, C., Christiansen, H.H., 2007. Internal structure of open system pingos, Adventdalen, Svalbard: the use of resistivity tomography to assess ground-ice conditions. Journal of Environmental and Engineering Geophysics 12, 113–126.

Rott, H., Siegel, A., 1999. Analysis of mass movement in alpine terrain by means of SAR interferometry. IEEE Geoscience and Remote Sensing Symposium, pp. 1933–1936. IGARSS'99.

Ryzhkin, I.A., Petrenko, V.F., 1997. Physical mechanisms responsible for ice adhesion. Journal of Physical Chemistry B 101, 6267–6270.

Salvigsen, O., 2002. Radiocarbon-dated Mytilus edulis and Modiolus modiolus from northern Svalbard: climatic implications. Norwegian Journal of Geography 56, 56–61.

Salzmann, N., Kääb, A., Huggel, C., Allgöwer, B., Haeberli, W., 2004. Assessment of the hazard potential of ice avalanches using remote sensing and GIS-modelling. Norwegian Journal of Geography 58, 74–84.

Salzmann, N., Nötzli, J., Hauck, C., Gruber, S., Hoelzle, M., Haeberli, W., 2007a. Ground surface temperature scenarios in complex high-mountain topography based on regional climate model results. Journal of Geophysical Research 112 (No. F2), F02S12. doi:10.1029/2006JF000527.

Salzmann, N., Frei, C., Vidale, P.-L., Hoelzle, M., 2007b. The application of Regional Climate Model output for the simulation of high-mountain permafrost scenarios. Global and Planetary Change 56, 188–202.

Sass, O., 2005a. Spatial patterns of rockfall intensity in the northern Alps. Zeitschrift für Geomorphologie 138, 51–65 N.F., Suppl.-Bd.

Sass, O., 2005b. Rock moisture measurements: techniques, results, and implications for weathering. Earth Surface Processes and Landforms 30, 359–374.

Schär, C., Vidale, P.L., Luthi, D., Frei, C., Haberli, C., Liniger, M.A., Appenzeller, C., 2004. The role of increasing temperature variability in European summer heatwaves. Nature 427, 332–336.

Scherler, M. 2006. Messung und Modellierung konvektiver Wärmetransportprozesse in der Auftauschicht von Gebirgspermafrost am Beispiel des Schilthorns. Diploma thesis Geographical Institute Zürich, University of Zürich, Switzerland.

Schiermeier, Q., 2003. Alpine thaw breaks ice over permafrost's role. Nature 424, 712.

Schneider, B., Schneider, H., 2001. Zur jährigen Messreihe der kurzfristigen Geschwindigkeitsschwankungen am Blockgletscher im Äusseren Hochebenkar, Ötztaler Alpen, Tirol. Zeitschrift für Gletscherkunde und Glazialgeologie. 37 (1), 1–33.

Schudel, L. 2003. Permafrost Monitoring auf dem Schilthorn mit geophysikalischen Methoden und meteorologischen Daten. Diploma thesis Geographical Institute Zürich, University of Zürich, Switzerland.

Scott, W., Sellmann, P., Hunter, J., 1990. Geophysics in the study of permafrost. In: Ward, S. (Ed.), Geotechnical and Environmental Geophysics. Society of Exploration Geophysics Tulsa, pp. 355–384.

Seierstad, J., Nesje, A., Dahl, S.O., Simonsen, J.R., 2002. Holocene glacier fluctuations of Grovabreen and Holocene snow-avalanche activity reconstructed from lake sediments in Groningstolsvatnet, western Norway. The Holocene 12 (2), 211–222.

Seppä, H., Birks, H.J.B., 2001. July mean temperature and annual precipitation trends during the Holocene in the Fennoscandian tree-line area: pollen-based climate reconstructions. The Holocene 11 (5), 527–539.

Seppä, H., Birks, H.J.B., 2002. Holocene climate reconstructions from the Fennoscandian tree-line area based on pollen data from Toskaljavri. Quaternary Research 57, 191–199.

Seppälä, M., 1983. Seasonal thawing of palsas in Finnish Lapland. Permfrost: Fouth International Conference. Proceedings. National Academy Press, Washington, D.C., pp. 1127–1132.

Seppälä, M., 1986. The origin of palsas. Geografiska Annaler 68A, 141–147.

Seppälä, M., 1988. Palsas and related forms. In: Clark, M.J. (Ed.), Advances in Periglacial Geomorphology. John Wiley & Sons Ltd, Chichester, pp. 247–278.

Seppälä, M., 1994. Snow depth controls palsa growth. Permafrost and Periglacial Processes 5, 283–288.

Seppälä, M., 1998. New permafrost formed in peat hummocks (pounus), Finnish Lapland. Permafrost and Periglacial Processes 9, 367–373.

Seppälä, M., 2003a. An experimental climate change study of the effect of increasing snow cover on active layer formation of a palsa, Finnish Lapland. In: Phillips, M., Springman, S.M., Arenson, L.U. (Eds.), Proceedings of the Eighth International Conference on Permafrost, vol. 2. Swets & Zeitlinger, Lisse, pp. 1013–1016.

Seppälä, M., 2003b. Surface abrasion of palsas by wind action in Finnish Lapland. Geomorphology 52, 141–148.

Seppälä, M., 2004. Wind as a geomorphic agent in cold climates. Cambridge University Press, Cambridge. 358 pp.

Seppälä, M., 2005. Dating of palsas. In: Ojala, A.E.K. (Ed.), Quaternary studies in the northern and Arctic regions of Finland. Geological Survey of Finland, Special Paper, vol. 40, pp. 79–84.

Seppälä, M., 1982. An experimental study of the formation of palsas. The Roger J.E. Brown Memorial Volume. Proceedings Fourth Canadian Permafrost Conference, Calgary, Alberta. National Research Council of Canada, pp. 36–42.

Shaopeng, H., Pollack, H.N., Po-Yu, S., 2000. Temperature trends over the past five centuries reconstructed from borehole temperatures. Nature 403 (6771), 756–758.

Schur, Y.I., 1988. The upper horizon of permafrost soils. In: Senneset, K. (Ed.), Proceedings of the Fifth International Conference on Permafrost. Tapir, Trondheim, pp. 867–871.

Shur, Y., Hinkel, K.M., Nelson, F.E., 2005. The transient layer: implications for geocryology and climate-change science. Permafrost and Periglacial Process 16, 5–17.

SLF/BUWAL, 2000. Richtlinien für den Lawinenverbau im Anbruchgebiet. EDMZ, Bern.

Slonosky, V.C., Jones, P.D., Davies, T.D., 2000. Variability of the surface atmospheric circulation over Europe, 1774–1995. International Journal of Climatology 20, 1875–1897.

Slonosky, V.C., Jones, P.D., Davies, T.D., 2001. Atmospheric cirkulation and surface temperature in Europe from the 18th century to 1995. International Journal of Climatology 21, 63–75.

Smith, L.B., Graham, J.P., Nixon, J.F., Washuta, A.S., 1991. Thermal-analysis of forced-air and thermosiphon cooling systems for the Inuvik Airport expansion. Canadian Geotechnical Journal 28 (3), 399–409.

Sollid, J.L., Sørbel, L., 1998. Palsa bogs as a climatic indicator — examples from Dovrefjell, southern Norway. Ambio 27, 287–291.

Sollid, J.L., Holmlund, P., Isaksen, K., Harris, C., 2000. Deep permafrost boreholes in western Svalbard, northern Sweden and southern Norway. Norwegian Journal of Geography 54, 186–191.

Sollid, J.L., Isaksen, K., Eiken, T., Ødegård, R.S., 2003. The transition zone of mountain permafrost on Dovrefjell, southern Norway. In: Phillips, M., Springman, S.M., Arenson, L.U. (Eds.), Proceedings Volume 2, Eight International Conference on Permafrost, Zurich, Switzerland, 21–25 July. Swets & Zeitlinger, Lisse, pp. 1085–1090.

Springman, S.M., Jommi, C., Teysseire, P., 2003. Instabilities on moraine slopes induced by loss of suction: a case history. Géotechnique 53 (1), 3–10.

Springman, S.M., Arenson, L.U., 2008. Recent advances in permafrost geotechnics. Proceedings ninth international conference on permafrost, volume 2, university of Alaska Fairbanks, 29 June–3 July 2008. In: Kane, D.L., Hinkel, K.M. (Eds.), Institute of Northern Engineering, University of Alaska Fairbanks, pp. 1685–1694.

Stähli, M., Jansson, P.E., Lundin, L.C., 1996. Preferential water flow in a frozen soil — a two domain model approach. Hydrological Processes 10, 1305–1316.

Steiner, W., Keusen, H.-R., Graber, U., 1996. Construction in Rock at 3550 meters elevation (Jungfraujoch, Switzerland). Proceedings Eurock.

Stocker-Mittaz, C., Hoelzle, M., Haeberli, W., 2002. Permafrost distribution modeling based on energy-balance data: a first step. Permafrost and Periglacial Processes 13 (4), 271–282.

Stoffel, M., Lièvre, I., Conus, D., Grichting, M.A., Raetzo, H., Gärtner, H.W., Monbaron, M., 2005. 400 years of debris-flow activity and triggering weather conditions: Ritigraben, Valais, Switzerland. Arctic, Antarctic, and Alpine Research, vol. 37, No. 3, pp. 387–395.

Strozzi, T., Kääb, A., Frauenfelder, R., 2004. Detecting and quantifying mountain permafrost creep from in-situ, airborne and spaceborne remote sensing methods. International Journal of Remote Sensing 25 (15), 2919–2931.

Sturm, M., Holmgren, J., König, M., Morris, K., 1997. The thermal conductivity of seasonal snow. Journal of Glaciology 43, 26–41.

Svendsen, J.I., Mangerud, J., 1997. Holocene glacial and climatic variations on Spitsbergen, Svalbard. The Holocene 7, 45–57.

Svensson, H., 1969a. Open fissures in a polygonal net on the Norwegian arctic coast. Biuletyn Peryglacjalny 19, 389–398.

Svensson, H., 1969b. Permafrost på Spetsbergen. Forskning och Framsteg 8, 20 (in Swedish).

Svensson, H., 1971. Pingos i yttre delen av Adventdalen. Norsk Polarinstitutt Årbok 1969, 168–174.

Svensson, H., 1976. Iskilar som Klimatindikator. Meddelanden från Lunds Universitets Geografiska Institutionen, No. 547, Svensk Geografisk Årsbok (Swedish Geographical Yearbook), 52, pp. 46–57 (in Swedish).

Svensson, H., 1982. Valley formation initiated by ice-wedge polygonal nets in terrace surfaces. Biuletyn Peryglacjalny 29, 139–142.

Svensson, H., 1988. Ice-wedge casts and relict polygonal patterns in Scandinavia. Journal of Quaternary Science 3, 57–67.

Svensson, H., 1996. Weather extremes — geomorphology. Svensk Geografisk Årsbok (Swedish Geographical Yearbook), pp. 173–179 (In Swedish).

Tanarro, L.M., et al., 2001. Permafrost distribution modelling in the mountains of the Mediterranean: Corral del Veleta, Sierra Nevada, Spain. Norwegian Journal of Geography 55 (4), 253–260.

Thalparpan, P., 2000. Lawinenverbauungen im Permafrost. Eidg. Institut für Schnee- und Lawinenforschung, Davos.

Thiis, T.K., Jaedicke, C., 2000. Changes in the snowdrift pattern caused by a building extension — investigations through scale modelling and numerical simulations. Proceedings of the Fourth International Conference on Snow Engineering, Trondheim, Norway, 19–21 June 2000, 363-375. Eds. E. Hjorth-Hansen, I. Holand, S. Løset, H. Norem. Balkema.

Tiljander, M., Saarnisto, M., Ojala, A.E.K., Saarinen, T., 2003. A 3000-year palaeoenvironmental record from annually laminated sediment of Lake Korttajarvi, central Finland. Boreas 26, 566–577.

Timofeev, V.M., Rogozinski, A.W., Hunter, J.A., Douma, M., 1994. A new ground resistivity method for engineering and environmental geophysics. Proceedings of the Symposium on the application of geophysics to engineering and environmental problems. EEGS, pp. 701–715.

Timur, A., 1968. Velocity of compressional waves in porous media at permafrost temperatures. Geophysics 33 (4), 584–595.

Tinner, W., Ammann, B., Germann, P., 1996. Treeline fluctuations recorded for 12,500 years by soil profiles, pollen and plant macrofossils in the Central Swiss Alps. Arctic and Alpine Research 28 (2), 131–147.

Ting, J.M., 1983. Tertiary creep model for frozen sands. Journal of Geotechnical Engineering 109 (7), 932–945.

Tveito, O.E., et al., 2001. Nordic climate maps. Report No. 06/01. DNMI, Oslo.

Varnes, D., 1984. Landslide hazard zonation : A review of principles and practice. UNESCO, Paris. 63 pp.

Völksch, I., 2004. Untersuchung und Modellierung kleinräumiger Unterschiede im Verhalten von Gebirgspermafrost. Diploma thesis, Departement Earth Sciences, ETH Zürich, Switzerland.

Vonder Mühl, D., Haeberli, W., 1990. Thermal characteristics of the permafrost within an active rock glacier (Murtèl/Corvatsch, Grisons, Swiss Alps). Journal of Glaciology 36 (123), 151–158.

Vonder Mühl, D., Stucki, T., Haeberli, W., 1998. Borehole temperatures in Alpine permafrost: a ten years series. In: Lewkowicz, A.G., Allard, M. (Eds.), Proceedings Seventh International Conference on Permafrost, Yellowknife, Canada, 23-27 June 1998. Centre d'Etudes Nordiques, Universite Laval, pp. 1089–1095. Collection Nordicana 57.

Vonder Mühl, D., Hauck, C., Lehmann, F., 2000. Verification of geophysical models in Alpine permafrost using borehole information. Annals of Glaciology 31, 300–306.

Vonder Mühl, D., Hauck, C., Gubler, H., McDonald, R., Russill, N., 2001. New geophysical methods of investigating the nature and distribution of mountain permafrost with special reference to radiometry techniques. Permafrost and Periglacial Process 12 (1), 27–38.

Vonder Mühl, D.S., Arenson, L.U., Springman, S.M., 2003. Temperature conditions in two Alpine rock glaciers. In: Phillips, Springman, Arenson (Eds.), Proceedings of the Eighth International Conference on Permafrost, 21–25 July, Zurich. A.A. Balkema, Zurich, Switzerland, pp. 1195–1200.

Vonder Mühl, D., Nötzli, J., Makowski, K., Delaloye, R., 2004. Permafrost in Switzerland 2000/2001 and 2001/2002. Glaciological report (permafrost). vol. 2/3. 86 pp.

Vonder Mühl, D., Noetzli, J., Roer, I., Makowski, K., Delaloye, R., 2007. Permafrost in Switzerland 2000/2003 and 2003/2004, Glaciological Report (Permafrost) No. 4/5 of the Glaciological Commission (GC) of the Swiss Academy of Sciences (SAS) and the Department of Geography, University of Zurich, 107pp.

Vonder Mühl, D., Noetzli, J., Roer, I., 2008. PERMOS — a comprehensive monitoring network of mountain permafrost in the Swiss Alps. 1869–1874. In: Kane, D.L., Hinkel, K.M. (Eds.), Proceedings Ninth International Conference on Permafrost, Volume 2, University of Alaska Fairbanks, 29 June–3 July 2008. Institute of Northern Engineering, University of Alaska Fairbanks, pp. 1869–1874.

Vorren, K.-D., 1972. Stratigraphical investigations of a palsa bog in northern Norway. Astarte 5, 39–71.

Vorren, K.-D., Vorren, B., 1975. The problem of dating a palsa. Two attempts involving pollen diagrams, determination of moss subfossils, and C14-datings. Astarte 8, 73–81.

Voytkovskiy, K.F., Golubev, V.N., 1973. Mechanical properties of ice as a function of the conditions of its formation. Paper presented at 2nd International Conference on Permafrost. Proceedings, National Academy of Sciences, Washington D.C.

Walder, J., Hallet, B., 1985. A theoretical model of the fracture of rock during freezing. Geological Society of America, Bull. 96 (3), 336–346.

Walder, J.S., Hallet, B., 1986. The physical basis of frost weathering: toward a more fundamental and unified perspective. Arctic and Alpine Research 18, 27–32.

Wangensteen, B., Guðmundsson, Á., Eiken, T., Kääb, A., Farbrot, H., Etzelmüller, B., 2006. Surface displacements and surface age estimates for creeping slope landforms in northern and eastern Iceland using digital photogrammetry. Geomorphology 80, 59–79.

Washburn, A.L., 1967. Instrumental observations of mass-wasting in the Mesters Vig district, Northeast Greenland. Meddelelser om Grønland. vol. 166. 318 pp.

Washburn, A.L., 1999. A high arctic frost creep/gelifluction slope, 1981–1989: Resolute Bay, Cornwallis Island, Northwest territories, Canada. Permafrost and Periglacial Processes 10, 163–186.

Wegmann, M. 1998. Frostdynamik in hochalpinen Felswänden am Beispiel der Region Jungfraujoch-Aletsch, PhD thesis, 144 pp, ETH Zürich, Zürich.

Wegmann, M., Gudmundsson, G.H., 1999. Thermally induced temporal strain variations in rock walls observed at subzero temperatures. In: Hutter, K., Wang, Y., Beer, H. (Eds.), Advances in Cold-Region Thermal Engineering and Sciences. Springer, Berlin, pp. 511–518.

Wegmann, M., Gudmundsson, G.H., Haeberli, W., 1998. Permafrost changes in rock walls and the retreat of alpine glaciers: a thermal modelling approach. Permafrost and Periglacial Processes 9 (1), 23–33.

Wen, Z., Sheng, Y., Ma, W., Qi, J.L., Wu, J.C., 2005. Analysis on effect of permafrost protection by two-phase closed thermosyphon and insulation jointly in permafrost regions. Cold Regions Science and Technology 43 (3), 150–163.

White, S.E., 1987. Differential movement across ridges on Arapaho rock glaciers, Colorado Front Range, US. Rock glaciers. Allen and Unwin, London, pp. 145–149.

Wick, L., Tinner, W., 1997. Vegetation changes and timberline fluctuations in the central airs as indicators of Holocene climatic oscillations. Arctic and Alpine Research 29, 445–458.

Williams, P.J., 1967a. Suction and its effects on unfrozen water of frozen soils. Publications of the Norwegian Geotechnical Institute 72, 27–35.

Williams, P.J., 1967b. Unfrozen water in frozen soils. Publications of the Norwegian Geotechnical Institute 72, 37–48.

Wright, J.F., Duchesne, C., Côté, M.M., 2003. Regional-scale permafrost mapping using the TTOP ground temperature model. In: Phillips, M., Springman, S.M., Arenson, L. (Eds.), Proceedings 8th International Conference on Permafrost. Swets and Zeitlinger, Lisse, pp. 1241–1246.

Yasufuku, N., Springman, S.M., Arenson, L.U., Ramholt, T., 2003. Stress-dilatancy behaviour of frozen sand in direct shear. 8th International Conference on Permafrost, Zurich. Balkema, Rotterdam, pp. 1253–1258 (2).

Yoshikawa, K., 1993. Notes on open-system pingo ice, Adventdalen, Spitsbergen. Permafrost and Periglacial Processes 4, 327–334.

Yoshikawa, K., Leuschen, C., Ikeda, A., Harada, K., Gogineni, P., Hoekstra, P., Hinzman, L., Sawada, Y., Matsuoka, N., 2006. Comparison of geophysical investigations for detection of massive ground ice (pingo ice). Journal of Geophysical Research 111, E06S19.

Zhang, T., Stamnes, K., 1998. Impact of climatic factors on the active layer and permafrost at Barrow. Alaska. Permafrost and Periglacial Processes 9 (3), 229–246.

Zhang, T., 2005. Influence of the seasonal snow cover on the ground thermal regime: an overview. Reviews of Geophysics 43, RG4002. doi:10.1029/2004RG000157.

Zhang, T., Barry, R.G., Haeberli, W., 2001. Numerical simulations of the influence of the seasonal snow cover on the occurrence of permafrost at high latitudes. Norwegian Journal of Geography 55, 261–266.

Zick, W., 1996. Bewegungsmessungen 1965–1994 am Blockgletscher Macun I (Unterengadin/Schweiz) — neue Ergebnisse. Zeitschrift für Geomorphologie N.F., Supplement-Band. 104, 59–71.

Zimmerman, R.W., King, M.S., 1986. The effect of freezing on seismic velocities in unconsolidated permafrost. Geophysics 51, 1285–1290.

Zimmermann, M., Haeberli, W., 1992. Climatic change and debris flow activity in high-mountain areas — a case study in the Swiss Alps. In: Boer, M., Koster, E. (Eds.), Catena Supplement 22, 59–72.

Zuidhoff, F.S., Kolstrup, E., 2000. Changes in palsa distribution in relation to climate change in Laivadalen, northern Sweden, especially 1960–1997. Permafrost and Periglacial Processes 11, 55–69.